Neural Underpinnings of Adaptive Control in Fronto-Subthalamic Networks

Submitted in fulfillment
for the degree of Doctor of Philosophy
Faculty of Human Sciences
The University of Cologne

by

Annika Elisa Sauter
ORCID: 0009-0007-8262-9775

Cologne,
August 2025

Neural Underpinnings of Adaptive Control in Fronto-Subthalamic Networks

Inauguraldissertation
zur Erlangung des Doktorgrades
der Humanwissenschaftlichen Fakultät
der Universität zu Köln

nach der Promotionsordnung
vom 10.09.2024
vorgelegt von
Annika Elisa Sauter
aus Zürich

Köln,
August 2025

Diese Dissertation wurde von der Humanwissenschaftlichen Fakultät der Universität zu Köln im Dezember 2025 angenommen.

Abstract

In an environment as complex and unpredictable as our human society, we cannot merely rely on hard-wired reflexes and short-term incentives for successful behavior. Instead, our brain uses cognitive control to derive expectations from current and prior information and adapts strategically to changing demands. Cognitive control involves interconnected processes that resist clear categorization, suggesting a shared core of control functions. Understanding this control architecture is crucial to understanding psychological and neuropsychiatric disorders that are linked to pathological control functions, as for example Parkinson's disease.

The aim of this thesis was to uncover the shared foundation that drives theoretically distinct aspects of control. Our focus was on the control required when a goal changes (response reprogramming) and the control employed when distractions occur (conflict resolution). Additionally, we assessed how these two aspects are modulated by expectations by varying their frequency of occurrence in a novel task. The integration of all these factors in one task allowed to test for interactions. Furthermore, the task processes were examined from different angles, which included neuroimaging data from healthy participants and electrophysiological data of people with Parkinson's disease that received deep brain stimulation of the subthalamic nucleus (STN DBS; neuromodulation).

In **Chapter 2**, we found behavioral evidence for a shared process behind reprogramming and conflict resolution in healthy participants. We predicted disproportionate performance decreases when these control demands coincided, reflecting limited resources for inhibition, flexibility or coordination, especially when they were unexpected. Indeed, we observed disproportionate error increases under these circumstances, suggesting a processing "bottleneck" that can be attenuated by anticipatory control (i.e., expectations).

The same task was employed in another sample of healthy participants while recording control-related brain activity with functional magnetic resonance imaging (fMRI; **Chapter 3**). We focused on shared cortical network activations, particularly in relation to cingulo-opercular and fronto-parietal control networks, which are both implicated in reprogramming and conflict resolution. Behaviorally, we replicated the main pattern of an expectation-dependent bottleneck for error rates, which we observed in **Chapter 2**. On a neural level, fronto-parietal

and cingulo-opercular activity was present in reprogramming as well as conflict resolution, while the shared engagement during both processes localized to the pre-supplementary motor area (pre-SMA), another key region in response control. Additionally, the right inferior frontal gyrus (IFG) was selectively activated when control demands coincided and were unexpected, which was linked to the error-related bottleneck.

In **Chapter 4**, we explored the role of the STN in these control processes in people with Parkinson's disease that received DBS of the STN. We recorded cortical electroencephalogram (EEG) and STN local field potentials (LFPs) to capture beta-band oscillatory signatures of inhibition and flexibility, which have been related to domain-general control. Behaviorally, active stimulation of the STN impaired control function during conflict, leading to increased errors. Moreover, reprogramming effects were generally attenuated as compared to a healthy population, indicating impaired motor preparation. Neurally, we observed both reprogramming and conflict-related beta signatures. Notably, elevated STN beta power increased error probability exclusively when reprogramming and conflict coincided, reflecting a putative bottleneck for flexible adaptations. Taken together, these findings are in line with a core involvement of beta dynamics and the STN in these control processes.

In sum, our findings support the notion that control arises from core regions within fronto-subthalamic networks, and is governed by general mechanisms that employ inhibition and flexibility across modalities. In case control demands are particularly elevated or complex, adaptive capacities may be limited and require additional coordination, which could explain the observed "bottleneck" effect.

Deutsche Zusammenfassung

Um sich unserer komplexen und schnelllebigen Umwelt erfolgreich anzupassen, genügt es nicht, unser Verhalten ausschließlich nach Reflexen und kurzfristigen Bedürfnissen auszurichten. Dafür besitzen wir die Fähigkeit zur kognitiven Kontrolle, welche es uns erlaubt, aus kontextuellen und vergangenen Informationen heraus Erwartungen zu formen und somit strategische Entscheidungen zu treffen. Die damit verbundenen Kontrollmechanismen sind eng miteinander verflochten und lassen sich nicht eindeutig abgrenzen, was auf ein zugrundeliegendes Kernsystem hindeutet. Das Verständnis dieser Kontrollhierarchie ist zentral für das Verständnis zahlreicher Krankheitsbilder, die durch dysfunktionale Kontrollmechanismen geprägt sind, wie z.B. die Parkinson-Erkrankung.

Um diese zugrundeliegenden Zusammenhänge zu verstehen, haben wir uns auf das Verhältnis zweier theoretisch unterschiedlicher Kontrollaspekte fokussiert: bei ersterem wird Kontrolle verlangt, um sich einem veränderten Ziel anzupassen (Antwort-Reprogrammierung), und bei zweiterem wird Kontrolle benötigt, um eine Ablenkung zu unterdrücken (Konfliktauflösung). Darüber hinaus haben wir untersucht, wie diese beiden Aspekte durch Erwartungen moduliert werden, indem wir die Häufigkeit ihres Vorkommens in einer neuartigen Aufgabe systematisch variierten. Die Integration der verschiedenen Kontrollaspekte in dieser Aufgabe erlaubte es, Interaktionen und Zusammenhänge zu prüfen, welche eine gemeinsame Grundlage nahelegen würden. Wir betrachteten dies aus verschiedenen Blickwinkeln, unter anderem mithilfe von Bildgebungs-Verfahren in einer gesunden Studienpopulation sowie durch elektrophysiologische Daten von Personen mit Parkinson-Erkrankung und Tiefer Hirnstimulation des Nucleus Subthalamicus (THS des STN; Neuromodulation).

In **Kapitel 2** haben wir Verhaltensparameter untersucht, welche in einer gesunden Studienpopulation auf einen gemeinsamen Kontrollprozess hinter Reprogrammierung und Konfliktauflösung hinweisen würden. In diesem Sinne erwarteten wir, dass die Leistung disproportional stark abnehmen würde, sobald diese Kontrollanforderungen zusammenfielen, was auf Verarbeitungsgrenzen hinsichtlich Inhibition, Flexibilität oder Koordination hinweisen würde. Zusätzlich erwarteten wir eine Verstärkung dieses Effekts,

sollten die Anforderungen unerwartet auftreten. Tatsächlich stellten wir disproportionale Fehlerzunahmen fest, sobald Reprogrammierung und Konfliktlösung gleichzeitig und unerwartet auftraten. Dies deutet auf einen Verarbeitungs-„Flaschenhals" hin, der durch antizipatorische Kontrolle (d. h. Erwartungen) abgeschwächt wird.

Dieselbe Aufgabe wurde in einer weiteren gesunden Stichprobe durchgeführt, während die Gehirnaktivität in einem fMRT aufgezeichnet wurde (**Kapitel 3**). Unser Fokus lag auf gemeinsamen kortikalen Aktivierungen, insbesondere in cingulo-opercularen und fronto-parietalen Kontrollnetzwerken. Auf Verhaltensebene konnten wir die allgemeinen Muster des erwartungsabhängigen "Flaschenhals"-Effektes (**Kapitel 2**) in der Fehlerrate replizieren, wenn Reprogrammierung und Konfliktlösung gleichzeitig auftraten. Darüber hinaus beobachteten wir cingulo-operculare und fronto-parietale Netzwerkaktivität in beiden Prozessen, die gemeinsame Aktivierung manifestierte sich jedoch in der präsupplementär-motorischen Region (pre-SMA), welche als eine weitere Kernstruktur in der Verhaltenskontrolle dient. Zudem konnten wir eine selektive Aktivierung des rechten inferioren Frontallappens (IFG) nachweisen, wenn Kontrollanforderungen zusammenfielen und zusätzlich unerwartet waren, was mit dem Flaschenhalseffekt bezüglich der Fehlerrate korrelierte.

In **Kapitel 4** lag der Schwerpunkt auf fronto-subthalamischen Netzwerken und der Rolle des Nucleus Subthalamicus (STN) in diesen Kontrollprozessen, was wir bei Personen mit Parkinson-Erkrankung und THS des STN untersucht haben. Wir zeichneten ein kortikales Elektroenzephalogramm (EEG) und lokale Feldpotenziale (LFPs) des STN auf, um oszillatorische Charakteristika von Inhibition und Flexibilität im Beta-Band zu erfassen, welches diese Kontrollprozesse möglicherweise domänenübergreifend moduliert. Zudem erwarteten wir eine Beeinträchtigung STN-bedingter Kontrollprozesse bei aktiver Stimulation. Auf Verhaltensebene konnten wir tatsächlich eine stimulationsabhängige Zunahme der Fehler in Konfliktsituationen beobachten. Darüber hinaus war die Reprogrammierungs-Anforderung im Vergleich zu einer gesunden Population insgesamt abgeschwächt, was auf eine unzureichende motorische Vorbereitung hindeutete. Auf neuronaler Ebene fanden wir Beta-Charakteristika für Reprogrammierung und Konfliktauflösung, die auf Inhibition und Anpassungsmechanismen in kortikalen Arealen und im STN hinweisen. Des Weiteren erhöhte eine verstärkte Beta-Aktivität im STN die Fehlerwahrscheinlichkeit, und zwar ausschließlich

wenn Reprogrammierung und Konflikt zusammenfielen, was auf einen "Flaschenhals"-Effekt für flexible Anpassungen hinweist. Zusammengefasst passen diese Resultate zu einem zugrundliegenden Kontrollmechanismus, welcher von Beta-Dynamiken und dem STN koordiniert wird.

Gesamthaft fügen sich unsere empirischen Resultate also in ein Rahmenmodell ein, demzufolge Kontrollprozesse aus Kernregionen in fronto-subthalamischen Netzwerken entstehen und universellen Mechanismen folgen, welche Inhibition und Flexibilität modalitätsübergreifend bestimmen. Abhängig von Art und Ausmaß der Kontrollanforderungen kann dies dazu führen, dass Anpassungskapazitäten limitiert sind, zusätzliche Koordination erfordern und einen „Flaschenhals"-Effekt hervorrufen, so wie er in unseren Studien beobachtet wurde.

Declaration of Authorship

I hereby declare that the empirical work of this thesis comprises my original research (conceptualization, data analysis, data collection, writing), conducted during the candidature for the degree of Doctor of Philosophy. Importantly, the work was carried out in collaboration with the co-authors and contributors who are credited in the **Author Contributions** section (page 164). All sources and materials included have been sufficiently referenced within the thesis.

Acknowledgements

At this point, I would like to thank all those whose essential contribution made this project possible in the first place. To begin with, I would like to thank my supervisors Simone Vossel and Juan Carlos Baldermann-Weiß for their guidance and support throughout this period. Thank you, Simone, for sharing your clear vision, and Carlos, for inspiring me with your ideas and always having an open ear for mine. Your combined perspectives helped to constantly advance this interdisciplinary project and my own understanding.

Additionally, I would like to thank Paola Mengotti and Thomas Schüller, who were key members of the project team and helped to shape the project on every level. Thank you also to Michael Barbe, for the valuable insights and help along the way, and for creating such a validating and supportive environment within the AG Barbe. It was a pleasure to be part of the Kappellchen crew.

Furthermore, I would like to thank Huiling Tan and the Tan group in Oxford, not only for sharing key analysis insights, but also for instantly making me feel a part of the team, and for their determination to give the best possible support in the shortest amount of time.

In addition to my mentors, I owe many thanks to everyone who stood by me throughout this period with steady support and encouragement. Thank you, Anna, for the many uplifting and insightful talks in the MRI room and all your help that I could never pay back with enough carrots. Thank you, Laura, for making everything feel less challenging after climbing mountains during storm warnings, next to all the research-related support, and all the fun times. Thank you, Katharina, for the many laughs (and of course, LMEs) in the basement of the psychiatry and beyond. Lea, I could write a whole chapter on your support, but for now, just a big thank you for everything. Thank you, Lisa and Lyle, for rescuing me from the rabbit hole time and again and for making everything better. Thank you, Jane and Ulises, for the amazing times and exchange together. Thank you also to my friends outside the PhD, for the patience and emotional support, and to my family, for always believing in me.

Table of Contents

List of Tables

Chapter 3

Appendix

Supplementary Material Chapter 2

Supplementary Material Chapter 4

List of Figures

General Introduction

Chapter 2

Chapter 3

Chapter 4

Appendix

Supplementary Material Chapter 2

Supplementary Material Chapter 3

Supplementary Material Chapter 4

List of Abbreviations

ACC	Anterior cingulate cortex
ANOVA	Analysis of variance
β	Beta; regression coefficient
BDI-II	Beck's Depression Index-II
BIC	Bayesian Information Criterion
BIS-11	Barratt Impulsiveness Scale-11
BOLD	Blood oxygenation level dependent
CBGTC (pathways)	Cortico-basal ganglia-thalamo-cortical (pathways)
CMRR	Center for Magnetic Resonance Research
CP	Congruency proportion
DBS	Deep brain stimulation
dlPFC	Dorsolateral prefrontal cortex
EEG	Electroencephalogram
EHI	Edinburgh Handedness Inventory
EPI	Echo-planar imaging
F	Referring to the statistical F-distribution
fMRI	Functional magnetic resonance imaging
FOG-Q	Freezing-of-Gait Questionnaire
GLM	Generalized linear model
GLME	Generalized linear mixed-effects model
IFG	Inferior frontal gyrus
LFP	Local field potential
LME	Linear mixed-effects model
min.	Minute
mm	Millimeter
MNI	Montreal Neurological Institute
MoCA	Montreal Cognitive Assessment
ms	Millisecond
p	*p*-value

PFC	Prefrontal cortex
pre-SMA	Presupplementary motor area
QUIP-PD	Questionnaire for Impulsive-Compulsive Disorders in Parkinson's disease
RM-ANOVA	Repeated measures analysis of variance
ROI	Region of interest
RT	Reaction time
SD	Standard deviation
SE	Standard error
sec.	Seconds
SEM	Standard error of the mean
SMA	Supplementary motor area
SPM	Statistical Parametric Mapping
T	Tesla
UPDRS-II	Unified Parkinson's disease Rating Scale-II
VP	Validity proportion

CHAPTER 1

General Introduction

1. Theory of cognitive control

In dynamic environments, we rely on cognitive control to translate complex information into goal-directed behavior. This ability is essential to strategically plan and flexibly adapt our course of action in spite of uncertainty and noise (Dosenbach et al., 2008; Miller & Cohen, 2001). To meet contextual demands, cognitive control implies many modalities (Dosenbach et al., 2006). But does the control that allows you to reroute in heavy traffic and the control that allows you to simultaneously ignore radio noise, rely on a similar mechanism? Different timescales and purpose naturally raise the question: does cognitive control entail a core, domain-general mechanism or does it combine separate sub-systems?

Research has yet to provide a conclusive answer to this question, even though most theoretical models agree on a domain-general core (Gratton et al., 2018). They mainly differ in their division of control components, resulting in distinct yet largely compatible concepts.

One approach to divide components is to define their main functional role. According to Gratton et al. (2018), this organization encompasses five key functions: (1) goal formation (direction) (2) information selection and updating (integration) (3) task set specification (translation) (4) shifting or orienting (adaptation) and (5) inhibition (complementary suppression). Importantly, although integral to cognitive control, attention is not typically considered a functional component. Rather, attention constitutes the filter per se that cognitive control processes, such as inhibition and updating, adapt and direct toward goal-relevant information (Gratton et al., 2018). The process is also referred to as "top-down" attention and guided by internal expectations and demands. In contrast, "bottom-up" attention is triggered by salient or unexpected stimuli that influence attention externally (Corbetta & Shulman, 2002).

The functional categorization by Gratton et al. (2018) provides a useful framework for testing theoretical assumptions. However, it likely reflects conceptual distinctions rather than fully separable functions, due to interdependencies and intersects. Along these lines, Miyake and Friedman (2012) focused on shared processes across experimental tasks and outlined inhibition as a ubiquitous factor that influences performance across categorizations. Accordingly, they termed it "common executive function". Unfortunately, the term "inhibition" lacks precision in the literature. In a narrow sense, it is depicted as the specific, transient suppression of a prepotent motor response in reaction to a stop cue (Aron et al., 2007). More broadly, it can be understood as a set of targeted or diffuse control processes that suppress or bias behavior in anticipation of or in adaptation to salient events (Wessel & Aron, 2017). With reference to a "common executive function", I will adopt the broader definition of "inhibition" for the scope of this thesis.

Notably, the term executive function is sometimes also used in place of cognitive control, but is by definition not equivalent (Badre, 2025). While executive function is specific to response formation and output, cognitive control relates to a more conceptual framework of regulatory control systems (e.g., Ritz et al., 2022). In this thesis' empirical work, the focus is on "response control", referring to cognitive control processes that are linked to executive function, which is more readily assessed in an experimental setting. This would exclude, for example, control over intrusive thoughts without an imminent output. Nonetheless, the presented empirical findings on response control processes may generalize to further aspects under the umbrella term of cognitive control.

Beyond a functional distinction, cognitive control processes can also be categorized in a temporal sense. Initially, cognitive control was thought to unfold in serial information processing stages, through which information flows in a sequential manner from perception to decision-making to action (Sternberg, 1969). However, growing evidence supports a parallel processing account including feedback loops, which seems more appropriate given the intertwined nature of cognitive control processes and the evolutionary advantage of enhanced flexibility in uncertain environments (Cisek, 2007). In the parallel model, the brain simultaneously generates, evaluates and adapts many potential courses of actions (e.g., Cisek

& Kalaska, 2010). A temporal categorization of control, known as the dual mechanisms of cognitive control, was proposed by Braver (2012), which distinguishes between anticipatory (proactive) and reactive (online) control components. A more gradual and sustained deployment of control is ascribed to anticipatory mechanisms, which support readiness and efficiency by advance preparation. Essentially, expectations introduce a selective bias that influences attention and decision thresholds. In contrast, reactive control mechanisms are employed "on demand" to enable flexible adaptations upon changing demands. This entails a more transient employment, which appears to be enhanced or diminished in relation to anticipatory control and expectations. Reactive control has been further divided into two stages: an initial "pause", marked by global inhibition, and a subsequent "retune" stage for selective adaptations (Hervault & Wessel, 2025).

The temporal account of cognitive control can be linked to the functional components defined by Gratton et al. (2018). In this regard, reactive control would correspond to flexible changes ascribed to shifting, while updating and inhibition are conceivably involved in both stages (e.g., Miyake & Friedman, 2012; Ridderinkhof et al., 2004). Updating allows us to adjust expectations during anticipation but also after reactive changes, and inhibition is required continuously for anticipatory bias as well as for reactive suppression and adaptation of premature responses. This underscores the conceptual intersections between theories that appear to be distinct in perspective rather than general assumption. Overall, the integrative nature of cognitive control processes may more closely resemble an emerging property than a clear component divide (e.g., Cisek & Kalaska, 2010). In order to get to the root of this, we need to investigate the underlying relationship of these processes.

In sum, cognitive control is pivotal for goal-oriented behavior in complex and uncertain environments, allowing us to diverge from hard-wired reactions in favor of strategic action. Despite its central contribution to human behavior, its multifaceted nature complicates empirical conclusions and theories are still lacking a comprehensive framework. However, neuroscientific advances and novel experimental techniques allow closer access to the abstract components of this construct and start to unravel its structure (e.g., Cavanagh & Frank, 2014). Clinically, impairments in cognitive control are associated with various neurological and psychiatric conditions, including Parkinson's disease, which has informed

theories on its neural foundations (e.g., Cools, 2006; Jahanshahi et al., 2015). Therefore, the need for translational research is rising that can bridge clinical and basic research, and thereby, the different components of cognitive control.

In the sections nr. 2 and 3 of the General Introduction, I will link the theoretical concepts of cognitive control to their neural counterparts, focusing on our control processes of interest, and discuss how these can be assessed experimentally. In this regard, I will explain a novel experiment in more detail that we employed in our empirical studies (**Chapter 2-4**) to reveal the underlying relationship between these control processes.

2. Neural architecture of cognitive control

2.1 Functional control networks

Theories about *where* the brain implements cognitive control were initially informed by observations of decreased behavioral flexibility and impaired decision-making in people with lesions of the prefrontal cortex (PFC) (e.g., Miller & Cohen, 2001). However, given the multidetermined nature of cognitive functions, a core control process may not entail a one-to-one mapping to one specific brain area (Gratton et al., 2018a). As outlined in the previous section, it may rather emerge from a dynamic interplay between different networks.

A common approach to investigate core control networks is to conduct meta-analyses of functional magnetic resonance imaging (fMRI) studies that include a variety of cognitive tasks. Typically, these tasks assess control processes linked to response formation, thus response control.

Dual-network model

Thus far, meta-analyses indicate that the interplay of two major networks contributes fundamentally to response control across domains: the cingulo-opercular network and the fronto-parietal network (dual-network model; Dosenbach et al., 2008). Additional hub regions, such as the pre-SMA, have also been consistently associated with control-related activity.

The cingulo-opercular network involves regions of the anterior PFC, the anterior lateral/frontal operculum, the dorsal ACC/medial superior frontal cortex, as well as the

thalamus. With respect to timing, it is thought to contribute to a more sustained and anticipatory control, while functionally serving aspects of updating and monitoring (Dosenbach et al., 2007). The control-conflict loop theory (e.g., Gratton et al., 2018) outlines specifically the ACC and pre-SMA as the core structures in conflict monitoring, acting in concert with the dorsolateral PFC (dlPFC), which would be in charge of implementing the control demand. The dlPFC is part of the fronto-parietal network, which further involves regions of the inferior parietal lobule, the inferior parietal sulcus, the dorsal frontal cortex, the precuneus and the middle cingulate cortex. Fronto-parietal network activity is temporally more transient and reactive, with a functional role relating to shifting and inhibition (Dosenbach et al., 2007). Notably, the functional intersections and interconnectivity among brain regions can lead to ambiguous interpretations (e.g., Rodríguez-Nieto et al., 2022). For instance, right frontal regions such as the IFG and the dlPFC are implicated in both the inhibition of premature responses and shifting of attention, likely reflecting shared rather than mutually exclusive processes. The right IFG, in particular, has been described as an attentional "circuit-breaker", involved during an emergency "pause" in reactive control (e.g., Corbetta & Shulman, 2002; Tatz et al., 2021), which may be triggered by both motor inhibition demands as well as the detection of salient events (Wessel & Aron, 2017).

It remains to be elucidated whether an activity pattern specific to the cingulo-opercular and fronto-parietal networks gives rise to domain-general control and in which way additional regions may contribute. Furthermore, key frontal control regions are also part of the cortico-basal ganglia-thalamo-cortical (CBGTC) pathways, which shape and implement control demands through a fronto-subthalamic route.

Cortico-basal-ganglia-thalamo-cortical pathways

Generally, the basal ganglia have been described as a "decision gatekeeper" (Redgrave et al., 1999), which do not generate goals themselves but serve to shape and authorize potential plans generated by the cortex. This "conditional routing" is based on integration of contextual, motivational, and sensory information to bias behavior toward the most adaptive outcome.

Structurally, the basal ganglia consist of a set of subcortical nuclei including the striatum (caudate nucleus and putamen), the globus pallidus (divided into internal and external segments), the substantia nigra, and the subthalamic nucleus (STN) (Albin et al., 1989; Parent & Hazrati, 1995). The STN entails a unique configuration, including widespread connectivity with frontal cortex, which makes it the basal ganglia's main integrative hub and gatekeeper. The classic tripartite model of the STN proposes a dorsolateral motor sector, a ventromedial associative region, and a medial limbic tip (Joel & Weiner, 2000). However, high-resolution tracing and imaging studies have revealed gradients across the STN rather than rigid borders (e.g., Alkemade et al., 2015; Haynes & Haber, 2013; Prasad & Wallén-Mackenzie, 2024). This architecture enables the STN to integrate a wide range of information, from motor specifications to value signals, rather than operating in strictly segregated channels (e.g., Drummond & Chen, 2020). Fronto-subthalamic projections are visualized in Figure 1. The function of the STN is initially excitatory with a net inhibitory effect, using glutamatergic projections to activate disinhibitory output structures (globus pallidus internus and substantia nigra), which in turn inhibit excitatory neuronal firing to the cortex, also known as "thalamocortical drive", which leads to movement suppression (Albin et al., 1989; Haynes & Haber, 2013; Figure 2 (top row)).

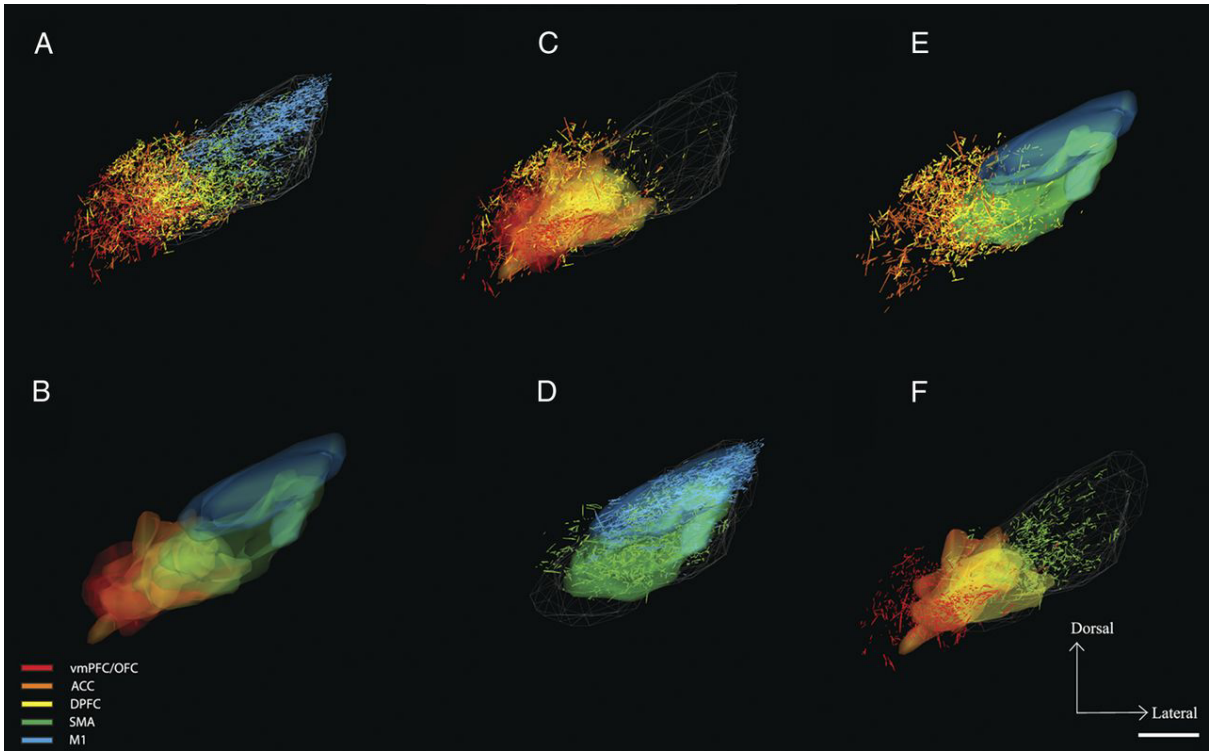

Fig. 1 Long-range projections of cortical regions to the STN, as indicated by different colors, which are associated with sensorimotor (e.g., SMA; green), cognitive (e.g., dPFC; yellow) and limbic (e.g., ACC; orange) domains. Illustrations A-F differ in emphasis on dense versus diffuse projections. All projections were derived with anterograde tracing in non-human primates. Importantly, the regional overlap among projections illustrates that domains are gradients rather than strictly segregated areas. Abbreviations: vmPFC: ventromedial prefrontal cortex (red); OFC: orbitofrontal cortex (red); ACC: anterior cingulate cortex (orange); dPFC: dorsal prefrontal cortex (yellow); SMA: supplementary motor area (green); M1: primary motor cortex (blue). (this figure is reproduced with permission of the Society for Neuroscience and was published under the Creative Commons Attribution-Noncommercial-Share Alike 3.0 Unported License (CC-BY-NC-SA; (https://creativecommons.org/licenses/by-nc-sa/3.0/) in Haynes & Haber, 2013).

Basal ganglia activity as a whole is commonly divided into three principal pathways: the hyperdirect and indirect pathways, related to inhibition via the STN, and the direct pathway, with net excitatory effects (e.g., Nambu et al., 2002). In the latter case, cortical input activates the striatum via the direct pathway, basal ganglia output structures (globus pallidus internus/substantia nigra) are inhibited, leading to disinhibition of thalamocortical drive and facilitated movement execution.

The fastest inhibitory route works via the hyperdirect pathway, which allows cortical areas, such as the pre-SMA, dlPFC or IFG, to directly excite the STN through monosynaptic

projections, leading to rapid global inhibition ("pause"; Hervault & Wessel, 2025; Nambu et al., 2002). For this reason, the STN is considered a "response brake" and crucial to reactive control (e.g., Aron, 2011; Frank et al., 2007). Furthermore, it is suggested that the initial "pause" grants time and clears activity for more selective adaptations during a subsequent stage ("pause and retune"; Hervault & Wessel, 2025). As increasingly acknowledged, the STN's contribution seems to extend beyond just implementing a "pause" to subsequently fine-tuning behaviorally relevant output, helping adjust motor vigor, timing, and flexibility (Jahanshahi et al., 2015; Nougaret et al., 2021). Moreover, its activity may also modulate anticipatory control, as demonstrated in preparation for stopping actions (e.g., Benis et al., 2014). However, precisely which control processes depend on the STN and how they relate to each other, is underexplored.

Notably, while the tripartite model of direct, indirect and hyperdirect pathways has provided a useful framework, accumulating evidence suggests it may be overly simplistic. The pathways are not completely segregated, and cross-talk among circuits (neural interconnections; Haber, 2003) introduces context-dependent dynamics that are not well accounted for in the classical model. Moreover, evidence from electrophysiological and imaging studies indicates that the pathways operate simultaneously, altogether suggesting more flexible, integrated modes of selection (Calabresi et al., 2014; Nambu et al., 2002).

2.2 Electrophysiological signatures of control

Not only where, but *how* the brain controls information processing can be investigated by studying oscillatory activity in electrophysiological recordings. Neural oscillations are cyclic fluctuations in excitability across groups of neurons which can be interpreted in a frequency-specific manner. A measured power in a frequency band reflects the degree of synchronization in a neuronal population, for example in response to a task stimulus, and provides crucial insight into the functional and temporal organization of information flow in the brain (Brittain & Brown, 2014). Enhanced synchronization is generally related to decreased information coding capacity (decreased entropy) and increased stability (e.g., Eusebio et al., 2009). By guiding information flow both locally and on a network-level, oscillations are thought to regulate neuronal spiking activity (Jensen & Mazaheri, 2010). Overall, activity in the theta

(~2-8 Hz) and beta (~13-30 Hz) frequency bands appears to play a central role in cognitive control (e.g., Cavanagh & Frank, 2014; Spitzer & Haegens, 2017).

Activity in the theta-band is involved in monitoring and signaling cognitive conflict both locally and within fronto-subthalamic pathways (e.g., Cavanagh et al., 2011; Zavala et al., 2016). Furthermore, its rhythm may serve to prevent conflict occurrence by organizing neural excitability and functional connectivity into alternating microstates of either sensory sampling (updating) or motor specification (Fiebelkorn et al., 2018). In short, the theta-band may be broadly attributed an organizational role in cognitive control, by boosting interareal coordination and temporospatial information structure (e.g., Cavanagh & Frank, 2014; Helfrich & Knight, 2016).

Peaks and troughs of beta power appear to balance inhibition and flexibility across domains. In the motor domain, beta synchronization (i.e., increase in beta power) is prominently observed during motor inhibition and movement termination, whereas beta desynchronization (i.e., decrease in beta power) is associated with motor initiation (Pfurtscheller, 2000; Pfurtscheller & Lopes Da Silva, 1999). Beyond motor functions, beta synchronization has been implicated in top-down attentional filtering and stabilization of a response plan (e.g., Dubey et al., 2023; Leventhal et al., 2012). Conversely, beta desynchronization is thought to promote flexibility, supporting adaptive changes and information encoding (e.g., Pierrieau et al., 2025; Spitzer & Haegens, 2017; Zavala et al., 2018). In line with a global function, beta appears as the most widespread cortical frequency and is closely linked to the dopamine network (Chikermane et al., 2024). Accordingly, beta dynamics may modulate synaptic connections in concert with dopamine to shape neural reinforcement at the cellular level (Cavallo & Neumann, 2024). Furthermore, Wessel and Anderson (2024) proposed that beta-band dynamics regulate inhibition and flexibility by tuning thalamocortical drive via fronto-subthalamic pathways, which was prominently related to the motor domain (Figure 2). The thalamus appears to be organized as a lower-level analogy of cortical networks, providing the structural means by which beta dynamics may selectively target cortical processes across domains (Hwang et al., 2017). However, it is still unclear whether this applies equally to different modes of inhibition, e.g., broad or selective suppression during anticipatory and reactive control. The initial "pause" during reactive control has been associated with frontocentral beta bursts (Wessel, 2020) and right-prefrontal

beta increases (Daniel et al., 2023), implementing broad inhibition. The subsequent "retune" stage, during which responses are flexibly adapted, has thus far been connected to theta increases (Hervault & Wessel, 2025), but may also rely on beta desynchronization for improved flexibility and performance (as indicated in Brittain et al., 2012; Pierrieau et al., 2025). These relationships warrant further investigation.

The significance of beta dynamics for adaptive control is further supported by a prominent role in Parkinson's disease pathology, where excessive beta synchronization is closely linked to impaired executive functions (Brown, 2003). This will be discussed in detail in section nr. 4 of the General Introduction, which focuses on Parkinson's disease.

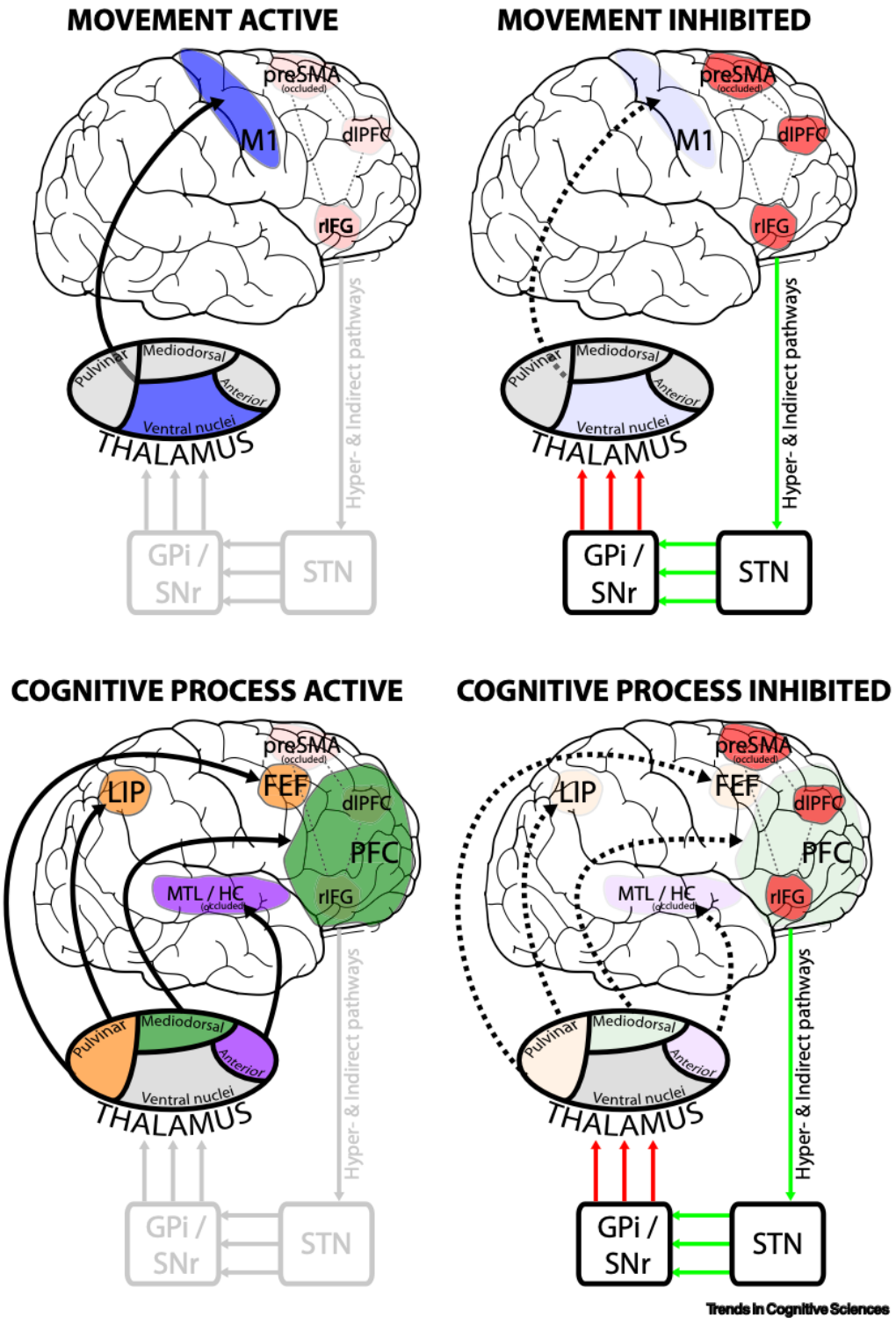

Fig. 2 Schematic representation of a putative domain-general mechanism of inhibitory control. The top row depicts the inhibitory mechanism as demonstrated for motor inhibition: the cortical areas depicted in red (pre-SMA, dlPFC and rIFG) transmit a stopping signal to the STN, which then implements the demand via GPi/SNr output nuclei. These suppress motor-related thalamic nuclei, thus thalamocortical drive to the motor cortex, which inhibits movement. The bottom row shows how the same inhibitory mechanism may work for other processes that are not

directly tied to movement execution. In these cases, alternative thalamic nuclei, such as the mediodorsal nucleus, may support the suppression of thalamocortical drive to modulate cortical areas that are, for example, involved in decision-making or perception. Abbreviations: pre-SMA: pre-supplementary motor area; dlPFC: dorso-lateral prefrontal cortex; rIFG: right inferior frontal gyrus; M1: primary motor cortex; GPi: globus pallidus internus; SNr: substantia nigra; LIP: lateral intraparietal cortex; MTL/HC: medial temporal lobe/hippocampal complex; FEF: frontal eye fields. (reprinted from Trends in Cognitive Sciences, 28(2), Wessel, J. R., & Anderson, M. C., Neural mechanisms of domain-general inhibitory control, 124–143, Copyright (2024), with permission from Elsevier)

3. Core control processes assessed in this thesis

Based on cognitive control's main concepts and their neural foundation, I will now discuss how they can be assessed experimentally. In particular, I will focus on two aspects of control that were investigated in this thesis, and describe how we examined their relationship to reveal shared underlying control processes. It should be noted that experimental tasks, including the one used in this thesis' work, typically measure control processes linked to response formation, i.e., response control. This represents a subcategory within the broader framework of cognitive control that is more accessible in an experiment.

Generally, experimental tasks that assess response control can be divided into four categories (Gratton et al., 2018): (1) continuous working memory paradigms, which primarily test updating (2) conflict paradigms, which introduce interference to probe inhibition of automated responses (3) response inhibition paradigms, which assess the suppression of prepotent (prepared) responses and (4) task-switching paradigms, which examine goal- or set-shifting.

For the scope of this thesis, we were interested in the relationship between response reprogramming and conflict resolution. During response reprogramming, an unexpected change in response demands requires inhibition of the prepared (prepotent) response and programming of an alternative (e.g., Aron & Verbruggen, 2008). Next to this, conflict resolution depicts the inhibition of interfering (automated) response activations that compete with the target activation (e.g., Botvinick et al., 2001). Generally, response reprogramming relates to response inhibition and conflict resolution to conflict paradigms, while response reprogramming also involves aspects of task-switching (e.g., Gratton et al., 2018). Testing

these aspects together highlights the interplay between different modalities of inhibition (prepotent activation vs. interference) and response adaptations (reprogramming and conflict suppression). Furthermore, we modulated expectations of reprogramming and conflict to determine how both of these reactive processes are influenced by anticipatory control. Together, these aspects encompass the key temporal and functional components of response control, providing a comprehensive framework to test common patterns.

Behaviorally, interactive patterns of control processes can be interpreted with the additive factors' method (Sternberg, 1969). This method posits that if two factors influence separate processing stages, their behavioral effects should be additive, and interaction would indicate that the factors influence the same processing stage. While this method has long served as a foundational tool for dissecting cognitive subprocesses (e.g., in the attentional network task; Fan et al., 2002), its assumptions have been criticized, as interactions could also arise from more complex coordinative dynamics or strategic adaptations (Pieters, 1983; Stafford & Gurney, 2011). Furthermore, the additive factors' method relies on a serial model of information processing, while a parallel processing framework with feedback loops appears more compatible with human neural architecture (Cisek & Kalaska, 2010).

Given these limitations, we adopted a more nuanced interpretation: rather than interpreting merely the presence or absence of statistical interactions, we focused on disproportionate decrements in performance under multiple demands (coinciding response reprogramming and conflict resolution), as an indication of mutual influence between the control mechanisms. This may reflect a partial overlap in control resources or elevated demands on their coordination. Such a limitation of processing capacities has been described as a processing "bottleneck", which indicates shared neural resources of the concurrent cognitive operations (Marois & Ivanoff, 2005; Pashler, 1994). The idea of a bottleneck provides an allegory for understanding how performance decreases could be linked to shared underlying substrates of theoretically distinct processes. Accordingly, we refer to the bottleneck account for identifying intersections among reprogramming and conflict resolution.

In the following, I will introduce standard tasks that have been used to test response reprogramming and conflict resolution individually and discuss their groundwork. Finally, I will present our novel task design, and explain how it integrates both of these aspects.

3.1 Response reprogramming

Generally, response inhibition tasks entail a primary task with an associated response (prepotent response) and an unexpected, reactive component, for which the prepotent response needs to be withheld. Response reprogramming, as an extension, entails not merely the inhibition of the prepotent but also the subsequent programming of an alternative response, relating to task-switching or shifting processes (Bestmann & Duque, 2016; Gratton et al., 2018). Accordingly, it is likely that measures of reprogramming reflect more than one main process.

Reprogramming has been studied using response cueing tasks, notably adaptations of the Posner cueing task (Posner, 1980) in the motor domain (Rushworth et al., 2001a; Rushworth et al., 1997). In these tasks, participants receive probabilistic cues that indicate the likely motor response to an upcoming target. Valid cues, which accurately predict the required response, typically result in faster and more accurate responses, whereas invalid cues lead to slower responses and increased error rates. This difference in performance, known as the "validity effect," reflects the ability to prepare for expected responses and the adaptation costs when these expectations are violated (Rushworth et al., 2001a).

Response preparation refers to the neural processes that induce readiness in the motor system for more efficient responding (Bestmann & Duque, 2016). One way to measure this is by assessing suppression of cortico-spinal excitability during the preparatory period, which reflects the responsiveness of pathways linking the primary motor cortex and the spinal cord (Duque & Ivry, 2009). Furthermore, advance preparation biases local primary motor cortex circuits, selectively suppressing competing activity (Hannah et al., 2018). For unimanual actions, interhemispheric inhibition was shown to selectively target the alternative response hand (Puri & Hinder, 2022). When cues are invalid, reprogramming requires a shift of this inhibitory bias, leading to release and adjustment (Neubert et al., 2011). Repetitive TMS over the left supramarginal gyrus has been shown to disrupt reprogramming after invalid cues,

demonstrating a principal role in response preparation and shifting (Kuhns et al., 2017; Rushworth et al., 2001b).

Anticipatory Modulation

Crucially, the magnitude of the validity effect is modulated by expectations of reprogramming, as manipulated by the frequency of valid versus invalid cues ("validity proportion"). It was demonstrated that participants implicitly learn the validity proportion (i.e., reliability of the cue) over time, adjusting their preparatory strategies accordingly (Bestmann et al., 2008; Kuhns et al., 2017). As the proportion of valid cues increases, so does the size of the validity effect, suggesting that heightened probabilities strengthen anticipatory control mechanisms, which in turn increases adaptation costs for invalid trials (e.g., Kuhns et al., 2017).

This expectation-dependent variability is mirrored at the neurophysiological level, where systematic manipulation of validity proportion appears to modulate cortico-spinal excitability in a graded manner, linking the expectation strength to both performance and readiness of the motor system (Bestmann et al., 2008). Similarly, Vossel et al. (2015) demonstrated that validity proportion affects how attentional resources are deployed through distinct network mechanisms. Another marker of cue-related anticipation may be linked to beta-band activity, as higher beta synchronization has been associated with more successful response inhibition (Benis et al., 2014).

3.2 Conflict resolution

Conflict resolution has been described as "refining representations" (Egner & Hirsch, 2005), in case similar response options compete for execution. This has been widely assessed with the arrow version of the Eriksen flanker task (Eriksen & Eriksen, 1974), in which participants are asked to respond according to the direction of the central target arrow. However, this arrow is flanked by distractor arrows pointing in either the same (congruent) or opposite (incongruent) direction. Incongruent flanker stimuli interfere (i.e., are in conflict) with the relevant target information and demand inhibition. The performance difference between these two trial types, as reflected in slower responses and increased errors on incongruent trials, is known as the "congruency effect" (e.g., Ridderinkhof et al., 2004).

To be precise, "conflict" and the "congruency effect" are terms used throughout a large range of task designs. Next to the Eriksen flanker task, the Stroop task (Stroop, 1935) and the Simon task (Simon & Rudell, 1967) are two other well-known paradigms to study the congruency effect. In the Stroop task, participants are typically required to name the ink color of a word that may denote a different semantic color name, creating stimulus-stimulus (S–S) conflict. The Simon task, in contrast, elicits a stimulus-response (S–R) conflict through stimuli that are spatially incongruent with the correct response side. The Eriksen Flanker task (Eriksen & Eriksen, 1974) has been primarily considered to elicit stimulus-response (S–R) conflict, but some researchers argue it also contains elements of stimulus-stimulus (S–S) conflict, depending on task parameters such as stimulus similarity and timing (Kornblum et al., 1990; van Veen et al., 2001). Nonetheless, the congruency effect in all three tasks may be explained by the same dual-route model (Rosenbaum & Kornblum, 1982), which posits that upon conflict, a fast, automated processing stream must be overridden by a slower processing route, which is guided by cognitive control. The crucial difference to inhibition of prepotent responses (classic response inhibition task) relates to timing: in conflict tasks, information about the correct target route is presented simultaneously to the distraction, while response inhibition tasks entail anticipatory response selection.

While conceptually similar, the congruency effect of the Eriksen flanker task, the Simon task and the Stroop task seem to engage partially distinct control processes. For instance, Egner (2008) and Liu et al. (2004) showed that Stroop and Simon conflicts activate partially distinct fronto-parietal regions. Similarly, Fan et al. (2003) found that these tasks differentially recruit the dorsal anterior cingulate cortex (ACC) and lateral prefrontal regions depending on conflict characteristics. Meta-analyses focusing on flanker conflict have consistently implicated frontal control regions such as the dorsolateral prefrontal cortex (dlPFC) of the fronto-parietal network and regions within the cingulo-opercular network, particularly the anterior insula, for conflict resolution (Cieslik et al., 2015; Nee et al., 2007).

Oscillatory activity provides further insight. Theta-band increases are a common marker of conflict, showing elevated power and coherence in the mPFC and STN during incongruent trials in a Stroop task (Ghahremani et al., 2018) and modulation of STN spiking during flanker conflict (Zavala et al., 2015). The beta-band is increasingly recognized as

another important signature of conflict resolution. Brittain et al. (2012) found that beta synchronization rises after conflict detection in a Stroop task, which is followed by pronounced desynchronization. In Parkinson's disease, Zavala et al. (2015) demonstrated that beta oscillations contribute to STN spike-phase locking during flanker conflict, potentially serving to inhibit premature responses. Similarly, Wessel et al. (2019) observed that beta-band activity in the STN influenced the primary motor cortex during Simon conflict, leading to increased suppression of cortico-spinal excitability and motor slowing, thereby relating conflict-related to motor-related inhibitory signatures.

Taken together, "conflict" appears to be a stretched concept and task characteristics introduce variability in related control demands. Nonetheless, these demands share the foundation of the dual-route model (Rosenbaum & Kornblum, 1982) and core similarities regarding network activations and oscillatory dynamics.

Anticipatory modulation

Similarly to the validity proportion in response cueing paradigms, anticipatory control also shapes the magnitude of the congruency effect (e.g., Derosiere et al., 2018). This can be achieved by systematically varying proportions of incongruent and congruent trials ("congruency proportion"). When conflict trials are frequent (i.e., expected), they usually decrease the congruency effect (Derosiere et al., 2018; Duque et al., 2016), which has been referred to as conflict adaptation (Botvinick et al., 2001). This effect is often interpreted with a conflict monitoring account, whereby the cognitive system would adjust attentional control depending on the expected likelihood of conflict (Botvinick et al., 2001), rather than preparing a specific response.

As top-down strategic control adjustments and lower-level learning are hard to dissociate in an experimental task, conflict monitoring effects have been strongly debated in the literature (e.g., Braem et al., 2019; Schmidt, 2013). For instance, in contingency learning, stimulus-response pairings that occur with unequal frequency can bias behavior, promoting processing short-cuts for automated response iterations (Schmidt & Besner, 2008). Another mechanism, temporal learning, proposes that participants adjust response thresholds based on experienced timing regularities, particularly in blocks dominated by either congruent or

incongruent trials (J. R. Schmidt, 2019). Moreover, sequence effects, described as the "Gratton effect" (Gratton et al., 1992), show that conflict occurrence in one trial reduces the congruency effect in the next. However, these adjustments are not mutually exclusive, as recent evidence suggests that both trial-by-trial and broader contextual adaptations may derive from similar processes, differing only in the level of abstraction involved (Braem et al., 2019). These processes could be conceptualized as specifying attentional weights to certain stimulus attributes, on both lower and higher levels (Gratton et al., 2018). Such level-dependent adjustments may account for inconsistent reports of network activity across studies, particularly regarding the involvement of the ACC (e.g., Aarts et al., 2008; Donohue et al., 2008).

On a neurophysiological level, the manipulation of congruency proportion has been related to different degrees of cortico-spinal excitability suppression for incongruent response activations, in association with conflict frequency (similarly to the validity proportion). The more frequently conflict occurred, the stronger it was expected, which was detected in enhanced suppression of cortico-spinal excitability (Bestmann & Duque, 2016; Duque et al., 2016).

Oscillatory signatures of conflict-related anticipation include the theta-band, which has been shown to increase with conflict expectation. Even so, it has been suggested that midfrontal theta reflects a general anticipatory state rather than conflict-specific anticipation (Asanowicz et al., 2022; Fan et al., 2007; Strack et al., 2013), which may result in ambiguous interpretations. In line with this, Zuure et al. (2020) identified distinct frontal theta components, possibly corresponding to different functional processes. In addition, the beta-band appears to play an important part in across-trial updating and adaptations of response thresholds in relation to conflict frequency (Zavala et al., 2018). Conflict trials were linked to subsequent attenuation of beta power, at the medial prefrontal cortex and the STN (Zavala et al., 2018), which supports the notion that a beta decrease amplifies adaptation capacities (R. Schmidt et al., 2019).

3.3 Novel response cueing/conflict task

The novel task that was employed in the thesis' empirical work integrates aspects of motor response cueing (Posner, 1980) and flanker conflict (Eriksen & Eriksen, 1974) tasks, including a modulation of anticipatory control, and was designed to assess the related core control processes. In this section, I will describe the novel response cueing/conflict task design in detail and review related integrative task designs.

The response cues indicated either a left- or right-hand response. Invalid cues, which indicated the wrong response, required response reprogramming upon target occurrence. Trials with invalid cues varied in frequency across blocks and either occurred at chance level (50% of trials; low validity proportion), or rarely (in 23% of trials; high validity proportion). This manipulated response expectations and amplified the validity effect when invalid trials occurred rarely (i.e., unexpected; Kuhns et al., 2017). In incongruent trials, flanker arrows indicated the opposite response as the target arrow, which created interference and required conflict resolution (Botvinick et al., 2001; Eriksen & Eriksen, 1974). The frequency of incongruent trials was also varied by block to modulate conflict expectations and increased the congruency effect when incongruent trials were rare (Duque et al., 2016). Blocks contained either frequent conflict (70% incongruent trials; low congruency proportion) or rare conflict (30% incongruent trials; high congruency proportion). Crucially, in invalid-incongruent trials, reprogramming coincided with conflict resolution, resulting in simultaneous control demands. The task design is depicted in Figure 3.

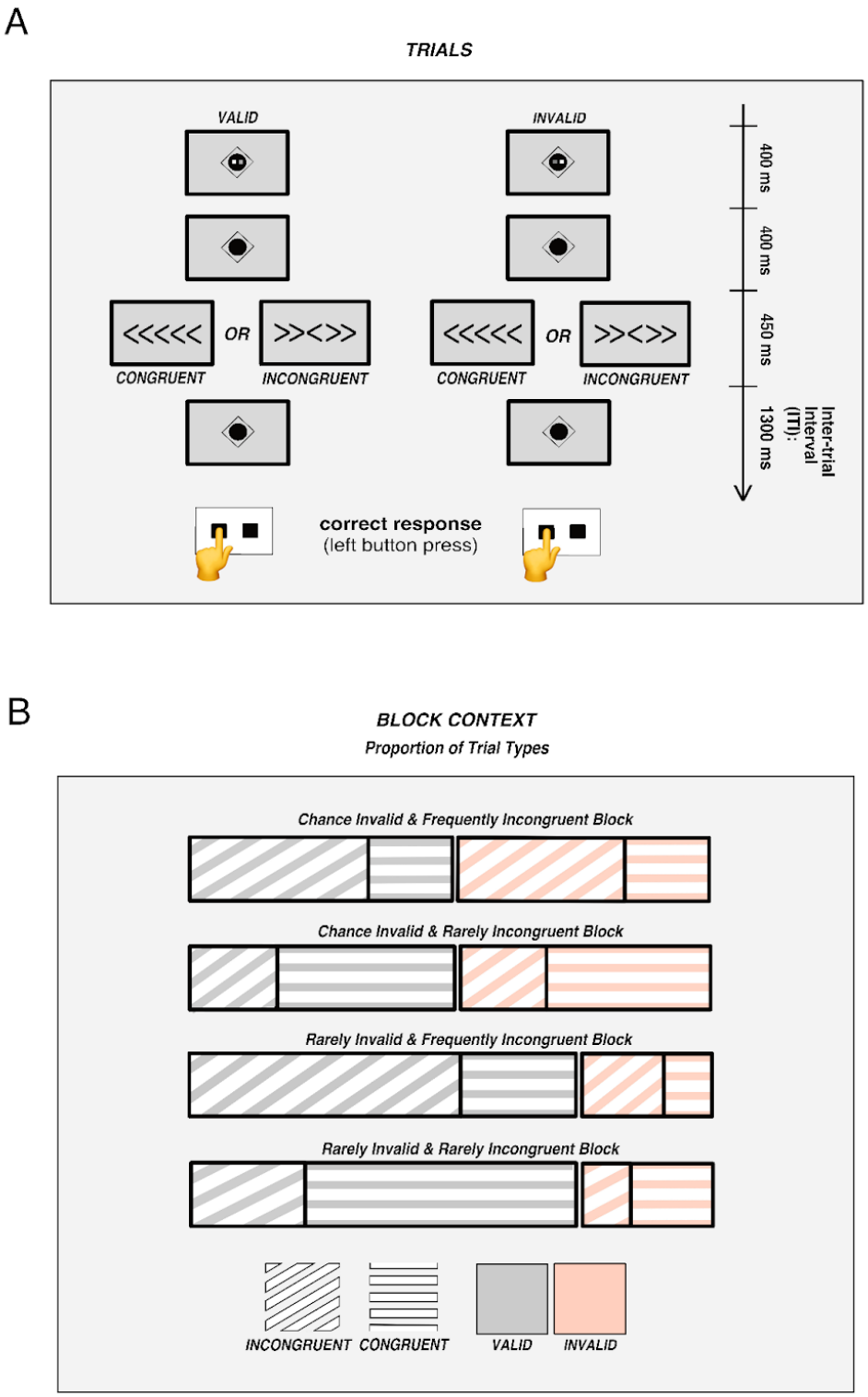

Fig. 3 Novel response cueing/conflict paradigm. (A) Trial structure: The top row shows the probabilistic motor response cues that indicated the likely upcoming response (white square: left/right button-press with left/right index finger). After a fixation interval (subsequent row), the target appeared (third row from top): a central arrow pointing left or right, requiring a corresponding button press (left button press in this example). In valid trials, the target matched the cued response; in invalid trials, the opposite response was required, necessitating response reprogramming. Central target arrows were flanked by either congruent or incongruent peripheral arrows. (B) Block

context: Four block types were defined by varying the proportions of valid vs. invalid and congruent vs. incongruent trials. (this figure is copied from Sauter et al. (2024), which is reprinted in **Chapter 2**, originally published under the Creative Commons Attribution 4.0 International License (https://creativecommons.org/licenses/by/4.0/) in Experimental Brain Research)

The relationships that we assessed with this task were two-fold: (1) anticipatory control of reactive reprogramming and conflict costs (facilitatory, neutral or amplifying influence) (2) coinciding reprogramming and conflict resolution (processing "bottleneck" or separate processes). While both of these relationships have been previously investigated, the novel response cueing/conflict task was, to our knowledge, the first that integrated all of these aspects in such a multidimensional way.

The most related task design was employed in a study by Wühr and Heuer (2017), which also integrated motor response cues with varying validity proportion (anticipatory response control) and flanker-induced conflict. However, the congruency proportion was kept constant at chance level, thus the researchers did not integrate anticipatory control related to conflict. They investigated a facilitatory effect of anticipatory response control on conflict resolution and found that only fully reliable response cues (100% validity proportion) eliminated the flanker congruency effect. This suggests that response preparation without uncertainty can prevent interference from distractors. However, when the validity proportion was reduced to 75%, this protective effect disappeared, indicating that fully dependable response preparation may be set apart from probabilistic preparation. In contrast, the novel response cueing/conflict task was focused on graded control demands with anticipatory control that always entailed uncertainty. In those task blocks by Wühr and Heuer (2017) that did involve uncertainty, validity proportion was high and invalid trials occurred rarely (25% of trials). This elicited the hypothesized validity effect, characterized by facilitated responding when response cues were valid and by reprogramming costs in invalid trials. However, reprogramming costs were unaffected by coinciding flanker conflict, i.e., no evidence of a processing bottleneck was observed. We examined this further using our task design with varying validity proportions that always entailed uncertainty and the additional manipulation of congruency proportions.

A processing bottleneck for simultaneous control demands has previously been related to spatial attention and conflict resolution. Valid spatial cues help to localize goal-relevant information through top-down attentional anticipation (Desimone & Duncan, 1995; Fan et al., 2002). Invalid cues, in contrast misdirect attention, which increases shifting demands and impairs performance. Trautwein et al. (2016) combined probabilistic spatial cueing with flanker conflict and found related activations in cingulo-opercular and fronto-parietal networks, including the anterior insula and the dorsal ACC. Most importantly, they observed a processing bottleneck related to simultaneous attentional shifting and conflict resolution in invalid–incongruent trials, reflected in disproportionate performance costs and activation of the left anterior insula. This indicates that adaptive capacities for multiple control demands may indeed be limited and arise from core structures within cingulo-opercular and fronto-parietal networks.

In view of a bottleneck between reprogramming and conflict resolution, evidence already indicates that both processes engage shared neural substrates in cingulo-opercular and fronto-parietal networks. Isherwood et al. (2021) found that tasks requiring global response inhibition show activation in similar regions as conflict tasks. Their meta-analysis identified common activation in the anterior insula, a key structure of the cingulo-opercular network. Another meta-analysis of Rodríguez-Nieto et al. (2022) delineated a core executive control network underlying inhibition, updating and shifting, which included fronto-parietal and cingulo-opercular structures, as well as the pre-SMA. The reliance on shared neural resources may limit control capacities when reprogramming and conflict resolution coincide.

Additionally, oscillatory dynamics related to reprogramming and conflict resolution bear similarities, which may further limit efficient control operations. For instance, beta-band synchronization within fronto-subthalamic pathways has been linked to both response and conflict inhibition (e.g., Wessel et al., 2019). Thus far, however, no study has directly examined whether this synchronization pattern is altered during simultaneous demand.

Importantly, functional imaging and electrophysiological methods mainly provide correlational evidence regarding brain–behavior relationships (Poldrack, 2006). To establish a more direct link, complementary approaches such as neurostimulation techniques (Siebner et al., 2009) or clinical investigations (Engel et al., 2005) are helpful. In this regard, the subsequent

section introduces Parkinson's disease, a neurological disorder with prominent executive control dysfunction. Its pathological signatures can be treated with neuromodulation through deep brain stimulation (DBS), which has informed the role of fronto-subthalamic pathways in the healthy brain (e.g., Morris et al., 2024). For the study in **Chapter 4**, we applied the novel response cueing/conflict task in people with Parkinson's disease receiving DBS of the STN to extend our understanding of the investigated control processes.

4. Control dysfunction in Parkinson's Disease

4.1 Pathology of Parkinson's disease

Parkinson's disease is one of the most prevalent neurodegenerative disorders, with increasing global health burden and no treatments to date that could slow disease progression (Kalia & Lang, 2015). Its pathogenesis is primarily associated with alpha-synuclein protein aggregates and their derivatives, called "Lewy-bodies", in dopaminergic neurons of the substantia nigra, which leads to progressive dopamine depletion (Braak et al., 2004). Accordingly, a strong genetic component of the disorder is related to heightened alpha-synuclein prevalence in predisposed people with Parkinson's disease. Furthermore, maladaptive immune responses and malfunctions of cellular organelles relate to alpha-synuclein aggregations and contribute to disease unfolding (Morris et al., 2024).

People affected by Parkinson's disease develop hallmark symptoms that are directly linked to impaired control and flexibility of motor execution. This includes progressive motor slowing (bradykinesia), stiffness (rigidity), gait disturbances and tremor. Other symptoms that are not directly linked to motor execution, such as depression and cognitive decline, strongly impact quality of life (Kalia & Lang, 2015; Morris et al., 2024). Clinical observations show that outwardly distinct symptoms may be intricately linked, as apparent, for example, in impaired motor execution under cognitive load, which points to intersecting mechanisms underlying these functions (Peterson et al., 2016). Furthermore, experimental studies demonstrate impaired performance in various control functions, such as inhibition of interference (Wylie et al., 2009), flexible set shifting (Cools, 2001), or updating of expectations (Galea et al., 2012) in people with Parkinson's disease. This points to a potential core foundation of control that is

impaired and emphasizes the clinical need to understand control processes from a broader perspective. In the following, I will explain how these Parkinsonian symptoms could be linked based on current models of the disease.

4.2 Models of Parkinson's disease

The rate model posits that the hallmark features of Parkinson's disease arise primarily from abnormal firing rates within specific basal ganglia nuclei, resulting from the degeneration of dopaminergic neurons in the substantia nigra (Obeso et al., 2000). In the healthy brain, dopaminergic input balances the activity of the direct and indirect pathways of the basal ganglia. Generally, the direct pathway, which facilitates movement, is enhanced by dopamine acting on D1 receptors, while the indirect pathway, which inhibits movement, is suppressed by dopamine acting on D2 receptors (Albin et al., 1989; DeLong, 1990). In Parkinson's disease, the loss of dopamine disrupts this balance, rendering an overactive indirect pathway, which shifts the balance towards inhibition. According to the rate model, this increased inhibitory signaling from the basal ganglia output nuclei to the thalamus would induce the pathological suppression of thalamocortical drive to motor areas of the cortex. This increased inhibition would be the principal mechanism of Parkinson's disease symptoms (DeLong, 1990).

However, the rate model alone fails to explain why Parkinsonian motor dysfunction persists even when average firing rates in basal ganglia nuclei are not significantly altered, and why treatments such as DBS are effective without consistently normalizing firing rates (McIntyre & Hahn, 2010; Wichmann & DeLong, 2006). These shortcomings brought forward the oscillatory model, which emphasizes the role of temporal structure, rather than just rate, of neuronal activity. The oscillatory model proposes increased oscillatory synchronization, particularly in the beta-band (13–30 Hz), as the key contribution to disease symptomatology (Brown, 2003).

In the healthy brain, neuronal firing across CBGTC pathways shows dynamic synchronization patterns, supporting flexible behavioral control (Brittain & Brown, 2014). In Parkinson's disease, dopamine depletion is related to increased synchronization and abnormally enhanced beta oscillations within and between basal ganglia nuclei and the cortex (Brown, 2003; Hammond et al., 2007; Iskhakova et al., 2021). This would also result in a

pathological suppression of thalamocortical drive, which impairs the initiation and scaling of movement, leading to bradykinesia and rigidity (Little & Brown, 2014). According to Wessel and Anderson (2024), suppression of thalamocortical drive may not merely modulate motor cortical areas but constitute a domain-general mechanism to adjust flexibility and inhibition of cortical processes. This may explain the range of impaired control functions observed in Parkinson's disease.

Supporting the oscillatory model, electrophysiological recordings from people with Parkinson's disease have consistently shown elevated beta-band activity in the STN, which is suppressed with dopaminergic medication and DBS (Kühn et al., 2006; Whitmer et al., 2012). Furthermore, the beta-band, and particularly, the lower beta sub-band (13–20 Hz), appear to correlate sensitively with motor-related symptoms (e.g., Neumann et al., 2016).

These findings suggest that Parkinsonian symptoms arise not solely from alterations in mean firing rates, but from the disruption of information flow due to excessive rhythmic synchronization. The oscillatory model aligns better with empirical data and has informed novel therapeutic strategies such as adaptive DBS, marking a critical evolution in therapeutic approaches (Little & Brown, 2014; Priori et al., 2013).

4.3 Deep brain stimulation and its effects on control functions

As the understanding of the underlying Parkinsonian disease mechanisms is advancing, the hope for disease-modifying treatments rises. But up to date, dopamine replacement therapy is the prevalent pharmaceutical option to treat the related motor impairments, by substituting for the dopaminergic loss in the substantia nigra (e.g., Olanow et al., 2009). Unfortunately, dopaminergic therapy is characterized by fluctuations in efficacy and can promote impulsive behaviors and compulsive use of medication (dopaminergic syndrome) (e.g., Cools, 2006).

Over the past 30 years and supported by recent technological advances, an additional therapeutic approach has gained primary attention, known as deep brain stimulation (DBS) (Lozano & Lipsman, 2013). After lesion surgeries of the STN had shown beneficial effects on Parkinsonian motor impairments, it was discovered that high-frequent electrical pulses

mimicked this lesion effect (Hariz & Blomstedt, 2022). Such chronically implanted DBS electrodes stimulate subcortical target structures, modulating their pathological activity to enhance motor control (Lozano et al., 2019) and allow for a substantial reduction of dopaminergic medication. Compared to a lesion, DBS can be safely applied bilaterally and adjusted postoperatively (Hariz & Blomstedt, 2022). During DBS surgery, bilateral lead electrodes are implanted into the target region, guided by preoperative magnetic resonance imaging and perioperative recordings of local brain activity. The leads are connected via subcutaneous cables to an implanted pulse generator that is placed within a collarbone pocket (Hariz & Blomstedt, 2022). Figure 4 provides a visual example of an implanted DBS device.

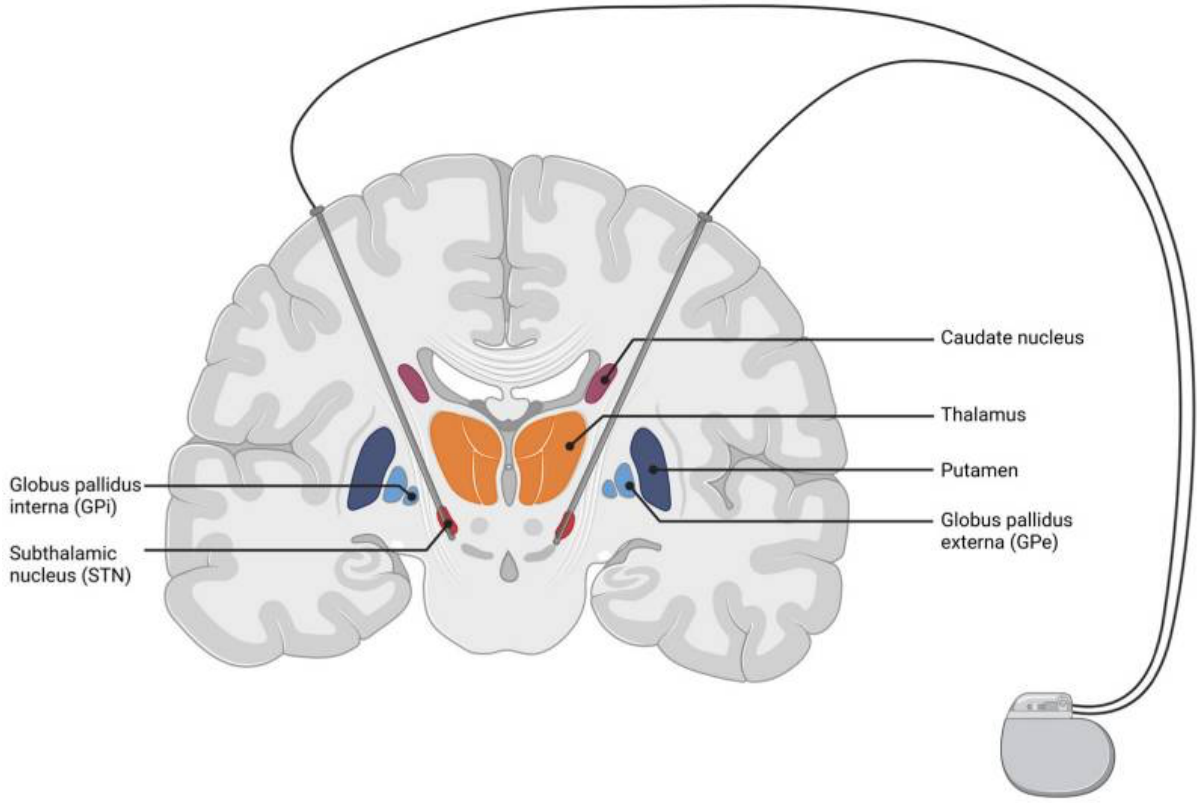

Fig. 4 Schematic illustration of a coronal cut of the human brain, depicting the main basal ganglia structures in color, with bilateral DBS electrodes targeting the STN (red). Electrodes are connected to the implanted pulse generator. (this figure is reproduced from Kricheldorff et al., 2022, and was published under an open access Creative Commons CC BY license (https://creativecommons.org/share-your-work/cclicenses/). The authors created the figure with the aid of biorender.com (accessed 1 February 2022))

The DBS mechanism of action is thought to be multi-fold and affect brain functions on various scales. On a cellular level, DBS modifies action potentials (Cameron et al., 2017), which can be influenced by cell-to-cell heterogeneity or stimulation direction (Balbinot et al., 2025). At the STN, recent evidence from mice optogenetic studies (Yoon et al., 2016; Yu et al., 2020) points to a far more nuanced DBS effect than merely "switching" STN function "ON" and "OFF". These studies have demonstrated that both driving as well as inhibiting STN function can affect Parkinsonian symptoms beneficially. Selective stimulation revealed that different cellular subtypes may fine-tune motor specifications, which extends the account of DBS and the STN substantially, could explain individual differences of efficacy and aid further refinement. On a circuit-level, DBS effects are mediated by temporospatial characteristics of functional brain circuits, which can determine whether intrinsic brain rhythms are either generated or disrupted (Balbinot et al., 2025). Primarily, its beneficial effect on motor control is ascribed to a substantial reduction of pathological beta-band activity (Kühn et al., 2006).

A novel approach to enhance stimulation selectivity is the aforementioned adaptive DBS, which considers symptom fluctuations and adjusts to real-time demands, thereby minimizing side effects and improving energy efficiency (e.g., Priori et al., 2013). Given the close correlation between the beta-band and Parkinson's disease symptoms (e.g., Neumann et al., 2016), adaptive DBS relies on beta oscillations as biomarkers for symptom fluctuations (e.g., Stanslaski et al., 2024).

Despite the apparent benefits of DBS over alternative therapeutic options, it cannot slow disease progression. Furthermore, there is generally no clear beneficial effect on symptoms such as cognitive decline (Fasano et al., 2010; Hariz & Blomstedt, 2022). Most importantly, while STN DBS can lead to marked improvements in motor function, these benefits may be accompanied by the onset of neuropsychiatric symptoms. This is related to the close anatomical and functional interconnectivity between motor, associative, and limbic domains that converge on the STN (e.g., Haynes & Haber, 2013). Through suppression of beta activity, DBS is thought to disrupt the pathological inhibition of thalamocortical drive, which shifts the balance towards disinhibition. While this facilitates deliberate motor initiation, it can concurrently impair the ability to withhold inappropriate or premature actions, thereby promoting impulsive and maladaptive behaviors (e.g., Frank et al., 2007; Witt et al., 2012).

Specifically, it was shown that DBS leads to maladaptive decision thresholds (Herz et al., 2018), favoring suboptimal choices during conflict tasks (e.g., Frank et al., 2007) or commission errors in response inhibition tasks, especially when wrong responses were highly prepotent (e.g., Georgiev et al., 2016). However, certain control functions may not be altered with DBS: people with Parkinson's disease have shown general impairments in cortico-spinal excitability suppression and related motor preparation, regardless of stimulation (Wilhelm et al., 2022, 2024).

Taken together, Parkinson's disease is a neurological disorder leading to impaired basal ganglia mechanisms and related control functions, most prominently motor control. Disease-related increases in fronto-subthalamic beta synchronization are counteracted by dopaminergic medication and DBS. However, this does not restore control per se, yet rather shifts the balance towards disinhibition (Hammond et al., 2007). It is crucial to dissect these pathological dynamics and their complex modulation by DBS to improve clinical care. Beyond this, studies in people with Parkinson's disease that receive STN DBS provide unique insights into STN function within fronto-subthalamic pathways, with valuable implications for control architecture in the healthy brain (e.g., Lozano et al., 2019; Lozano & Lipsman, 2013). In this regard, the novel response cueing/conflict task was also employed in people with Parkinson's disease receiving DBS of the STN (study presented in **Chapter 4**).

5. Methodological framework

This section introduces the neural measures of the study in **Chapter 3**, which used functional magnetic resonance imaging (fMRI), and the study in **Chapter 4**, which combined electroencephalogram (EEG) with local field potential (LFP) recordings.

5.1 Functional magnetic resonance imaging

The method behind fMRI is non-invasive and entails strong magnetic fields to manipulate the alignment of hydrogen nuclei in the body. Depending on the nuclei's state transitions, they emit signals that are detected and converted to characteristic tissue images (Huettel et al., 2004). Furthermore, neural activity increases blood flow and oxygenation, which

changes blood-related magnetic properties. This is captured as blood-oxygen-level-dependent (BOLD) signals, which allow researchers to infer cognitive processing across the brain with high spatial resolution (Huettel et al., 2004). Accordingly, brain regions can be related to specific functions and shared activity or interplays between different networks can be investigated (e.g., Davis & Poldrack, 2013). To this end, researchers commonly employ contrasts (e.g., incongruent vs. congruent conditions) to isolate functional activation related to a specific condition. Furthermore, conjunction analyses are used to identify regions reliably activated across multiple task demands, indicating shared engagement (Conjunction null hypothesis; Friston et al., 2005). In addition, interaction analyses such as analyses of variance (ANOVAs) are a means to investigate whether regional activation patterns in one condition are crucially modulated by another condition, revealing interdependent contributions. We employed these methodological tools to explore shared and distinct network activations relating to our novel response cueing/conflict task (**Chapter 3**).

5.2 Electrophysiological recordings

Electrophysiological brain signals, such as electroencephalogram (EEG) recordings and local field potentials (LFPs), capture neuronal currents with high temporal precision (e.g., Buzsáki et al., 2012). Scalp EEG provides a macroscopic view of cortical dynamics, while intracranial LFPs are recorded from depth electrodes and offer finer spatial resolution and access to subcortical structures. LFPs reflect the summed synaptic potentials in the electrode's vicinity, as for example of the STN when recording from DBS electrodes (Yin et al., 2021).

However, the collection of viable LFP recordings via DBS electrodes is a major challenge when investigating STN function (Thenaisie et al., 2021). While perioperative (intra- and postoperative recordings) recordings provide access to the STN, they suffer from the impact of surgery-related distress or sedatives on the task-related cognitive processes (Soh et al., 2025). Furthermore, perioperative settings do not allow for prolonged recordings with active stimulation, which are crucial when delineating the direct contribution of STN function to processes of interest (Soh et al., 2025).

Percept PC recordings (Medtronic, Inc.)

Recent technological advances introduced a novel LFP recording device that circumvents the described perioperative issues: the Percept PC and RC (Medtronic, Inc., Minneapolis, USA) are advanced sensing-enabled implanted pulse generators that allow for chronic recording of LFPs from DBS electrodes in outpatient settings (i.e., outside the perioperative setting; Yin et al., 2021). These devices enable continuous LFP monitoring and provide direct insight into subcortical activity during cognitive tasks under more generalizable conditions. LFPs are wirelessly transmitted from the implanted pulse generator via an external communicator to a clinician tablet. The "streaming" mode enables the recording of LFPs with both active and inactive stimulation, from two contacts surrounding the stimulation contact (Thenaisie et al., 2021).

Integrating these subcortical signals with simultaneous EEG recordings opens new avenues for investigating the time-sensitive cortico-subcortical interplay during experimental tasks (Soh et al., 2024). This technique has already yielded important findings for adaptive DBS protocols, and provided deeper insights into the role of basal ganglia structures in cognitive control (Feldmann et al., 2022; Oehrn et al., 2024; Soh et al., 2024).

The research potential of outpatient recordings with Percept (Medtronic, Inc.) is, however, compromised by missing digital task-event markers in these recordings, which reduces alignment precision with simultaneous EEG signals (Soh et al., 2025). "Power cycling", i.e., brief activation and inactivation of stimulation, stands out as the most practical and safe current synchronization method, without the need for further equipment. It induces a cascade of DBS artifacts that are visible in LFP and EEG channels (Soh et al., 2025). This method was used for LFP/EEG synchronization in the study presented in **Chapter 4**.

6. Research aims

The present thesis investigates two key aspects of response control - response reprogramming and conflict resolution - in a novel, integrated experimental framework to reveal their shared underlying control processes and dependence on expectations.

Specifically, we aimed to test whether simultaneous control demands produce a bottleneck effect, indicating limitations in processing capacities when mechanisms overlap.

To this end, we developed the novel response cueing/conflict task, which integrates response reprogramming and conflict resolution. We varied the frequency of these control demands, thereby modulating expectations (anticipatory control). This task was employed in three complementary studies, each offering a different perspective on the related control processes.

Chapter 2

Behavioral study in healthy participants (peer-reviewed publication)

Firstly, we employed the novel task in young, healthy participants (published in Sauter et al., 2024). The aim was to test whether expectation-dependent response reprogramming and conflict resolution interact at the behavioral level and produce a bottleneck effect. Since this study was the first to employ the task, it also served as a reference to validate the hypothesized effects in a healthy population.

Chapter 3

Functional imaging study in healthy participants (study description)

The same task was used in an fMRI setting with young, healthy participants, in order to identify shared neural activity underlying expectation-dependent response reprogramming and conflict resolution. We hypothesized to find control-related activations within the fronto-parietal and cingulo-opercular networks, and a bottleneck effect when reprogramming and conflict resolution coincided.

Chapter 4

Electrophysiological study in people with Parkinson's disease receiving DBS of the STN (manuscript in preparation)

Additionally, we employed the task in people with Parkinson's disease receiving DBS of the STN, focusing on control-related oscillations in the beta-band within fronto-subthalamic

pathways. Participants performed the task with active and inactive stimulation while we recorded cortical EEG and STN LFPs. Our goal was to investigate whether reprogramming and conflict resolution are modulated by shared, STN-dependent dynamics in the beta-band.

Together, these studies provide a comprehensive view on intersections between main response control processes, how they are modulated by anticipatory and reactive control, and how they are expressed behaviorally, neurally, and pathologically. By integrating these findings, this thesis contributes to a broader understanding of the core processes underlying response control. The theoretical implications will be reviewed in the **General Discussion**.

Chapter 2 contains a reprinted manuscript originally published in Sauter et al. (2024), *Experimental Brain Research*, under the Creative Commons Attribution 4.0 International License *(https://creativecommons.org/licenses/by/4.0)*

CHAPTER 2

Response and conflict expectations shape motor responses interactively

Annika E. Sauter[1,2,3,4], Adam Zabicki[1,4], Thomas Schüller[2,3], Juan Carlos Baldermann[2,5], Gereon R. Fink[1,2], Paola Mengotti[1], Simone Vossel[1,4]

[1] Cognitive Neuroscience, Institute of Neuroscience & Medicine (INM-3), Forschungszentrum Jülich, 52425 Jülich, Germany

[2] Department of Neurology, Faculty of Medicine and University Hospital Cologne, University of Cologne, 50937 Cologne, Germany

[3] Department of Psychiatry, Faculty of Medicine and University Hospital Cologne, University of Cologne, 50937 Cologne, Germany

[4] Department of Psychology, Faculty of Human Sciences, University of Cologne, 50923 Cologne, Germany

[5] Department of Psychiatry and Psychotherapy, Faculty of Medicine, Medical Center – University of Freiburg, 79104 Freiburg, Germany

Corresponding author

Annika E. Sauter

Cognitive Neuroscience, Institute of Neuroscience and Medicine (INM-3)

Forschungszentrum Jülich,

Leo-Brandt-Str. 5, 52425 Jülich, Germany

Phone: +49-2461-61-50326, fax: +49-2461-61-1518

Email: a.sauter@fz-juelich.de

ORCID ID: 0009-0007-8262-9775

Acknowledgments

The authors gratefully acknowledge support from the Deutsche Forschungsgemeinschaft (DFG, German Research Foundation) (Project-ID 431549029 - SFB 1451). Furthermore, we thank our colleagues from the Institute of Neuroscience and Medicine (INM-3) for their valuable support and discussions.

JCB is funded by the Else Kroener-Fresenius-Stiftung (2022_EKES.23).

Abstract

Efficient responses in dynamic environments rely on a combination of readiness and flexibility, regulated by anticipatory and online response control mechanisms. The latter are required when a motor response needs to be reprogrammed or when flanker stimuli induce response conflict and they are crucially modulated by anticipatory signals such as response and conflict expectations. The mutual influence and interplay of these control processes remain to be elucidated. Our behavioral study employed a novel combined response cueing/conflict task designed to test for interactive effects of response reprogramming and conflict resolution and their modulation by expectations. To this end, valid and invalid response cues were combined with congruent and incongruent target flankers. Expectations were modulated by systematically manipulating the proportions of valid versus invalid cues and congruent versus incongruent flanker stimuli in different task blocks. Reaction time and accuracy were assessed in thirty-one healthy volunteers. The results revealed response reprogramming and conflict resolution interactions for both behavioral measures, modulated by response and conflict expectations. Accuracy decreased disproportionally when invalidly cued targets with incongruent flankers were least expected. These findings support coordinated and partially overlapping anticipatory and online response control mechanisms within motor-cognitive networks.

Introduction

Our motor responses result from competitive advantages over alternative options, constantly updated to optimize behavior. This process is guided by preparing relevant motor responses and prioritizing the optimal response among alternatives (H. Brown et al., 2011; Cisek & Kalaska, 2010). An optimal response, however, is situational and subject to internal and external dynamics. A constant influx of information is concurrently transformed into viable response plans to accommodate these dynamics. Efficient responding involves balancing between readiness and flexibility based on current expectations. Readiness is promoted by anticipatory response control, allowing for adequate preparation. Complementarily, online control mechanisms enable flexibility during response execution, in case expectations are violated or distractions occur (Aron, 2011; H. Brown et al., 2011; Cisek & Kalaska, 2010).

The flexible online control can particularly be probed in two situations: First, in situations that require the suppression of the prepared response and the programming of an alternative (Mars, Piekema, et al., 2007). Second, in case of competing response representations that demand conflict resolution (Duque et al., 2013; Heekeren et al., 2008). Experimentally, response preparation and reprogramming have been assessed with response cueing tasks such as motor versions of the Posner attention task (Posner, 1980; Rosenbaum & Kornblum, 1982; Rushworth et al., 1997; 2001). In these tasks, probabilistic response cues induce motor preparation of the indicated response. Valid cues lead to faster responses with fewer errors, whereas invalid cues result in slower and more erroneous responses. These behavioral (reaction time (RT) or accuracy) differences between invalid and valid trials are termed the "validity effect". In the case of response conflict, similar response options compete for execution and require additional selection effort (Cisek & Kalaska, 2010). This situation can be created in an experimental setting by introducing irrelevant distractor stimuli associated with alternative responses, as in the Erikson flanker task (Eriksen & Eriksen, 1974). In the arrow version of this task, a central target arrow is "flanked" by peripheral distractor arrows with either congruent or incongruent directions. Behavioral differences between incongruent and congruent trial types are termed the "congruency effect".

Beyond online control, response reprogramming and conflict resolution are affected by anticipatory control mechanisms through expectations. In the cueing task, the frequency of

valid and invalid cues (i.e., the expectation that the cue will be valid in a given trial) modulates the validity effect through varying preparation strength and surprise, even when these probabilities are unknown and need to be inferred from trial-wise observations (Bestmann et al., 2008; H. Brown et al., 2011; Kuhns et al., 2017; Mengotti et al., 2020; Vossel et al., 2014). Bestmann and colleagues (2008) showed that RTs, as well as corticospinal excitability (CSE), covaried with information-theoretic measures of entropy (i.e., context-derived expectations) and surprise (i.e., how unexpected the event is within this context). Kuhns et al. (2017) observed that the size of the validity effect increases with an increasing probability of valid cues (i.e., when invalid trials are less expected). Similarly to the validity effect, expectations regarding conflict occurrence (i.e., the frequency of incongruent trials) influence the congruency effect, with increased error rates for infrequent incongruent trials (Derosiere et al., 2018; Duque et al., 2016; Logan, 1980). The exact mechanisms underlying the proportion congruency effect are still debated (Schmidt, 2013; Braem et al., 2019). Whereas it has initially been attributed to anticipatory conflict adaptation (Botvinick et al., 2001), alternative explanations involve modulations due to stimulus-response contingency or temporal learning. Still, conflict adaptation and lower-level learning processes may also go hand in hand (Braem et al., 2019), and it has been shown that the effect of varying congruency proportions can be described by formal volatility-based reinforcement learning schemes that predict control demands (Jiang et al., 2015), similar to the validity proportion effect in cueing tasks (Kuhns et al., 2017). It is currently unclear whether a common control mechanism coordinates online response reprogramming and conflict resolution and their modulation by expectations. Hence, by manipulating these factors within the same task, we wanted to test at which levels mutual influences (interactions) may occur. More generally, it has been proposed that dynamic response requirements align with a neural system that can operate in parallel processing streams (e.g., Cisek, 2007; Cisek & Kalaska, 2010). Rather than operating as a functionally designated and locally confined mechanism, response control may arise from the interactions among distributed subprocesses (Ridderinkhof et al., 2011).

In line with this view, a recent study found partially distinct but coordinated neural signatures of anticipatory and online control (Asanowicz et al., 2022). Hence, distributed neural subnetworks may encode the selection and specification of response plans (e.g., Crammond & Kalaska, 2000). An integral control mechanism may involve mutual inhibition and excitement

(Cisek, 2006), as well as neural interconnections across functional boundaries (Haber, 2003). Furthermore, it is well known that an intricate balance between inhibitory and disinhibitory forces in the basal ganglia loops shapes cortically-generated response programs. Cortical regions such as the anterior cingulate cortex (ACC) and fronto-parietal areas are robustly activated by interference tasks including the flanker task (Isherwood et al., 2021), and subcortico-cortical interplays may be relevant for coordinating response control subprocesses. In contrast to the effect of spatial attention cues on conflict processing, which has been investigated by numerous behavioral and neuroimaging studies using variants of the Attention Network Test (ANT; Fan et al., 2002), and for which interactive "bottleneck"-effects have been reported in the insula (Trautwein et al., 2016), studies on the interplay of response cues and flankers are scarce. Since pathological disturbances of these motor-cognitive subprocesses, e.g., in Parkinson's Disease, generate maladjusted response outcomes (e.g., Aron et al., 2016; Bonnevie & Zaghloul, 2019; Galea et al., 2012), a further understanding of the underlying control mechanisms and subprocesses is also relevant from a clinical perspective.

Previous studies have tested for a putative interaction between response cueing and conflict resolution in different ways, mainly using conflict tasks other than flanker tasks (e.g., Simon tasks: Proctor et al., 1992; Wascher and Wolber, 2004). Findings from Simon effect tasks have shown that valid response preparation can enlarge rather than reduce the Simon effect (e.g., Wascher & Wolber, 2004), suggesting that response preparation effects on conflict processing may be masked by additional stimulus-induced factors such as attention shifts.

A study by Wühr & Heuer (2017) aimed to shed more light on the counterintuitive findings regarding response cueing and the Simon effect. This study most closely resembles the current study design, since it employed a non-spatial response cueing and Flanker conflict paradigm in healthy participants and manipulated the frequency of valid and invalid cues to vary response expectations. Trials with incongruent and congruent flankers occurred with equal probability. The results showed that the flanker-induced congruency effect was eliminated in a condition with 100% valid cues (i.e., without response uncertainty). However, in a condition with 75% valid cues, the congruency effect was unaffected by valid or invalid response cues. This finding provides the first evidence for an interaction between the two response control processes induced by cue and flanker stimuli that may depend on response

expectations. However, since cues were 100% valid, response expectations were never violated in this condition. A follow-up study by Wühr et al. (2018) replicated the finding of decreased flanker interference (conflict) upon 100% valid response cues with a task modulation that ensured attentional processing of the target. Neither of the two studies (Wühr et al., 2018; Wühr & Heuer, 2017), however, tested the effect of expectations regarding conflict occurrence since incongruent trials occurred with the same frequency as congruent trials throughout the task.

The current study aimed to elucidate concurrent expectation-dependent response reprogramming and conflict resolution in a novel response cueing and conflict task. Specifically, the task combined valid and invalid motor response cues with congruent and incongruent target flankers, resulting in four trial types. The invalid-incongruent trial type combined reprogramming of the response after an invalid cue and resolving conflict from flanker interference. Furthermore, varying proportions of these trial types were presented in different blocks to manipulate response and conflict expectations. Based on previous work, we hypothesized to find validity and congruency effects that would be modulated by block-specific expectations. Notably, we asked whether response reprogramming and flanker-induced conflict interacted and further aimed to contextualize this interaction of online response control mechanisms with anticipatory control. This allowed us to assess multiple subprocesses of response control within the same task and to test for their potential non-additivity, comparable to the additive factors method (Sternberg, 1969; see also studies on the ANT for a similar procedure, e.g., Fan et al., 2002). While the exact conclusions drawn from interactive effects in the additive factors method are debated (e.g., Pieters, 1983; Stafford & Gurney, 2011), we assumed that a disproportionate performance decline under simultaneous demands (reprogramming and conflict resolution) - potentially amplified in case of strongly violated expectations - would provide a demonstration of a mutual influence of the different motor-cognitive control subprocesses in this task. This influence may be caused by a partial overlap between the control mechanisms or increased coordinatory demands.

Methods

Participants

Thirty-six young healthy participants were recruited for the study. Per inclusion criteria, participants were between the ages of 18-40, native speakers of German, unaffected by any neurological or psychiatric condition, right-handed (handedness was verified with the Edinburgh Handedness Inventory (EHI; mean (± SD) laterality quotient: 78.77 ± 14.64, ranging from 50 to 100; Oldfield, 1971), and not taking centrally-acting medication or drugs. All participants gave their written informed consent. The German Psychological Society's ethics committee approved the study performed following the Ethic's Code of the World Medical Association (Declaration of Helsinki).

Two participants were excluded after data collection due to exceedingly low accuracy scores (5.83% and 14.09%), suggesting they did not follow the instructions. The performance of three additional participants deviated more than two standard deviations from mean accuracy (91.37 ± 5.51% mean accuracy: lower accuracy limit at 80.34%), leading to their exclusion from further evaluations. Accordingly, data from 31 participants (mean age: 25.13 ± 5.27 years, ranging from 19 to 36 years; 13 female and 18 male) were considered for the analyses. The sample size was based on the behavioral study by Wühr and Heuer (2017), which employed a comparable response cueing/conflict task.

The Barratt Impulsiveness Scale (BIS-11; Patton et al., 1995) was assessed at the beginning of an experimental session and considered for the potential contribution of impulsiveness to individual differences in task performance (Harrison et al., 2009; Landau et al., 2012).

Experimental set-up

The task was presented on a 47.39 cm x 29.62 cm computer screen while participants sat 94 cm away on a comfortable chair. Left and right index fingers were resting on adjacent response pad keys (response pad "RB-830" by cedrus®). Participants positioned their heads on a chin rest during the experiment, individually adjusted to a suitable height. A camera

monitored the participants inside the experiment booth to capture any behavior that might have affected task performance.

Eye-tracking

An EyeLink® 1000 eye-tracker was used to record eye movements during the experiment (sampling rate: 1000 Hz) to control for central fixation. Either left eye or right eye movements were recorded. The eye-tracker was calibrated before the training and before the main task. Participants were instructed to fixate on the screen's center during a trial. Eye-tracking data that were distorted by glasses/contact lenses or movement (data of nine participants in total) were considered unreliable and thus not included in the analysis.

Task

The paradigm was based on the motor version of a Posner-type cueing task (Posner, 1980; M. F. S. Rushworth et al., 1997) and the arrow version of the Erikson flanker task (Eriksen & Eriksen, 1974). Combining these two tasks allowed us to assess motor preparation and reprogramming, response conflict, and their modulation by expectations. The paradigm was programmed with the Presentation® software (Version 18.0, Neurobehavioral Systems, Inc., Berkeley, CA).

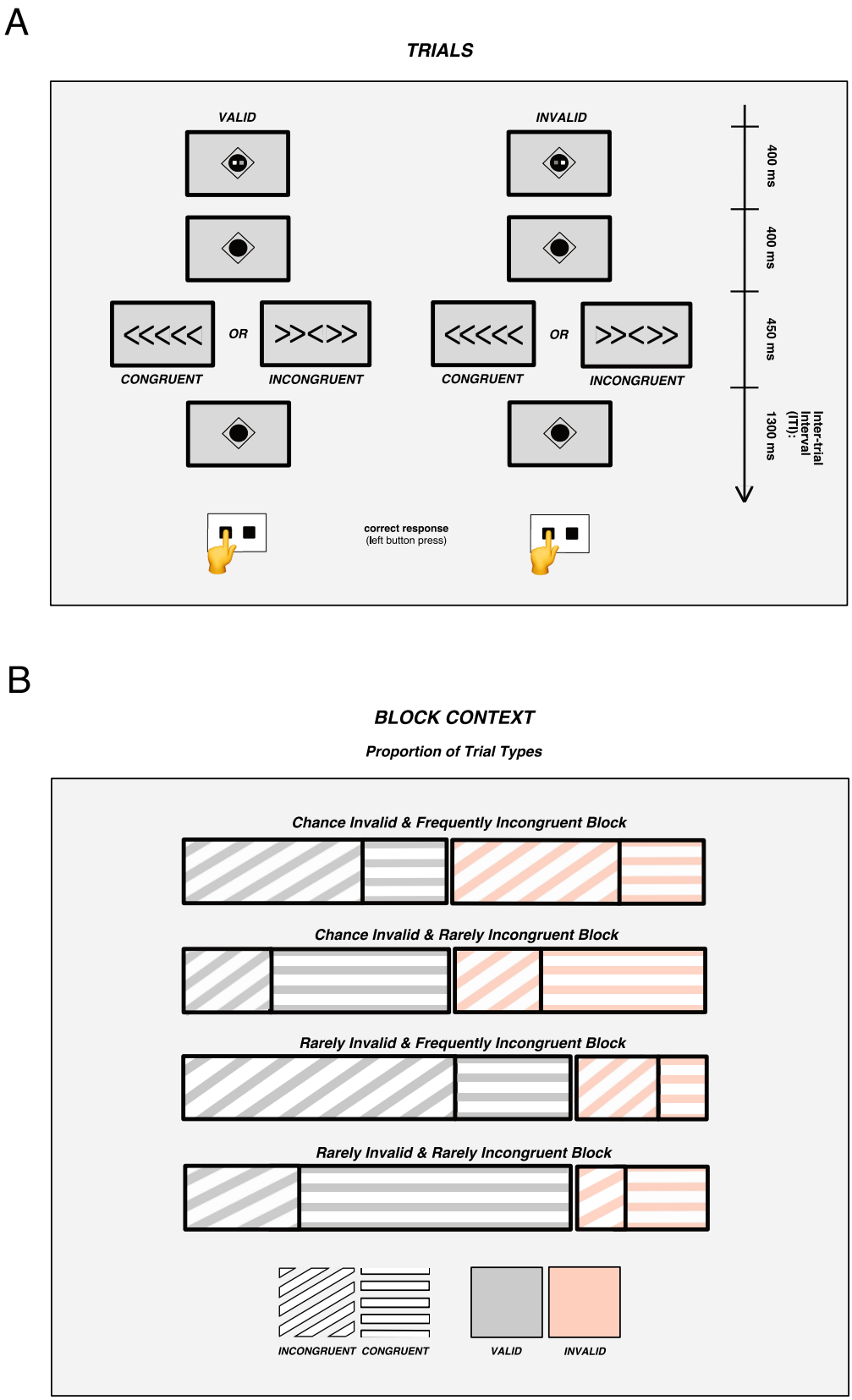

Fig. 1 Schematic illustration of the response cueing/conflict paradigm.

(A) Trials: The motor response cues are displayed in the first row. The white square indicated the probable response to the upcoming target (button press with left/right index finger). The target (third row) was shown after a fixation

interval (second row). A left/right central target arrow required a left/right-hand button press (left-hand press demanded in this example). In valid trials, the target required the cued response. In invalid trials, the target required the alternative response, i.e., response reprogramming. The central target arrows were presented with either congruent or incongruent peripheral flanker arrows

(B) Block context: Four block types were realized by manipulating the proportions of valid to invalid and congruent to incongruent trials. Each block type was presented thrice in a fixed pseudorandomized order

Trial structure

At the start of each trial, a motor response cue was presented for 400 ms (Figure 1A; cue dimension: 2 degrees visual angle). The cue depicted the two response keys (left and right square), of which the white key (square) denoted the upcoming response side. In valid trials, the cue indicated the response to the target correctly, while it displayed the incorrect (alternative) response in invalid trials. After the cue, a fixation point ("diamond") appeared for 400 ms, followed by the target, displayed for 450 ms. The target was a chevron-type arrow in the center of the screen, pointing either to the left or right, thereby demanding a response with the left or right index finger. Two peripheral distractor arrows were displayed on each side of the central target arrow (dimension of one arrow: 1.25 degrees; total stimulus length: 6.61 degrees; arrow spacing: 0.09 degrees). The distractor arrows pointed uniformly either in the same direction as the target (congruent trial) or in the opposite direction (incongruent trial). Following the target presentation, the fixation point reappeared in the inter-trial interval that lasted for 1300 ms, during which responses were still registered. In total, a trial lasted for 2550 ms. Each block contained eight null trials, which showed only the fixation point. These trials lasted for 1700 ms and were used to jitter the inter-trial interval.

Block structure

Main experiment

Varying proportions of valid to invalid and congruent to incongruent trials were employed in different blocks to manipulate expectations regarding the upcoming trial type (Figure 1B). Each block was presented thrice in a pseudorandom order, which was identical for all participants. In addition, the trial sequence within each block was pseudorandom and identical for all participants (but different for the different block repetitions). This is a standard procedure in studies using computational modeling of stimulus probabilities or contingencies

to ensure comparable learning processes (e.g., Iglesias et al., 2013), which we considered an additional analysis option for this study. Blocks of the same type did not follow each other consecutively. Please refer to Supplementary Figure SF5 for a schematic display of the block sequence.

Regarding validity proportions, valid and invalid trials occurred at chance level (50% valid trials, i.e., validity proportion) in half of the blocks. In these blocks, there was maximal uncertainty about the required motor response. In contrast, in the remaining blocks, most trials were valid (77% validity proportion), thereby reducing the uncertainty about the motor response to the target. This manipulation was similar to previous studies in which the validity proportion varied between 50% and 90% (e.g., Kuhns et al., 2017), allowing for a comparison of conditions with different levels of uncertainty about the upcoming motor response.

Concerning congruency proportions, congruent trials were more likely than incongruent trials (70% congruent trials, i.e., congruency proportion) in half of the blocks, while this relation was reversed in the other half of blocks (30% congruency proportion). These congruency proportions were similar to those realized by Derosiere et al. (2018) and Duque et al. (2016).

Combining the different validity and congruency proportions systematically resulted in four unique block types (Figure 1B). Each block type was repeated thrice, resulting in 12 blocks of 70 trials each (approximate overall duration: 35 minutes). Self-paced breaks separated the blocks of the main experiment. The four unique trial types (valid/invalid cue and congruent/incongruent target) within the four unique block types generated a total of 16 distinct conditions, thereby amounting to a 2 (*validity*: valid/invalid) x 2 (*congruency*: congruent/incongruent) x 2 (*validity proportion*: rarely invalid [77% validity proportion]/chance invalid [50% validity proportion]) x 2 (*congruency proportion*: rarely incongruent [70% congruency proportion]/frequently incongruent [30% congruency proportion]) factorial design. Within each condition, left- and right-hand responses were distributed evenly.

Before the start of each block, participants were presented with information on screen as to whether the upcoming block would contain mainly incongruent or congruent trials (to adhere to the Derosiere et al. (2018) and Duque et al. (2016) implementation of congruency

proportions). No information about the validity proportion was provided (to follow the Kuhns et al. (2017) approach to implementing validity proportions).

Training

Before the main experiment, participants performed a training session with three blocks of 40 trials each (approximately 5 minutes overall), separated by self-paced breaks between blocks. The first two blocks of the training showed only the central arrow without distractor arrows to accustom the participants to the general speed and sequence of events. The first block comprised mostly valid trials (80% validity proportion), while the second block used an equal proportion of valid and invalid trials (50% validity proportion). The third block introduced the flanking distractor arrows next to the target and mainly contained valid trials (80% validity proportion) and congruent/incongruent trials at chance level (50% congruency proportion). The training trials appeared in a pseudorandomized and fixed order within a block, with no null trials. As in the main task, left- and right-hand responses were evenly distributed within each condition.

Data analysis

Behavioral data

Only trials with correct responses were considered for RT analyses. Anticipatory responses (faster than 100 ms) were discarded. Regarding accuracy scores, missed trials and trials with an incorrect response were treated as erroneous trials. Missed responses amounted on average to 6.40 ± 12.25%.

Our aim was firstly to investigate the main effects of a trial's validity and congruency as well as their potential interaction, and secondly, whether and how block-wise expectations modulated these trial-level effects. For this, each participant's condition-specific mean RTs and accuracy scores were analyzed with separate 2 (*validity*: valid/invalid) x 2 (*congruency*: congruent/incongruent) x 2 (*validity proportion*: rarely invalid [77% validity proportion]/chance invalid [50% validity proportion]) x 2 (*congruency proportion*: rarely incongruent [70% congruency proportion]/frequently incongruent [30% congruency proportion]) repeated-measures (RM) ANOVAs. Additionally, we repeated these analyses with each participant's

inverse efficiency (RTs divided by accuracy) to account for differential accuracies between conditions with a compound measure (Snodgrass et al., 1985) (see Supplementary Material). Given the tendency of accuracy results to display skewness, we additionally used the non-parametric Wilcoxon signed-rank test to compare the congruency effect (accuracy incongruent trials minus congruent trials) between conditions, further supporting our accuracy findings.

We expected to find significant main effects of validity and congruency, reflecting the well-described behavioral costs after invalid cues and incongruent flankers. Moreover, we expected significant *validity x validity proportion* and *congruency x congruency proportion* interactions, reflecting the expectation-dependent modulation of response reprogramming and conflict resolution reported previously (e.g., Kuhns et al. 2017; Duque et al. 2016). We then checked for an interaction effect reflecting an interplay between the respective response control processes in dependency of expectations. We confirmed in an additional analysis that our results of interest would not change when considering only RTs within 3 standard deviations of the individual mean RT (i.e. when discarding trials with outlier RT) (cf. Supplementary Table ST2; the only deviation was a significant two-way interaction of *validity proportion* and *congruency proportion*, which, however, was not relevant for our hypotheses, which focused on interaction effects between these block-level and the trial-level factors).

A potential influence of impulsivity on the outcome parameters, assessed with the Barratt Impulsiveness Scale (BIS-11), was tested with additional RM-ANOVAs that included the BIS-11 score as a covariate. The total score and the motor impulsivity sub-score were evaluated in this way to test for associations with individual task performance.

Analyses were carried out with MATLAB (The MathWorks Inc. (2022). MATLAB version: 9.13.0 (R2022a), Natick, Massachusetts: The MathWorks Inc. https://www.mathworks.com) and JASP (JASP Team (2023). JASP (Version 0.17.1)).

Eye-tracking data

We conducted an eye-tracking analysis to confirm that participants fixated in the center of the display and refrained from making eye movements in the direction of the motor response cues. Pupil coordinates of the right or left eye were analyzed throughout the trial

period from cue onset until the end of the target presentation to ensure central fixation. A circle with a diameter of twice the cue dimension (2 degrees to each side) was defined as a region of interest for valid central fixation during this period. Cumulative valid fixation points were expressed as a percentage for each trial and averaged across trials for each participant, of which a grand average over all participants was determined.

The eye-tracking data was analyzed with MATLAB (The MathWorks Inc. (2022). MATLAB version: 9.13.0 (R2022a), Natick, Massachusetts: The MathWorks Inc. https://www.mathworks.com).

Results

Eye-tracking data

The analysis of eye-tracking coordinates confirmed a central fixation throughout the cue-target period within a region-of-interest of 2° to each side 92.33 ± 6.15% (ranging from 76.70% to 99.88%) of the time as an average over all participants with valid eye-tracking data (only data without distortion by movements or glasses/contact lenses: 22 out of 31 participants). Hence, participants attended sufficiently to the region-of-interest during a trial.

Reaction Time

Validity and Congruency Effects at Trial-Level

The RM-ANOVA on RTs revealed significant main effects of *validity* ($F_{(1,30)}$ = 37.68, p < .001, η_p^2 = 0.56) and *congruency* ($F_{(1,30)}$ = 737.88, p < .001, η_p^2 = 0.96). Invalid cues lead to increased RTs (423.27 ± 40.97 ms) as compared to valid cues (396.64 ± 33.93 ms), and incongruent flankers evoked increased RTs (447.66 ± 39.52 ms) in contrast to congruent flankers (372.25 ± 33.09 ms). Furthermore, *validity* and *congruency* interacted significantly at the trial level ($F_{(1,30)}$ = 7.51, p = .01, η_p^2 = 0.20), with larger congruency effects for valid (79.48 ± 16.51 ms) than invalid trials (71.34 ± 18.51 ms). This effect was mainly driven by faster responses to targets with congruent flankers in validly (as opposed to invalidly) cued trials (valid-

congruent: 356.90 ± 32.09 ms; valid-incongruent: 436.38 ± 37.53 ms; invalid-congruent: 387.60 ± 39.02 ms; invalid-incongruent: 458.94 ± 44.79 ms) (see Figure 2).

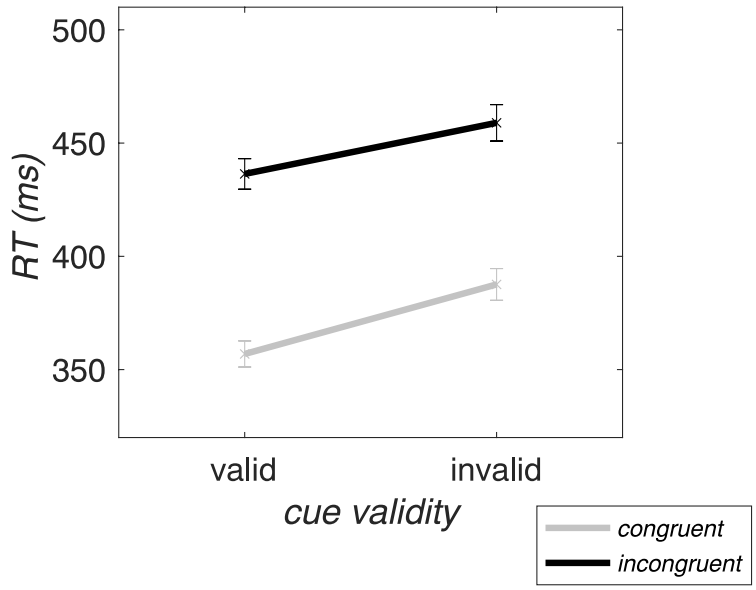

Fig. 2 Trial-wise RTs averaged over all block types. The congruency effect is visible as the RT difference (distance) between congruent (gray) and incongruent (black) lines. On the x-axis, the validity effect is reflected in the slope of the lines between valid and invalid trial RTs. The error bars depict the standard error of the mean

Validity and Congruency Effects at Block-Level

Considering the impact of block-specific trial proportions (expectations) in the ANOVA revealed that RTs were significantly shaped by validity and congruency proportions. More specifically, the two-way *validity x validity proportion* ($F_{(1,30)}$ = 21.84, p < .001, η_p^2 = 0.42) and *congruency x congruency proportion* ($F_{(1,30)}$ = 82.20, p < .001, η_p^2 = 0.73) interactions reached significance. As expected, the validity effect increased with a higher validity proportion (when invalid trials were less expected: 33.17 ± 29.14 ms at 77% validity proportion) compared to the chance level (20.09 ± 20.96 ms at 50% validity proportion). Likewise, the congruency effect was enhanced with a higher congruency proportion (when incongruent trials were less expected: 86.76 ± 18.24 ms at 70% congruency proportion), in contrast to a context of frequent incongruent trials (64.06 ± 15.57 ms at 30% congruency proportion). Next to this, the highest-order effects that reached significance were two significant three-way interactions: *validity x congruency x congruency proportion* ($F_{(1,30)}$ = 6.20, p < .05, η_p^2 = 0.17) as well as *validity x congruency x validity proportion* ($F_{(1,30)}$ = 10.89, p < .01, η_p^2 = 0.27). These interactions reflected

modulations of the *validity-by-congruency* interaction by expectations about the motor response and conflict occurrence and are described below in more detail. The four-way interaction was not significant. A complete list of effects that resulted from the RM-ANOVA at inter- and intra-trial- and block levels is provided in Supplementary Table ST1.

Response Expectation-dependent Modulation of the Validity Effect by Congruency

A closer look at the three-way interaction of *validity*, *congruency*, and *validity proportion* revealed that for congruent trials (no flanker-induced conflict), RTs were slower for invalid trials when they were rare (77% validity proportion; 393.14 ± 41.61 ms) than when they occurred at chance level (50% validity proportion; 382.07 ± 37.82 ms). In a complementary manner, valid cueing induced faster RTs (352.28 ± 29.40 ms) within rarely invalid blocks, compared to chance invalid blocks (361.52 ± 35.41 ms) in congruent trials. Therefore, without conflict by incongruent flankers, the RT validity effect (difference between invalid and valid trial RTs) increased as expected when invalid trials were rare. In contrast, in incongruent trials (conflict present), in which RTs were generally higher, the modulation by validity proportion was attenuated (i.e., varying response expectations; see Figure 3).

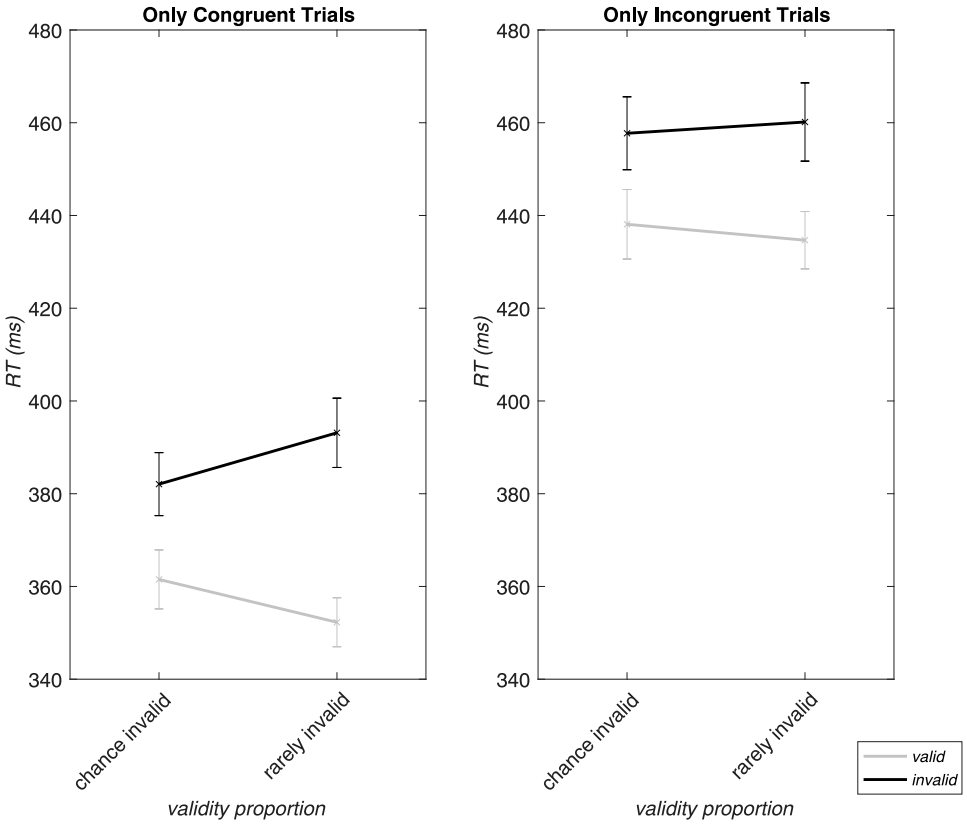

Fig. 3 Modulation of the RTs in invalid and valid trials (i.e., the validity effect) by response expectations (validity proportion), separated by trial congruency. This figure visualizes the three-way interaction for RTs of validity, congruency, and validity proportion. Line graphs show differences between chance (50% validity proportion) and rarely invalid (77% validity proportion) block types for valid (grey lines) and invalid (black lines) trials. The error bars show standard errors of the mean

Conflict Expectation-dependent Modulation of the Congruency Effect by Validity

As indicated by the three-way interaction of *validity*, *congruency*, and *congruency proportion*, the modulation of the congruency effect (RT incongruent minus RT congruent trials) was dependent on the validity of a trial. While the congruency effect was, as expected, generally larger in the context of rare incongruent trials (70% congruency proportion) compared to frequent incongruent trials (30% congruency proportion), the effect was further enhanced when a trial was also valid as compared to invalid (i.e., when response expectations were not violated; Figure 4).

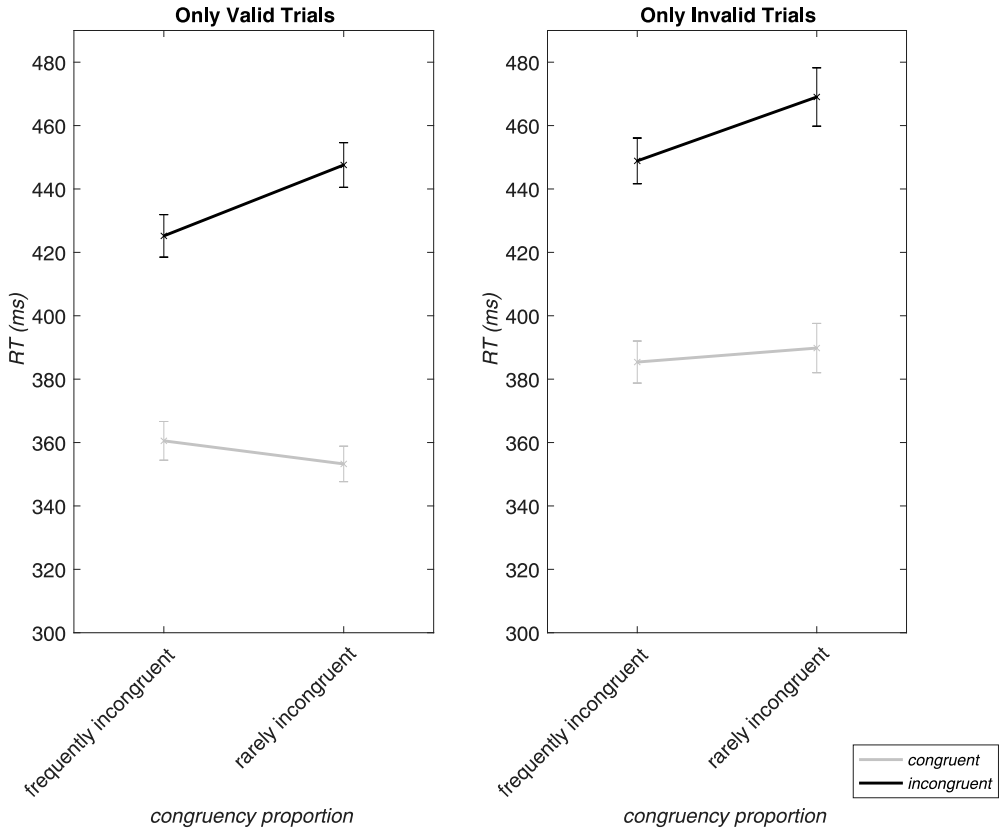

Fig. 4 Modulation of the RTs in incongruent and congruent trials (i.e., the congruency effect) by conflict expectations (congruency proportion) for valid and invalid trials. The x-axis depicts frequently incongruent (30% congruency proportion) and rarely incongruent (70% congruency proportion) block types with mean RTs for congruent (grey lines) as well as incongruent (black lines) trials. Error bars display the standard errors of the mean. This figure depicts the three-way interaction for RTs of validity, congruency, and congruency proportion

Figure 5 summarizes the congruency effects in the different blocks. A summary figure and table with data for all conditions are provided in the Supplementary Material (Supplementary Figure SF4 and Table ST3).

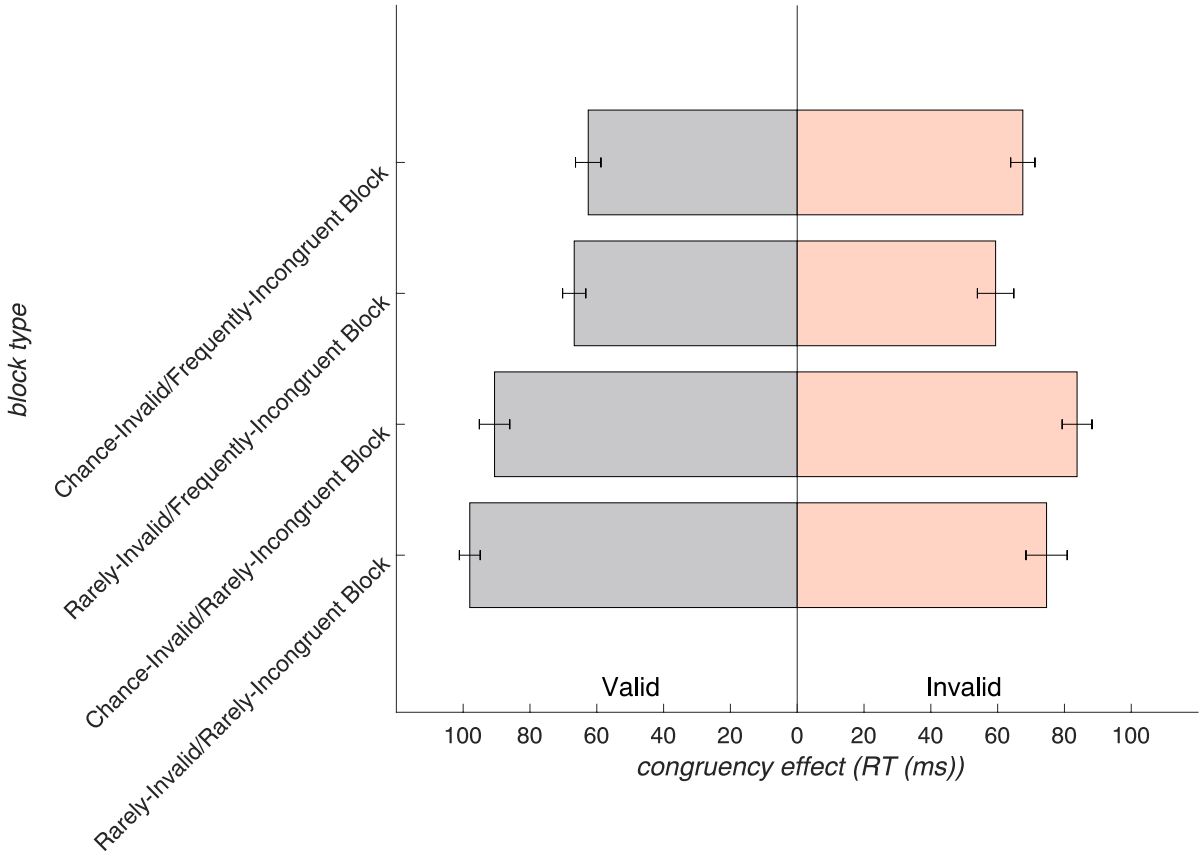

Fig. 5 The congruency effect (RT incongruent trials – congruent trials) is shown for each block type (y-axis), separated by valid (gray bars) and invalid (orange bars) trials on the x-axis. For valid trials, the rarely-incongruent blocks clearly show the expected larger congruency effect compared to the frequently-incongruent blocks, which is also larger than in the invalid rarely-incongruent blocks. Error bars depict the standard error of the mean

Accuracy

Validity and Congruency Effects at Trial-Level

As for the ANOVA on RTs, the RM-ANOVA on accuracy yielded significant main effects of *validity* ($F_{(1,30)} = 21.24$, $p < .001$, $\eta_p^2 = 0.41$) and *congruency* ($F_{(1,30)} = 108.53$, $p < .001$, $\eta_p^2 = 0.78$), with lower accuracy in invalid (88.80 ± 8.14%) than valid (93.94 ± 3.72%) and in incongruent (84.60 ± 8.84%) than congruent (98.14 ± 2.97%) trials. Again, as for RTs, the trial-level interaction between *validity* and *congruency* was significant ($F_{(1,30)} = 22.48$, $p < .001$, $\eta_p^2 = 0.43$). However, in contrast to RTs, it manifested in larger congruency effects for invalid (16.90 ± 9.98%) than valid trials (10.19 ± 6.01%) (Figure 6).

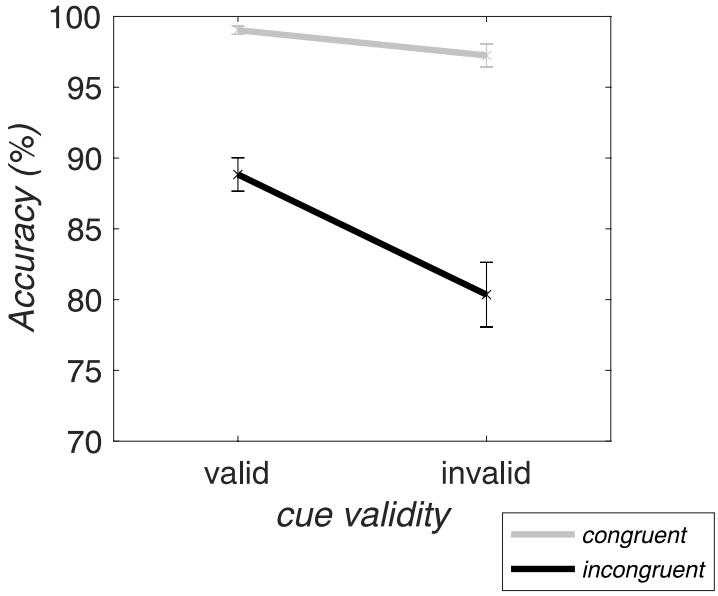

Fig. 6 Accuracy on trial-level, averaged over all block types. The difference between the congruent (gray) and incongruent (black) lines shows the congruency effect, which is larger for invalid than valid trials. The validity effect is visible as the slope of the lines between valid and invalid trials (on the x-axis). Error bars indicate the standard error of the mean

Validity and Congruency Effects at Block-Level

Block-level effects contributed to a significant four-way interaction in the RM-ANOVA ($F_{(1,30)} = 7.11$, $p < .05$, $\eta_p^2 = 0.19$). Additionally, every lower-order effect was significant, except for the three-way interaction of *validity x congruency x validity proportion*. A complete RM-ANOVA table for accuracy effects is presented in Supplementary Table ST1. Repeating this analysis with inverse efficiency scores revealed similar effects (see Supplementary Material).

The significant four-way interaction became most apparent within the incongruent trials, where the distinctively lowest accuracy was observed for invalid-incongruent trials in the context of strongly violated expectations for both response and conflict (rare invalid [77% validity proportion]/rare incongruent [70% congruency proportion] blocks, see Figure 7). This finding reflects that the trial- and block-specific effects on accuracy were not additive but disproportionally enhanced in this condition (68.28 ± 21.56% accuracy; post-hoc paired samples t-tests against all other conditions were significant (all $p < .001$) when applying Bonferroni correction). Additionally, due to the skewness of accuracy measures, we applied non-parametric Wilcoxon signed-rank tests to compare the congruency effect of this condition against those of the remaining seven conditions (Figure 7). These comparisons

revealed significant differences after Bonferroni correction (all $p < 0.05$), affirming our findings obtained with parametric tests.

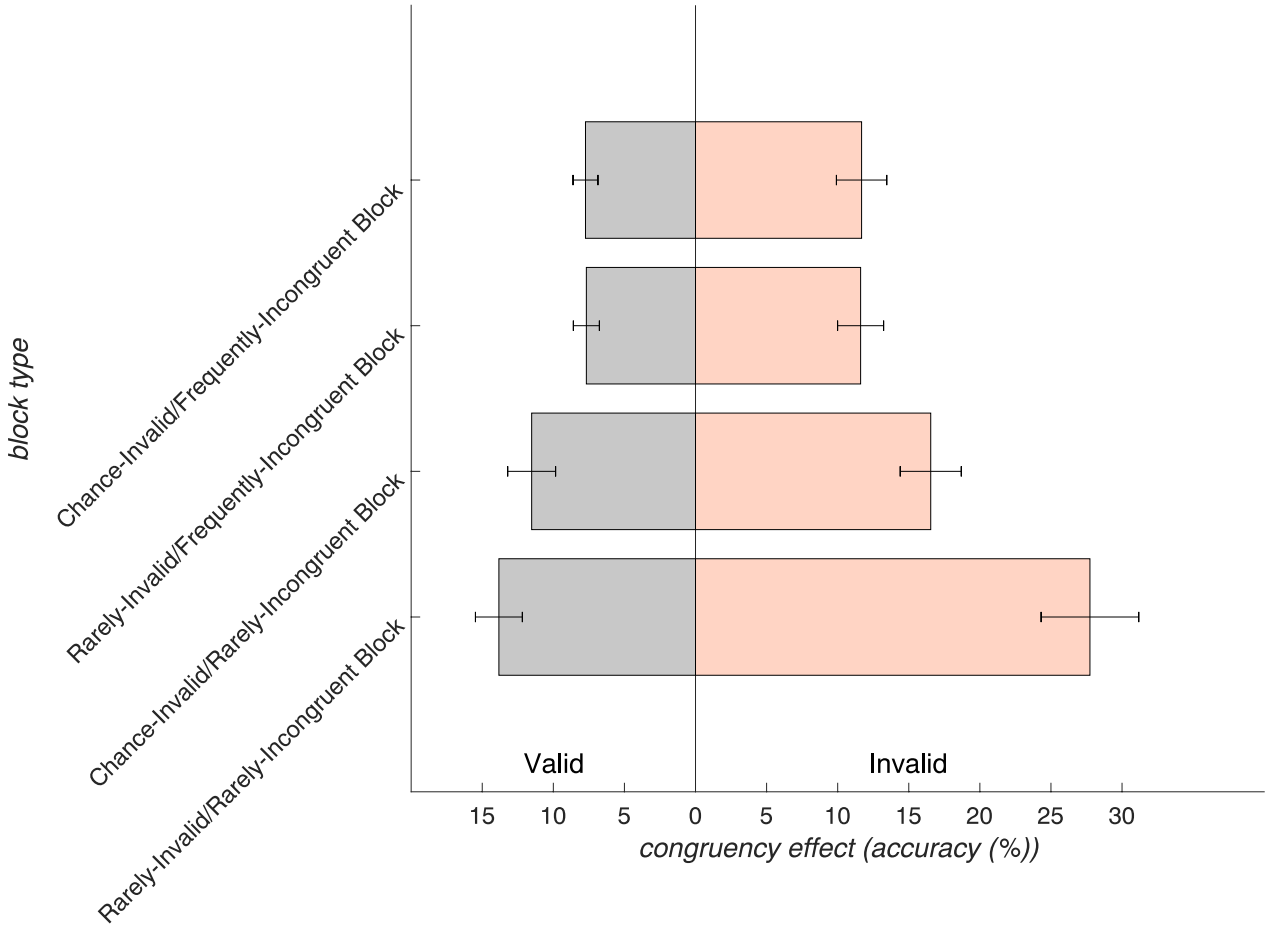

Fig. 7 Congruency effects (accuracy incongruent trials – congruent trials) for each block type (y-axis), divided by valid (gray bars) and invalid (orange bars) trials on the x-axis. This visualizes the disproportionate increase of the congruency effect within invalid trials for the rarely-invalid/rarely-incongruent block. The error bars show standard errors of the mean

BIS-11 Score

The mean (±SD) BIS-11 total score amounted to 57.58 ± 5.99, and the motor impulsivity sub-score to 13.26 ± 2.00. The RM-ANOVAs on RTs, accuracy, and inverse efficiency that included either BIS-11 score as a covariate did not reveal any significant effects (all $p > 0.1$) of those impulsivity measures on the response control processes assessed in our paradigm.

Discussion

This study employed a novel response cueing/conflict paradigm that assessed expectancy-dependent response reprogramming and conflict resolution, along with their behavioral interactions in RTs and accuracy. Previous studies have employed motor response cues to induce response preparation and reported lower performance for invalid rather than valid cueing conditions. The current study observed this validity effect for both behavioral outcomes. Similarly, peripheral arrows that are presented together with a target stimulus have been shown to decrease performance when incongruent (i.e., associated with an alternative motor response) rather than congruent to the target. Again, we replicated this congruency effect for RTs and accuracy. Moreover, in both measures, our findings revealed significant interactions between validity and congruency effects.

Consistent with related studies (Derosiere et al., 2018; Duque et al., 2016; Kuhns et al., 2017), we observed that the magnitude of the validity effect was dependent on the expectations of invalid cues, while the size of the congruency effect was influenced by expectations regarding incongruent stimuli. These effects were evident in both RTs and accuracy. Consequently, the varying frequencies of trial types in different blocks influenced both online response reprogramming and conflict resolution, potentially through anticipatory control mechanisms. Specifically, as reported in Kuhns et al. (2017), the reprogramming of a prepared response was slower and more often unsuccessful when invalid trials were less frequent and thus less expected. In contrast, stronger motor preparation due to predictive cues facilitated response execution in valid trials. Similarly, less frequent and thus less expected incongruent trials amplified the congruency effect (as in, e.g., Duque et al., 2016).
Our data extend these findings by showing interactions between validity and congruency at the trial-level, and higher-level interactions with expectancy-dependent modulations. Validity-by-congruency interactions were present for RT and accuracy, with different conditions driving the interactions. Whereas the congruency effect in accuracy was enhanced via a reduction of accuracy with invalid cueing in incongruent trials, the congruency effect in RTs was enhanced via facilitation by valid cues in congruent trials. This latter effect bears similarity to findings from the Simon effect (e.g., Wascher & Wolber, 2004). Hence, although our data show a robust main effect of validity on both RTs and accuracy, preparation processes for a response and for

stimuli processing cannot be unequivocally disentangled here, as the cue is indicative of both response type and stimulus appearance. Therefore, it cannot be ruled out that the validity effect in our study reflects additional factors beyond response preparation. Still, our finding aligns with previous studies investigating expectation-dependent response preparation with response cues that have been shown to rely on other mechanisms than feature or spatial cueing (Kuhns et al., 2017).

Moreover, for RTs and accuracy, the expectancy-dependent modulations of validity and congruency effects were interdependent, i.e., the validity effect modulation depended on the congruency of the target display and the congruency effect modulation depended on the validity of the cue. The four-way interaction among all factors was not significant for RTs, but for accuracy. This was driven by a disproportionate (more-than-additive) decrease in performance when a strong expectation about an imminent response was violated, and the target was unexpectedly combined with incongruent flanker stimuli (invalid-incongruent trials in rarely-invalid/rarely-incongruent blocks). Notably, this effect could not merely be attributed to the rare occurrence (i.e., general surprise) of this trial type: Since the task also comprised a block with reversed congruency proportions, the number of trials with rare invalid cues and rare incongruent flankers was identical to the number of trials with rare invalid cues and rare congruent flankers (see Figure 1B), where this performance decrement was not observed. Instead, the interaction effect presumably resulted from simultaneous demands for online control of response reprogramming and conflict resolution, in particular when unexpected. This may be attributed to partially shared mechanisms of the different online control subprocesses leading to mutual interference, or to a bottleneck in coordinatory processes. While the anticipatory conflict adaptation account of the proportion congruency effect is debated (e.g., Braem et al., 2019), the validity proportion effects more directly reflect cue-induced preparatory response control. Our finding that both manipulations interactively shape accuracy in invalid-incongruent trials may point to similar or converging anticipatory mechanisms. These could be characterized in future neuroimaging or electrophysiological studies with the present task.

Relating these results to other cueing/conflict paradigms in the literature, the combined response cueing/flanker task used by Wühr and Heuer (2017) is most comparable

to the present study. In contrast to their results, the present study found significant interactions between validity and congruency despite using probabilistic cues that were valid in 50% or 77% (not 100%) of the trials. Differences in the stimuli and study design may account for these discrepancies. Notably, the study by Wühr and Heuer (2017) used letters as flankers, whereas the present study used arrows, which may elicit more automatic and, thus, more robust response activation (Ridderinkhof et al., 2021), potentially promoting an interaction between the cued response and target congruency in our task. Furthermore, Wühr & Heuer (2017) did not manipulate conflict expectations, and manipulated the validity proportion in different experiments with different groups of participants.

One could speculate that differences between RTs and accuracy in the present study may be due to strategies prioritizing speed over accuracy, resulting in increased errors without the corresponding change in RTs. Along these lines, Draheim et al. (2021) found that the RT measures alone may inadequately represent performance in flanker and Stroop tasks due to individual speed-accuracy trade-offs. The studies by Duque et al. (2016) and Derosiere et al. (2018) employed similar manipulations of block-wise congruency proportions. Analyses regarding the directionality of the interaction effect revealed that the two studies obtained the same pattern of results for accuracy, while their findings differed for RTs. More specifically, the interaction was driven by the difference in RTs in incongruent trials in Duque et al. (2016) and by the RT difference in congruent trials in Derosiere et al. (2018). Concerning accuracy, however, both studies found that the incongruent trials in the rarely incongruent context were more prone to errors.

While studies that manipulate motor preparation and conflict resolution within the same task are scarce, similar interactions between validity and congruency effects have been extensively studied in the attention domain. For instance, the Attention Network Test (ANT; Fan et al., 2002) assesses the functions of three partially independent attention networks: alerting, spatial orienting, and executive attention (conflict resolution of incongruent flankers). In the revised ANT task (ANT-R; Fan et al., 2009), invalid cues were introduced alongside predictive valid cues. The results revealed uncorrelated behavioral scores (Fan et al., 2002) and differential involvement of specific brain networks (Fan, Kolster, et al., 2007) and brain oscillatory patterns (Fan, Byrne, et al., 2007) for each of the attentional subdomains. Nonetheless, the subdomains also seem to draw on partially shared resources. When

contrasting orienting (spatial and temporal information) and alerting (temporal information only) cues, it was found that alerting cues increased the congruency effect, while orienting cues interacted positively with the executive domain by reducing the congruency effect when the target location was validly cued (Fan et al., 2009) and modulated congruency-related activation in the insula (Trautwein et al., 2016). At the neural level, the anterior cingulate cortex (ACC), a crucial structure for conflict processing (Matsumoto & Tanaka, 2004; Pochon et al., 2008), may also be involved in uncertainty processing (Behrens et al., 2007) of cues containing alerting (i.e., no spatial) information, thereby increasing the processing load. This relates to the potential underlying neural processes associated with our behavioral effects, as the ACC might be activated by uncertainty during response reprogramming after violated expectations and by conflict processing required by an incongruent target (the invalid-incongruent condition in our task). Supporting this, Kuhns et al. (2017) reported increased ACC (and left parietal) activation in an fMRI study when invalid motor cues were more unexpected. In the current motor response cueing/conflict task, a shared reliance on specific cingulo-opercular and fronto-parietal structures may potentially account for the pronounced decrease in performance observed in our rare invalid-incongruent condition. Moreover, neurons in the primary motor cortex, onto which all modulatory signals converge, could also contribute to a shared reliance.

Future studies could employ the present task to test whether shared network activations, putatively involving the ACC, underlie the behavioral interactions of unexpected response reprogramming and conflict resolution reported in this study. In a clinical setting, this task could be employed in patients with impaired cortico-basal ganglia-thalamo-cortical (CBGTC) pathways to provide a more profound understanding of the common structure behind motor-cognitive response control mechanisms and their neural underpinnings.

Conclusion

The current study explored the interplay between anticipatory and online response control mechanisms, revealing a behavioral interaction between expectation-dependent response reprogramming and conflict resolution. These results suggest coordinated and

partially overlapping anticipatory and online response control mechanisms within motor-cognitive networks.

Data Availability Statement

The behavioral and eye-tracking data files and the relevant code used for analyses (MATLAB) will all be made available on the online GIN repository G-Node (https://gin.g-node.org/asauter/2023_Sauter_ResponseControl (last accessed: 20.07.2023)).

Author Contributions

Conceptualization: S.V., P.M., J.C.B., T.S., A.E.S. and G.R.F.; Data Analysis: A.E.S., S.V., P.M.; Data collection: A.E.S.; Project administration: S.V.; Writing - original draft: A.E.S.; Writing - review & editing: A.E.S., S.V., P.M., T.S., J.C.B., A.Z. and G.R.F. All authors have read and agreed to the published version of the manuscript.

Conflict of Interest

The authors have no competing interests to declare.

References

Aron, A. R. (2011). From Reactive to Proactive and Selective Control: Developing a Richer Model for Stopping Inappropriate Responses. Biological Psychiatry, 69(12), e55–e68. https://doi.org/10.1016/j.biopsych.2010.07.024

Aron, A. R., Herz, D. M., Brown, P., Forstmann, B. U., & Zaghloul, K. (2016). Frontosubthalamic Circuits for Control of Action and Cognition. The Journal of Neuroscience, 36(45), 11489–11495. https://doi.org/10.1523/JNEUROSCI.2348-16.2016

Asanowicz, D., Kotlewska, I., & Panek, B. (2022). Neural Underpinnings of Proactive and Preemptive Adjustments of Action Control. Journal of Cognitive Neuroscience, 34(9), 1590–1615. https://doi.org/10.1162/jocn_a_01884

Behrens, T. E. J., Woolrich, M. W., Walton, M. E., & Rushworth, M. F. S. (2007). Learning the value of information in an uncertain world. Nature Neuroscience, 10(9), 1214–1221. https://doi.org/10.1038/nn1954

Bestmann, S., Harrison, L. M., Blankenburg, F., Mars, R. B., Haggard, P., Friston, K. J., & Rothwell, J. C. (2008). Influence of Uncertainty and Surprise on Human Corticospinal Excitability during Preparation for Action. Current Biology, 18(10), 775–780. https://doi.org/10.1016/j.cub.2008.04.051

Bonnevie, T., & Zaghloul, K. A. (2019). The Subthalamic Nucleus: Unravelling New Roles and Mechanisms in the Control of Action. The Neuroscientist, 25(1), 48–64. https://doi.org/10.1177/1073858418763594

Botvinick, M. M., Braver, T. S., Barch, D. M., Carter, C. S., & Cohen, J. D. (2001). Conflict monitoring and cognitive control. Psychological Review, 108(3), 624–652. https://doi.org/10.1037/0033-295X.108.3.624

Braem, S., Bugg, J. M., Schmidt, J. R., Crump, M. J. C., Weissman, D. H., Notebaert, W., & Egner, T. (2019). Measuring Adaptive Control in Conflict Tasks. Trends in Cognitive Sciences, 23(9), 769–783. https://doi.org/10.1016/j.tics.2019.07.002

Brown, H., Friston, K., & Bestmann, S. (2011). Active inference, attention, and motor preparation. Frontiers in Psychology, 2(SEP), 1–10. https://doi.org/10.3389/fpsyg.2011.00218

Cisek, P. (2006). Preparing for Speed. Focus on "Preparatory Activity in Premotor and Motor Cortex Reflects the Speed of the Upcoming Reach". Journal of Neurophysiology, 96(6), 2842–2843. https://doi.org/10.1152/jn.00857.2006

Cisek, P. (2007). Cortical mechanisms of action selection: The affordance competition hypothesis. Philosophical Transactions of the Royal Society B: Biological Sciences, 362(1485), 1585–1599. https://doi.org/10.1098/rstb.2007.2054

Cisek, P., & Kalaska, J. F. (2010). Neural Mechanisms for Interacting with a World Full of Action Choices. Annual Review of Neuroscience, 33(1), 269–298. https://doi.org/10.1146/annurev.neuro.051508.135409

Crammond, D. J., & Kalaska, J. F. (2000). Prior Information in Motor and Premotor Cortex: Activity During the Delay Period and Effect on Pre-Movement Activity. Journal of Neurophysiology, 84(2), 986–1005. https://doi.org/10.1152/jn.2000.84.2.986

Derosiere, G., Klein, P.-A., Nozaradan, S., Zénon, A., Mouraux, A., & Duque, J. (2018). Visuomotor Correlates of Conflict Expectation in the Context of Motor Decisions. The Journal of Neuroscience, 38(44), 9486–9504. https://doi.org/10.1523/JNEUROSCI.0623-18.2018

Draheim, C., Tsukahara, J. S., Martin, J. D., Mashburn, C. A., & Engle, R. W. (2021). A toolbox approach to improving the measurement of attention control. Journal of Experimental Psychology: General, 150(2), 242–275. https://doi.org/10.1037/xge0000783

Duque, J., Olivier, E., & Rushworth, M. (2013). Top–Down Inhibitory Control Exerted by the Medial Frontal Cortex during Action Selection under Conflict. Journal of Cognitive Neuroscience, 25(10), 1634–1648. https://doi.org/10.1162/jocn_a_00421

Duque, J., Petitjean, C., & Swinnen, S. P. (2016). Effect of Aging on Motor Inhibition during Action Preparation under Sensory Conflict. Frontiers in Aging Neuroscience, 8. https://doi.org/10.3389/fnagi.2016.00322

Eriksen, B. A., & Eriksen, C. W. (1974). Effects of noise letters upon the identification of a target letter in a nonsearch task. Perception & Psychophysics, 16(1), 143–149. https://doi.org/10.3758/BF03203267

Eriksen, C. W., & Schultz, D. W. (1979). Information processing in visual search: A continuous flow conception and experimental results. Perception & Psychophysics, 25(4), 249–263. https://doi.org/10.3758/BF03198804

Fan, J., Byrne, J., Worden, M. S., Guise, K. G., McCandliss, B. D., Fossella, J., & Posner, M. I. (2007). The Relation of Brain Oscillations to Attentional Networks. Journal of Neuroscience, 27(23), 6197–6206. https://doi.org/10.1523/JNEUROSCI.1833-07.2007

Fan, J., Gu, X., Guise, K. G., Liu, X., Fossella, J., Wang, H., & Posner, M. I. (2009). Testing the behavioral interaction and integration of attentional networks. Brain and Cognition, 70(2), 209–220. https://doi.org/10.1016/j.bandc.2009.02.002

Fan, J., Kolster, R., Ghajar, J., Suh, M., Knight, R. T., Sarkar, R., & McCandliss, B. D. (2007). Response Anticipation and Response Conflict: An Event-Related Potential and Functional Magnetic Resonance Imaging Study. Journal of Neuroscience, 27(9), 2272–2282. https://doi.org/10.1523/JNEUROSCI.3470-06.2007

Fan, J., McCandliss, B. D., Sommer, T., Raz, A., & Posner, M. I. (2002). Testing the Efficiency and Independence of Attentional Networks. Journal of Cognitive Neuroscience, 14(3), 340–347. https://doi.org/10.1162/089892902317361886

Galea, J. M., Bestmann, S., Beigi, M., Jahanshahi, M., & Rothwell, J. C. (2012). Action reprogramming in Parkinson's disease: Response to prediction error is modulated by levels of dopamine. Journal of Neuroscience, 32(2), 542–550. https://doi.org/10.1523/JNEUROSCI.3621-11.2012

Haber, S. N. (2003). The primate basal ganglia: Parallel and integrative networks. Journal of Chemical Neuroanatomy, 26(4), 317–330. https://doi.org/10.1016/j.jchemneu.2003.10.003

Harrison, E. L. R., Coppola, S., & McKee, S. A. (2009). Nicotine deprivation and trait impulsivity affect smokers' performance on cognitive tasks of inhibition and attention. Experimental and Clinical Psychopharmacology, 17(2), 91–98. https://doi.org/10.1037/a0015657

Heekeren, H. R., Marrett, S., & Ungerleider, L. G. (2008). The neural systems that mediate human perceptual decision making. Nature Reviews Neuroscience, 9(6), 467–479. https://doi.org/10.1038/nrn2374

Iglesias, S., Mathys, C., Brodersen, K. H., Kasper, L., Piccirelli, M., DenOuden, H. E. M., & Stephan, K. E. (2013). Hierarchical Prediction Errors in Midbrain and Basal Forebrain during Sensory Learning. Neuron, 80(2), 519–530. https://doi.org/10.1016/j.neuron.2013.09.009

Isherwood, S. J. S., Keuken, M. C., Bazin, P. L., & Forstmann, B. U. (2021). Cortical and subcortical contributions to interference resolution and inhibition – An fMRI ALE meta-analysis. Neuroscience & Biobehavioral Reviews, 129, 245–260. https://doi.org/10.1016/j.neubiorev.2021.07.021

JASP Team. (2023). JASP (Version 0.16.2) [Computer software]. JASP. https://jasp-stats.org/

Jiang, J., Beck, J., Heller, K., & Egner, T. (2015). An insula-frontostriatal network mediates flexible cognitive control by adaptively predicting changing control demands. Nature Communications, 6(1), 8165. https://doi.org/10.1038/ncomms9165

Kuhns, A. B., Dombert, P. L., Mengotti, P., Fink, G. R., & Vossel, S. (2017). Spatial Attention, Motor Intention, and Bayesian Cue Predictability in the Human Brain. Journal of Neuroscience, 37(21), 5334–5344. https://doi.org/10.1523/JNEUROSCI.3255-16.2017

Landau, A. N., Elwan, D., Holtz, S., & Prinzmetal, W. (2012). Voluntary and involuntary attention vary as a function of impulsivity. Psychonomic Bulletin & Review, 19(3), 405–411. https://doi.org/10.3758/s13423-012-0240-z

Logan, G. D. (1980). Attention and automaticity in Stroop and priming tasks: Theory and data. Cognitive Psychology, 12(4), 523–553. https://doi.org/10.1016/0010-0285(80)90019-5

MathWorks. (2022). MATLAB (Version R2022a) [Computer software]. https://www.mathworks.com/.

Mars, R. B., Piekema, C., Coles, M. G. H., Hulstijn, W., & Toni, I. (2007). On the programming and reprogramming of actions. Cerebral Cortex, 17(12), 2972–2979. https://doi.org/10.1093/cercor/bhm022

Matsumoto, K., & Tanaka, K. (2004). Conflict and Cognitive Control. Science, 303(5660), 969–970. https://doi.org/10.1126/science.1094733

Mengotti, P., Kuhns, A. B., Fink, G. R., & Vossel, S. (2020). Age-related changes in Bayesian belief updating during attentional deployment and motor intention. Psychological Research, 84(5), Article 5. https://doi.org/10.1007/s00426-019-01154-w

Oldfield, R. C. (1971). The assessment and analysis of handedness: The Edinburgh inventory. Neuropsychologia, 9(1), 97–113. https://doi.org/10.1016/0028-3932(71)90067-4

Patton, J. H., Stanford, M. S., & Barratt, E. S. (1995). Factor structure of the Barratt impulsiveness scale. Journal of Clinical Psychology, 51(6), 768–774. https://doi.org/10.1002/1097-4679(199511)51:6<768::aid-jclp2270510607>3.0.co;2-1

Pieters, J. P. (1983). Sternberg's additive factor method and underlying psychological processes: Some theoretical considerations. Psychological Bulletin, 93(3), 411–426. https://doi.org/10.1037/0033-2909.93.3.411

Pochon, J.-B., Riis, J., Sanfey, A. G., Nystrom, L. E., & Cohen, J. D. (2008). Functional Imaging of Decision Conflict. The Journal of Neuroscience, 28(13), 3468–3473. https://doi.org/10.1523/JNEUROSCI.4195-07.2008

Posner, M. I. (1980). Orienting of Attention. Quarterly Journal of Experimental Psychology, 32(1), 3–25. https://doi.org/10.1080/00335558008248231

Proctor, R. W., Lu, C.-H., & Van Zandt, T. (1992). Enhancement of the Simon effect by response precuing. Acta Psychologica, 81(1), 53–74. https://doi.org/10.1016/0001-6918(92)90011-2

Richard Ridderinkhof, K., Forstmann, B. U., Wylie, S. A., Burle, B., & van den Wildenberg, W. P. M. (2011). Neurocognitive mechanisms of action control: Resisting the call of the Sirens. WIREs Cognitive Science, 2(2), 174–192. https://doi.org/10.1002/wcs.99

Ridderinkhof, K. R., Wylie, S. A., van den Wildenberg, W. P. M., Bashore, T. R., & van der Molen, M. W. (2021). The arrow of time: Advancing insights into action control from the arrow version of the Eriksen flanker task. Attention, Perception, & Psychophysics, 83(2), 700–721. https://doi.org/10.3758/s13414-020-02167-z

Rushworth, M. F. S., Nixon, P. D., Renowden, S., Wade, D. T., & Passingham, R. E. (1997). The left parietal cortex and motor attention. Neuropsychologia, 35(9), 1261–1273.

Schmidt, J. R. (2013). Questioning conflict adaptation: Proportion congruent and Gratton effects reconsidered. Psychonomic Bulletin & Review, 20(4), 615–630. https://doi.org/10.3758/s13423-012-0373-0

Snodgrass, J. G., Townsend, J. T., & Ashby, F. G. (1985). Stochastic Modeling of Elementary Psychological Processes. The American Journal of Psychology, 98(3), 480. https://doi.org/10.2307/1422636

Stafford, T., & Gurney, K. N. (2011). Additive Factors Do Not Imply Discrete Processing Stages: A Worked Example Using Models of the Stroop Task. Frontiers in Psychology, 2. https://doi.org/10.3389/fpsyg.2011.00287

Sternberg, S. (1969). The discovery of processing stages: Extensions of Donders' method. Acta Psychologica, 30, 276–315. https://doi.org/10.1016/0001-6918(69)90055-9

Trautwein, F.-M., Singer, T., & Kanske, P. (2016). Stimulus-Driven Reorienting Impairs Executive Control of Attention: Evidence for a Common Bottleneck in Anterior Insula. Cerebral Cortex, 26(11), 4136–4147. https://doi.org/10.1093/cercor/bhw225

Vossel, S., Mathys, C., Daunizeau, J., Bauer, M., Driver, J., Friston, K. J., & Stephan, K. E. (2014). Spatial Attention, Precision, and Bayesian Inference: A Study of Saccadic Response Speed. Cerebral Cortex, 24(6), 1436–1450. https://doi.org/10.1093/cercor/bhs418

Wascher, E., & Wolber, M. (2004). Attentional and intentional cueing in a Simon task: An EEG-based approach. Psychological Research, 68(1), 18–30. https://doi.org/10.1007/s00426-002-0128-z

Wühr, P., Frings, C., & Heuer, H. (2018). Response Preparation With Reliable Cues Decreases Response Competition in the Flanker Task. Experimental Psychology, 65(5), 286–296. https://doi.org/10.1027/1618-3169/a000411

Wühr, P., & Heuer, H. (2017). Response Preparation, Response Conflict, and the Effects of Irrelevant Flanker Stimuli. Advances in Cognitive Psychology, 13(1), 70–82. https://doi.org/10.5709/acp-0208-3

CHAPTER 3

Response cueing and conflict in an fMRI Study: methods and preliminary results

The following sections provide an outline of the fMRI study's methods and preliminary results for reference. These results will be reviewed more thoroughly in the **General Discussion**. The purpose of this study was to investigate shared and interacting cortical networks underlying response reprogramming and conflict resolution.

1. Methods

1.1 Participants

Thirty healthy participants gave their written informed consent to participate in this study. They were between 18 and 40 years old, right-handed (confirmed with the Edinburgh Handedness Inventory; EHI; Oldfield, 1971), unaffected by any neuropsychiatric disorders or centrally-acting medication, and safe to go into the 3 Tesla MRI scanner (e.g., no metal implants). Subsequent to data collection, we had to exclude three participants whose accuracy deviated more than two standard deviations from the mean across participants (accuracy below 68.08%). Furthermore, one participant was excluded whose frame-wise head displacement during scanning exceeded the threshold of 2 mm translation and 2 degree rotation. Therefore, the final dataset included behavioral and imaging data of 26 participants (mean age: 28 years, ranging from 19 to 35 years; 13 female and 13 male). The study was conducted in ethical compliance with the Declaration of Helsinki and approved by the German Psychological Society (22.06.22).

1.2 Procedure

Prior to performing the experiment in the MRI, participants completed questionnaires regarding MRI safety, inclusion criteria, right-handedness (EHI) and impulsivity (Barratt

Impulsiveness Scale 11 (BIS-11); Patton et al., 2011). The BIS-11 was, however, not considered for the preliminary analysis presented here. Subsequently, participants received task instructions and completed a short training session (~ 5 min.) outside the scanner to get accustomed to the pace and requirements of the task.

The main experiment was performed in a 3 Tesla (3T) Prisma MRI scanner, in which the task was displayed on a computer screen at 264 cm distance from the participants. The screen was visible to the participants as a reflection in the mirror of a 64-channel head coil. Responses were given with left- and right index fingers, resting on the respective keys of the MRI-suitable response box. An EyeLink® 1000 eye-tracker recorded the participant's pupil coordinates during the task to ensure they attended the central task stimuli.

Before starting the main task, the eye-tracker was calibrated. Subsequently, the task was presented on-screen with a total duration of approximately 40 min. (including 11 breaks of 30 sec. that separated the task blocks). Task-related brain activity was registered with T2*-weighted EPI (echo-planar imaging) images and BOLD contrast, using a Center for Magnetic Resonance Research (CMRR) multi-band EPI sequence (multi-band factor 8; repetition time of 0.8 sec.; echo time of 37 ms; https://www.cmrr.umn.edu/multiband/). Overall, 3'052 EPI volumes were collected with anterior-to-posterior phase encoding, complemented by additional 10 EPI volumes with posterior-to-anterior phase encoding, in order to support distortion correction. Each EPI volume comprised 72 axial slices. After completing the main task, participants underwent a T1-weighted structural scan (~ 7 min.; sequence: MPRAGE; sagittal slices: 208; voxel size: 0.9 mm^3; 2500 ms repetition time; 2.22 ms echo time; field of view of 256 mm). Altogether, participants were in the scanner for around 60 minutes. The participation was compensated with 15 Euros per hour.

1.3 Task design

This study employed the novel response cueing/conflict task from Sauter et al. (2024), which was only adjusted with regard to the breaks between task blocks and the block sequence. While the design in Sauter et al. (2024) entailed self-paced breaks (participants decided individually when to continue), the blocks in this MRI-suitable version were separated by fixed breaks of 30 sec., signaled with a countdown presented on screen. Additionally, we employed the same block sequence as in Sauter et al. (2024) in half of the participants, while the remaining participants were presented with a different sequence (also pseudorandomized; depicted in Supplementary Fig. SF1, Appendix). With this adjustment, we aimed to counterbalance any effects relating to the chronological block order. For further task details, we refer to the description in Sauter et al. (2024), which is presented in **Chapter 2**.

Towards the end of the data collection, an error was detected that occurred while the task was adjusted for the MRI presentation. This resulted in the incorrect presentation of the block information regarding conflict frequency in half of the blocks. More specifically, information was presented just prior to a block to let the participant know about the frequency of conflict in the upcoming trials (following Derosiere et al., 2018), thus shaping their expectations and potentially control strategies. However, due to the error, participants were consistently told that blocks would primarily contain congruent trials (i.e., that conflict would be infrequent, thus unexpected). This was incorrect for half of the blocks, in which incongruent trials were actually more frequent than congruent trials. A comparative analysis between the data of Sauter et al. (2024), where instructions were always accurate, and the behavioral data of this MRI study, confirmed that this change of prior information affected the congruency effect. To circumvent this issue, we restricted the analyses to blocks in which the instructions were correct and matched the actual conflict frequency (i.e., the ones with unexpected (infrequent) conflict) in this fMRI study. Accordingly, the factor of conflict expectation did not vary in the analyzed data and was not included as a predictor. Despite the reduced dataset, the main behavioral results of interest remained largely consistent with Sauter et al. (2024).

1.4 Data analysis

Behavior

Our behavioral analysis was adapted from Sauter et al. (2024), with the only exception that the factor of congruency proportion was not considered, as only blocks with high congruency proportion (unexpected conflict) were included in the final dataset.

The primary aim was to test for main effects of validity (response reprogramming) and congruency (conflict resolution), as well as their interaction. Moreover, we explored whether these effects were further modulated by varying response expectation (*validity proportion*). Accordingly, we calculated repeated-measures ANOVAs for RTs and accuracy with the following within-subject factors: *validity* (valid vs. invalid), *congruency* (congruent vs. incongruent), and *validity proportion* (unexpected reprogramming [77% validity proportion] vs. chance expectation [50% validity proportion]).

Our RT analyses included correct trials that were above 100 ms (no anticipatory responses). Accuracy was calculated as the percentage of correct trials (> 100 ms) per condition. Incorrect button presses and missed responses (no response) were equally treated as incorrect trials.

Even though the analyses were performed without the factor of congruency proportion, we hypothesized to replicate the significant main effects of validity and congruency and a *validity-by-congruency* interaction that was observed in our behavioral study for both RTs and accuracy, employing the same task (Sauter et al., 2024). Furthermore, we expected to again find a significant interaction between *validity* and *validity proportion*, indicating that expectations modulate response reprogramming (Kuhns et al., 2017; Sauter et al., 2024). We also examined a three-way interaction reflecting disproportionate performance decrements when unexpected reprogramming was demanded simultaneously with conflict resolution. This would align with the bottleneck for elevated control demands that was observed in Sauter et al. (2024) and reflected in disproportionate error increases when both unexpected control demands (reprogramming and conflict resolution) coincided.

The behavioral analyses were performed using MATLAB (The MathWorks Inc., 2022, Version 9.13.0 R2022a, Natick, MA) and JASP (JASP Team, 2023, Version 0.17.1 (behavior) and Version 0.19.1 (imaging-related)).

Imaging

All imaging data were processed and analyzed using the SPM12 software (Wellcome Department of Imaging Neuroscience, London; Friston et al., 1995; http://www.fil.ion.ucl.ac.uk/spm). The first six volumes were discarded during preprocessing to prevent T1 equilibration effects, resulting in 3'046 task-based fMRI volumes for analysis. Functional images were realigned to each participant's mean EPI image, corrected for geometric distortions using the HySCO module in the ACID toolbox (http://www.diffusiontools.org/), and bias-field corrected. Next to that, the T1-weighted structural scan was skull-stripped, co-registered to the mean EPI volume, and segmented to estimate deformation fields. The latter were then applied to normalize all images to Montreal Neurological Institute (MNI) space with a voxel resolution of 2 mm^3. Subsequently, normalized functional images were smoothed using an 8 mm full-width at half-maximum Gaussian kernel.

General Linear Model (GLM) analyses were performed, modeling the eight trial conditions of interest along with regressors that accounted for incorrect trials, pauses, and head motion parameters at the single-subject level. Subject-specific contrast images were computed for each condition and entered into second-level group analyses.

At the group level, random effects analyses were conducted using the 2 × 2 x 2 factorial design of the behavioral ANOVA: *validity* (valid vs. invalid) x *congruency* (congruent vs. incongruent) x *validity proportion* (unexpected reprogramming [77% validity proportion] vs. chance expectation [50% validity proportion]).

Validity (invalid minus valid) and congruency (incongruent minus congruent) effects were firstly analyzed in separate, planned t-contrasts to identify the individual activations related to reprogramming and conflict, respectively. Moreover, planned t-tests were used to test for interaction effects between all factors.

In order to find network regions that were reliably engaged for both reprogramming and conflict resolution, we conducted a conjunction analysis on the common activity between the validity and congruency contrasts (Conjunction null hypothesis; Friston et al., 2005).

All second-level analyses applied a voxel-wise statistical threshold of $p < .001$. Cluster-level Family-Wise Error (FWE) correction was used to control for multiple comparisons, and results were considered significant at a corrected cluster-level threshold of $p < .05$.

Since no significant interaction effects were observed at the whole-brain level, more sensitive region-of-interest (ROI) analyses were performed. For the identification of these regions, a Global null hypothesis analysis was conducted, testing for areas that showed either validity or congruency effects (Friston et al., 2005). To localize peak coordinates in the two networks of interest (i.e., the cingulo-opercular and fronto-parietal network), a significance threshold of $p < .00001$ and an extent threshold of 10 voxels was employed. Parameter estimates for peaks in the two networks were extracted and analyzed with separate 2 × 2 x 2 ANOVAs with the factors *validity* (valid vs. invalid) x *congruency* (congruent vs. incongruent) x *validity proportion* (unexpected reprogramming [77% validity proportion] vs. chance expectation [50% validity proportion]).

Anatomical localization of activation peaks relied on maximum probability maps from the Anatomy Toolbox (Eickhoff et al., 2005) for mapped regions to assign each peak voxel to the most probable brain region.

2. Results

2.1 Behavior

Reaction time

The repeated-measures ANOVA on RTs revealed the expected main effects of *validity* ($F_{(1,25)} = 52.11$, $p < .001$, $\eta p^2 = 0.68$) and *congruency* ($F_{(1,25)} = 298.52$, $p < .001$, $\eta p^2 = 0.92$), reflecting the expected RT costs of reprogramming and conflict resolution. Different from our previous study (Sauter et al., 2024), there was no *validity-by-congruency* interaction in RTs.

Regarding the influence of response expectations, we found the hypothesized increase of the validity effect when reprogramming was unexpected (77% validity proportion), reflected in a significant *validity-by-validity proportion* interaction ($F_{(1,25)} = 11.55$, $p < .01$, $\eta p^2 = 0.32$).

Accuracy

The repeated-measures ANOVA on accuracy yielded main effects of *validity* ($F_{(1,25)} = 18.82$, $p < .001$, $\eta p^2 = 0.43$) and *congruency* ($F_{(1,25)} = 54.91$, $p < .001$, $\eta p^2 = 0.69$), as expected from previous results (Sauter et al., 2024) for error-related reprogramming and conflict costs, and as reported for RTs. In contrast to RTs, but in line with Sauter et al. (2024), the *validity-by-congruency* interaction was significant for accuracy ($F_{(1,25)} = 9.84$, $p < .01$, $\eta p^2 = 0.28$).

Response expectations shaped the validity effect similarly to RTs, by eliciting larger effects in blocks with rare invalid trials (77% validity proportion; i.e., unexpected reprogramming). This was represented as a significant interaction of *validity-by-validity proportion* ($F_{(1,25)} = 14.80$, $p < .001$, $\eta p^2 = 0.37$).

Furthermore, there was a significant interaction between *validity, validity proportion and congruency* ($F_{(1,25)} = 5.96$, $p < .05$, $\eta p^2 = 0.19$), reflecting disproportionate error increases when unexpected reprogramming coincided with conflict resolution. This hints at a bottleneck for concurrent control demands, particularly when reprogramming is unexpected.

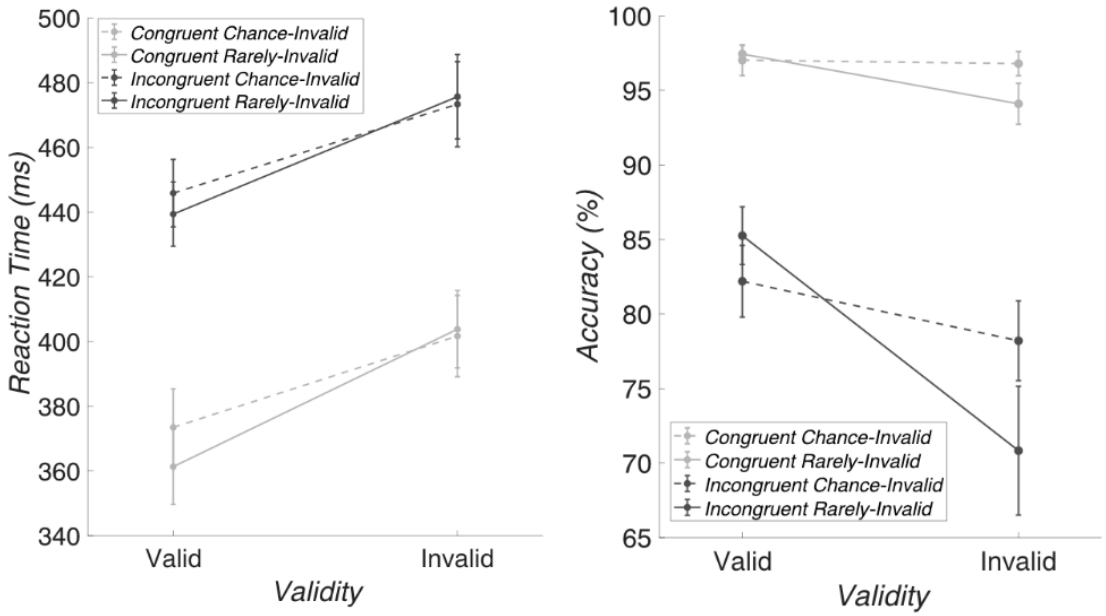

Fig. 1 Behavioral validity and congruency effects as modulated by the frequency of invalid trials (validity proportion, i.e., response expectation). Left: Light grey lines depict congruent trials, dark grey lines represent incongruent trials. Dashed lines indicate blocks in which invalid trials occurred at chance level, while continuous lines represent blocks with rare invalid trials (unexpected reprogramming). The x-axis shows the validity of the trial and reflects the validity effect as the slope between valid and invalid trials. The congruency effect, on the other hand, is represented as the difference between congruent (light grey) and incongruent lines (dark grey). Right: This depicts the same parameters as the left graph but this time for accuracy. Invalid-incongruent trials in the rare-invalid blocks (unexpected reprogramming) show the disproportionate accuracy decrease that is reflected in the significant interaction between validity, validity proportion and congruency ($F_{(1,25)} = 5.96$, $p < .05$, $\eta p^2 = 0.19$)

2.2 Imaging

Contrasts of reprogramming and conflict resolution

Validity: reprogramming

The planned t-contrast of activity between invalid (reprogramming) and valid trials revealed significant peak activations in five main clusters, which are listed in detail in Table 1. They entailed the pre-SMA, the right dorsal premotor cortex, the bilateral insular cortex extending into the frontal operculum cortex, as well as the right middle temporal/temporoparietal cortex (see also Figure 2, left panel).

Congruency: conflict resolution

The difference between incongruent (conflict resolution) and congruent trials, as calculated in the planned t-contrast, manifested in five main activity clusters, with some large clusters extending to multiple brain regions. These comprised the bilateral occipital cortex, the bilateral superior parietal lobule and intraparietal sulcus, the left cerebellum, the bilateral dorsal premotor cortex, the inferior/middle frontal gyrus, and the right insular cortex. These activations are further specified in Table 1 and presented in Figure 2 (right panel).

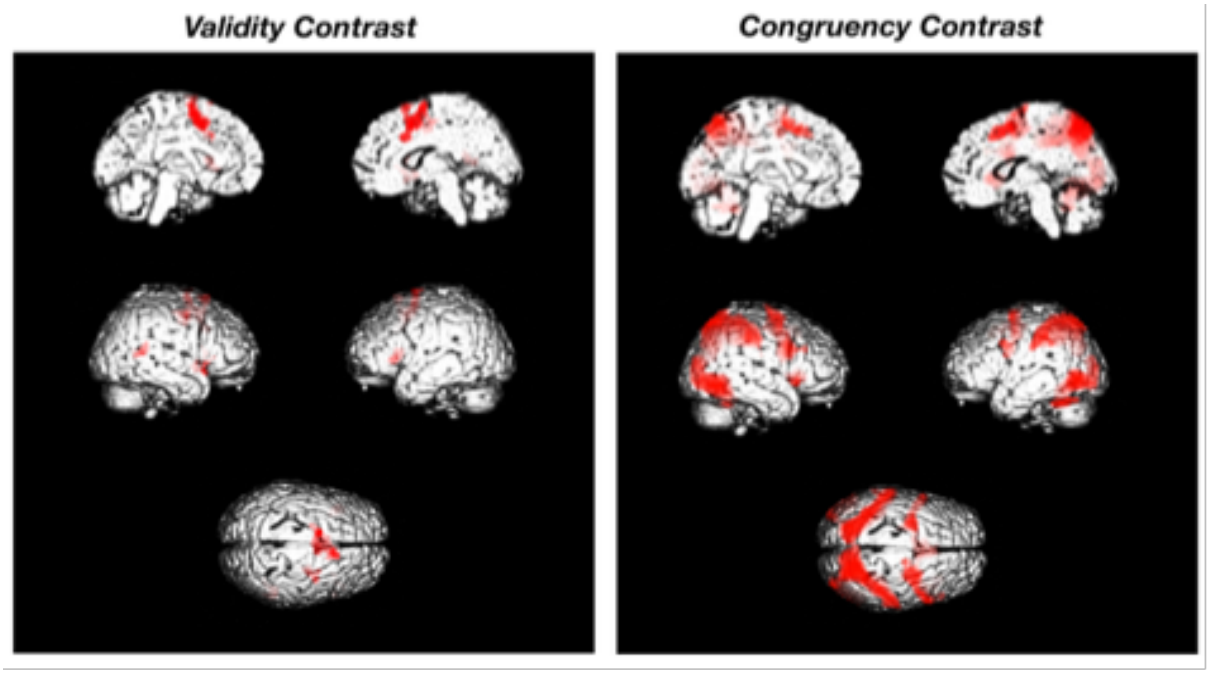

Fig. 2 Left: activations of the validity t-contrast of invalid minus valid trials, showing areas involved in response reprogramming ($p < .05$ FWE corrected at cluster-level (cluster-forming threshold $p < .001$)). Right: conflict-related activity as revealed by the t-contrast of incongruent minus congruent trials ($p < .05$ FWE corrected at cluster-level (cluster-forming threshold $p < .001$))

REGION	SIDE	COORDINATES			VOXEL	Z-SCORE
		X	Y	Z		
Response Reprogramming (invalid > valid)						
pre-SMA (Area 6mr)	L	-8	2	56	1296	4.94
dorsal premotor cortex (Area 6d3)	R	30	2	46	279	3.98
insular cortex, frontal operculum cortex (Area Id7, Area OP8, Area Id6, Area OP9)	L	-36	20	4	258	4.50
insular cortex, frontal operculum cortex (Area Id6, Area Id5)	R	40	6	-4	243	3.86
middle temporal gyrus, temporo-parietal junction	R	48	-46	12	236	4.24
Conflict Resolution (incongruent > congruent)						
lateral occipital cortex (Area FG2)	R	48	-58	-10	12141	7.51
with subpeaks in:						
superior parietal lobe (Area 7A)	R	22	-66	56		
intraparietal sulcus (Area hIP8)	R	30	-70	40		
intraparietal sulcus (Area hIP5)	R	30	-66	36		
intraparietal sulcus (Area hIP2)	R	42	-36	40		
intraparietal sulcus (Area hIP6)	L	-24	-62	54		
intraparietal sulcus (Area hIP8)	L	-22	-68	42		
intraparietal sulcus (Area hIP1)	L	-38	-38	40		
lateral occipital cortex (Area hOc4la, Area hOc5)	L	-46	-70	-4	2796	6.52
with subpeaks in:						
cerebellum	L	-38	-52	-28		
temporal occipital fusiform cortex (FG4)	L	-40	-50	-14		
dorsal premotor cortex (Area 6d3)	R	26	-2	48	2173	5.24
with subpeaks in:						
precentral/inferior frontal gyrus (Area 44)	R	56	12	32		
pre-SMA (Area 6mr)	R	9	0	68		
dorsal premotor cortex (Area 6d3)	L	-24	-6	50	1985	5.83
with subpeaks in:						
pre-SMA (Area 6mr)	R	2	14	52		
insular cortex (Area Id6)	R	40	18	0	558	4.73

Table 1 Peak cluster activations (and subpeaks for clusters extending into multiple brain regions) for validity and congruency contrasts, depicting cluster region, side (L = left, R = right), MNI-coordinates, cluster size (in number of voxels) and z-scores

Conjunction of reprogramming and conflict resolution

The contrasts of the validity and congruency effects were further evaluated for consistently shared activation patterns (i.e., testing a Conjunction null hypothesis in SPM12;

Friston et al., 2005), which revealed a significant conjunction effect in the pre-SMA region with extension into the SMA (see Figure 3, more specifics are listed in Table 2).

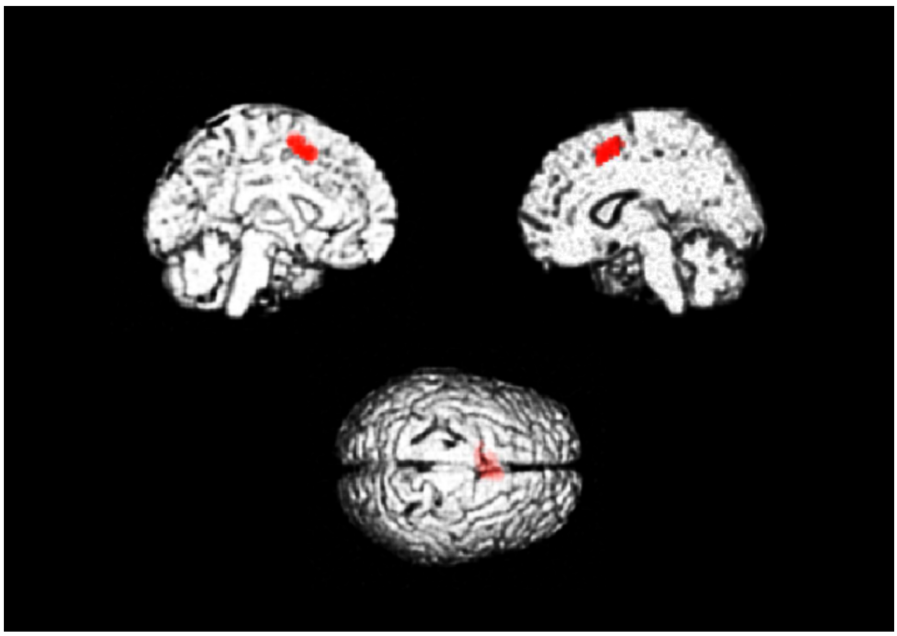

Fig. 3 Shared activation between reprogramming and conflict resolution, as derived from the conjunction of validity and congruency contrasts, manifests in the pre-SMA region (extending into the SMA) ($p < .05$ FWE corrected at cluster-level (cluster-forming threshold $p < 0.001$))

Interactions

At the whole-brain level, no interaction contrast reached significance. Our ROI analyses, as derived from the peaks of the global null analysis of validity and congruency effects (displayed in Table 2), focused specifically on interactive activity patterns within our networks of interest. This analysis revealed a three-way interaction in the right precentral gyrus adjacent to the inferior frontal gyrus ($F_{(1,25)} = 6.60$, $p < .05$). This region was deactivated in all conditions except for the invalid-incongruent condition with a high validity proportion, thus when reprogramming was unexpected and coincided with conflict resolution. Moreover, activation in this condition was negatively correlated with accuracy scores ($r = -0.45$; $p < .05$). In addition, activity in the right superior parietal lobule showed a *validity-by-congruency* interaction ($F_{(1,25)} = 4.33$, $p < .05$), with strongest activation during invalid-incongruent trials. In

all other regions, there were no significant interaction effects of *validity* and *congruency*, nor of all three factors.

REGION	SIDE	COORDINATES			VOXEL	Z-SCORE
		X	Y	Z		
Conjunction Null Hypothesis						
pre-SMA (Area 6mr)	L	-4	2	56	477	4.34
Global Null Hypothesis						
dorsal premotor cortex (Area 6d3)	L	-26	-8	48	259	6.13
dorsal premotor cortex (Area 6d3)	R	30	2	46	220	5.96
pre-SMA (Area 6mr)	R	6	6	56	361	5.51
precentral gyrus	R	48	2	34	89	4.90
precentral gyrus	R	34	4	26	10	4.59
insular cortex (Area Id6)	R	40	16	-6	250	5.02
insular cortex (Area Id6)	L	-32	18	10	122	6.02
intraparietal sulcus (Area hIP1)	L	-38	-36	36	82	5.43
intraparietal sulcus (Area hIP3)	L	-28	-50	50	10	4.53
intraparietal sulcus (Area hIP2)	R	38	-36	40	163	5.70
superior parietal lobe	L	-18	-54	52	17	4.73
superior parietal lobe (Area 7A)	R	14	-64	70	15	4.96
cerebellum*	L	-38	-46	-30	31	5.25
intraparietal sulcus (Area hIP5)*	L	-28	-68	24	19	5.05
lateral occipital cortex (Area hOc4la)*	L	-46	-84	-8	15	4.58
inferior temporal gyrus (Area FG4)*	R	50	-48	-20	11	4.85
lateral occipital cortex (Area hOc5)*	L	-40	-72	0	10	4.59

Table 2 Peak cluster activations for conjunction and global null analyses, depicting cluster region, side (L = left, R = right), MNI-coordinates, cluster size (in number of voxels) and z-score. The asterisk (*) indicates regions that are not part of the networks of interest and were therefore not included in the ROI analyses

3. References

Derosiere, G., Klein, P.-A., Nozaradan, S., Zénon, A., Mouraux, A., & Duque, J. (2018). Visuomotor Correlates of Conflict Expectation in the Context of Motor Decisions. The Journal of Neuroscience, 38(44), 9486–9504. https://doi.org/10.1523/JNEUROSCI.0623-18.2018

Eickhoff, S. B., Stephan, K. E., Mohlberg, H., Grefkes, C., Fink, G. R., Amunts, K., & Zilles, K. (2005). A new SPM toolbox for combining probabilistic cytoarchitectonic maps and functional imaging data. NeuroImage, 25(4), 1325–1335. https://doi.org/10.1016/j.neuroimage.2004.12.034

Friston, K. J., Holmes, A. P., Poline, J.-B., Grasby, P. J., Williams, S. C. R., Frackowiak, R. S. J., & Turner, R. (1995). Analysis of fMRI Time-Series Revisited. NeuroImage, 2(1), 45–53. https://doi.org/10.1006/nimg.1995.1007

Friston, K. J., Penny, W. D., & Glaser, D. E. (2005). Conjunction revisited. *NeuroImage*, *25*(3), 661–667. https://doi.org/10.1016/j.neuroimage.2005.01.013

JASP Team. (2023). JASP (Version 0.16.2) [Computer software]. JASP. https://jasp-stats.org/

Kuhns, A. B., Dombert, P. L., Mengotti, P., Fink, G. R., & Vossel, S. (2017). Spatial Attention, Motor Intention, and Bayesian Cue Predictability in the Human Brain. The Journal of Neuroscience, 37(21), 5334–5344. https://doi.org/10.1523/JNEUROSCI.3255-16.2017

MathWorks. (2022). MATLAB (Version R2022a) [Computer software]. https://www.mathworks.com/.

Oldfield, R. C. (1971). The assessment and analysis of handedness: The Edinburgh inventory. Neuropsychologia, 9(1), 97–113. https://doi.org/10.1016/0028-3932(71)90067-4

Patton, J. H., Stanford, M. S., & Barratt, E. S. (2011). Barratt Impulsiveness Scale-11 [Dataset]. https://doi.org/10.1037/t05661-000

Sauter, A. E., Zabicki, A., Schüller, T., Baldermann, J. C., Fink, G. R., Mengotti, P., & Vossel, S. (2024). Response and conflict expectations shape motor responses interactively. Experimental Brain Research, 242(11), 2599–2612. https://doi.org/10.1007/s00221-024-06920-w

Wellcome Trust Centre for Neuroimaging. (2020). SPM12 [Computer software]. https://www.fil.ion.ucl.ac.uk/spm/

CHAPTER 4

Beta dynamics control general response flexibility in a fronto-subthalamic network

Abstract

Flexible fronto-subthalamic control mechanisms support adaptive behavior in response to changing goals or conflict. Within these networks, the subthalamic nucleus (STN) is central to control implementation, including outright motor inhibition, as well as more flexible adjustments to reprogram responses or resolve conflict. Whether these functions rely on a shared mechanism remains unclear, though preliminary evidence suggests that beta-band dynamics, prominently linked to motor inhibition, may govern control across domains. In Parkinson's disease, pathological beta activity reflects a shift toward excessive inhibition, which can be suppressed by deep brain stimulation (DBS) of the STN. We investigated whether beta dynamics reflect a common response control process using a novel task combining response reprogramming (via probabilistic cues) and conflict resolution (via congruent/incongruent flanker stimuli) while recording EEG activity of 27 people with Parkinson's disease ON and OFF STN DBS. In a subsample of 10 participants, sensing-enabled DBS systems (Percept PC, Medtronic, Inc.) allowed for simultaneous STN local field potential (LFP) recordings. We examined two post-target windows, reflecting an early global inhibition (beta synchronization) and subsequent adaptations (beta desynchronization). Our results showed initial right-prefrontal beta synchronization during conflict when DBS was OFF, followed by widespread beta desynchronization (prefrontal, motor, and STN regions) that was unaffected by DBS. Reprogramming effects appeared during response adaptation, with right-prefrontal beta desynchronization when DBS was OFF. STN beta power in this period predicted RTs and error rates, relating to decreased flexibility with higher beta power. Particularly, error rates increased with beta power when response adaptations for reprogramming and conflict resolution coincided. These findings support a general role of

fronto-subthalamic beta in mediating inhibition and flexibility, while partially distinct manifestations may reflect different response adjustments for reprogramming and conflict.

1. Introduction

Adaptive behavior in dynamic environments requires the brain to flexibly control neural activity. While intentions bias response plans towards an expected goal-direction, flexible adaptations are demanded when conditions change. In case of violated response expectations, the anticipated response plan needs to be inhibited while an alternative is programmed. Moreover, distractions may demand conflict resolution of interfering response activations. Therefore, efficient responding depends on adaptive brain network activity, precisely the cortico-basal-ganglia-thalamo-cortical (CBGTC) pathways, which regulate activations of competing response plans (e.g., Bonnevie & Zaghloul, 2019).

A key decision point within these CBGTC pathways is the subthalamic nucleus (STN), which integrates inputs across domains to adapt responses according to internal goals and external demands. Importantly, hyperdirect cortical projections allow for rapid transmission of contextual information to the STN for fast response inhibition. This "braking" function is a crucial control mechanism to prevent premature responding and to grant more time for response selection (e.g., Chen et al., 2020; Frank et al., 2007).

In the healthy brain, neuronal firing across CBGTC pathways is dynamic and supports flexible response adaptations. In Parkinson's disease, however, dopamine depletion is related to excessive synchronization in the beta-band (~13–30 Hz) within the STN and its cortical connections (Brown, 2003; Hammond et al., 2007; Iskhakova et al., 2021). This over-synchronization results in heightened inhibition of thalamocortical drive, which impairs flexible control functions and contributes to symptoms such as rigidity.

Deep brain stimulation (DBS) of the STN is a treatment to counteract this inhibition by suppressing aberrant beta activity (Kühn et al., 2006; Little & Brown, 2014). Studies in people with Parkinson's disease receiving STN DBS provide unique insight into STN function, particularly through recordings of STN local field potentials (LFPs). These findings increasingly outline a role of the STN beyond just a behavioral "brake", but as a dynamic modulator of

response thresholds and flexible adaptations (Herz et al., 2022; Jahanshahi et al., 2015; Nougaret et al., 2021), potentially mediating these processes through a similar mechanism.

Beta-band dynamics, prominently linked to motor functions, are increasingly recognized as a mechanism that governs cognitive-behavioral flexibility and inhibition across domains. While beta desynchronization (i.e., decreases in beta power) supports adaptive changes, as observed during movement initiation, updating, or conflict processing (e.g., Brittain et al., 2012; Tan et al., 2016), beta synchronization (i.e., increases in beta power) can stabilize cognitive-behavioral states, as seen in motor termination, attentional filtering or response selection (e.g., Chandrasekaran et al., 2019; Dubey et al., 2023; Leventhal et al., 2012). In line with this, beta represents the most globally distributed cortical frequency, coordinating processes across regions and domains (e.g., Chikermane et al., 2024; Spitzer & Haegens, 2017).

According to the "pause-then-retune" model (Hervault & Wessel, 2025), reactive response control comprises two sequential stages with distinct neurophysiological signatures. The initial "pause" is related to transient global inhibition via the STN (“brake”), presumably through the hyperdirect pathway (Wessel et al., 2022). This is accompanied by frontocentral beta bursts (Wessel, 2020), that are thought to reflect subcortical-cortical communication (Diesburg & Wessel, 2021), and right-lateralized increases of beta power (e.g., Daniel et al., 2023). This temporary pause creates a window to recalibrate (“retune”) responses through more selective adaptations (Wessel & Aron, 2017). The “retune” stage is dependent on the complexity and type of these adaptations (Hervault & Wessel, 2025), and may relate to beta desynchronization for enhanced cognitive-behavioral flexibility (e.g., Brittain et al., 2012).

While increased beta has been linked to maintenance of the current state, potentially slowing responses (Engel & Fries, 2010), investigations of the relationship between beta and behavior have mainly highlighted context-dependencies (e.g., Chandrasekaran et al., 2019; Senkowski, 2005). A recent study by Pierrieau et al. (2025), however, provides a new explanation to this variability. They propose the motor flexibility hypothesis, suggesting that beta desynchronization reflects adaptive performance rather than RTs per se (motor vigor hypothesis; Niv et al., 2007). A stronger beta desynchronization, particularly in the lower sub-band (~13–20 Hz), is linked to enhanced adaptive capacities and improved task performance.

While Pierrieau et al. (2025) focused on cortical beta dynamics, findings by Herz et al. (2023) indicate similar dynamics at the STN.

In the current study, we aimed to contribute to the emerging framework of a general fronto-subthalamic control process that is governed by beta-band dynamics. We focused on two theoretically distinct control demands - response reprogramming and conflict resolution - and integrated them in a novel task to examine their shared control signatures.

Response reprogramming involves anticipatory preparation of a response using a probabilistic cue that biases motor readiness. Invalid cues (violated response expectations) required reactive inhibition of the prepared response and programming of an alternative. In healthy participants, anticipatory response preparation in this task has been shown to improve performance for valid cues and to deteriorate performance for invalid ones (Sauter et al., 2024), which is known as the "validity effect" (Mars et al., 2007; Posner, 1980; Rosenbaum & Kornblum, 1982; Rushworth et al., 2001a; Rushworth et al., 1997).

Conflict resolution, in contrast, entails the inhibition of interfering, automated response activations that are in conflict with the correct response. Here, we employed a variant of the Eriksen flanker task (Eriksen & Eriksen, 1974), in which irrelevant, directionally incongruent stimuli interfere with response selection. The resulting performance cost, relative to congruent trials, is referred to as the "congruency effect" (e.g., Ridderinkhof et al., 2004).

Reactive control demands, as measured in validity and congruency effects, can be modulated by anticipatory control. In cueing tasks, frequent (expected) valid cues increase preparatory strength and surprise for invalid trials, leading to stronger validity effects at high validity proportions (Bestmann et al., 2008; Kuhns et al., 2017). Similarly, the proportion of incongruent trials modulates the congruency effect, showing larger effects when incongruent trials are unexpected (high congruency proportion) (e.g., Derosiere et al., 2018). The latter is often interpreted as conflict adaptation, implying anticipatory top-down adjustments, though alternative explanations link this effect to low-level learning processes (Braem et al., 2019; J. R. Schmidt, 2019). In order to explore the contribution of anticipatory control processes in our task, we systematically varied trial proportions and thus expectations in different task blocks.

Our novel response cueing/conflict task has never been studied in people with Parkinson's disease receiving STN DBS. This allowed us to gain a novel perspective on the task processes by assessing their dependence on STN function through DBS modulation. We recorded high-density cortical EEG while participants (n = 27) performed the task ON and OFF DBS. In a sub-group of 10 participants, who were equipped with an implanted Percept PC pulse generator (Medtronic, Inc.), we were able to simultaneously record STN LFPs alongside the cortical EEG. Based on the literature, we focused on right-prefrontal and motor-cortical EEG activity next to the STN as our regions of interest (e.g., Hervault & Wessel, 2025; Wessel et al., 2019).

Behaviorally, we expected the described validity and congruency effects, reflecting costs of invalid cues (response reprogramming) and incongruent targets (conflict resolution), in line with prior findings (Sauter et al., 2024). We further hypothesized an interaction between these effects, suggesting shared control processes (as in Sauter et al., 2024). As DBS reduces inhibition and facilitates prepotent responses (Appleby et al., 2007; Frank et al., 2007), we expected larger validity and congruency effects ON DBS. On a neural level, we expected beta synchronization after invalid and incongruent targets relating to the "pause" stage (initial inhibition), followed by beta desynchronization during the "retune" stage, reflecting adaptive reprogramming and conflict resolution. We explored whether these beta dynamics interact during invalid-incongruent trials and whether STN beta power would predict behavioral performance according to control demands. Furthermore, we expected altered beta dynamics ON DBS, considering the attenuation of beta activity through stimulation.

Taken together, our findings support a general account of fronto-subthalamic beta dynamics in mediating behavioral flexibility and performance in response reprogramming and conflict resolution, which may generalize to further domains. Crucially, next to related beta signatures, a dominant congruency effect and differential modulation by DBS suggest partially distinct control requirements during these processes.

2. Methods

2.1 Participants

An overall number of 27 people with Parkinson's disease and bilaterally implanted STN DBS electrodes gave their written informed consent to participate in the present study, which received approval from the local ethics committee (01.09.2022; 22-1135) and was carried out in compliance with the Declaration of Helsinki. Ten of the included participants had a Percept PC implanted pulse generator (Medtronic, Inc., Minneapolis, USA), which allowed for the wireless outpatient recording of STN LFPs alongside the cortical EEG. Participants were only included when meeting the criteria of an idiopathic Parkinson's disease diagnosis and ongoing DBS treatment for a minimum of three months. Exclusion criteria comprised severe cognitive impairments, psychiatric comorbidity requiring treatment or any other severe mental illnesses.

Two participants (with EEG only) were unable to complete the OFF stimulation condition and another participant (with EEG only) was unable to complete the task for either stimulation condition due to pronounced occurrence of tremor and fatigue. Next to these cases, a technical error prevented registration of task events in the EEG file for another participant (with EEG only), therefore only the behavioral data could be analyzed. In total, data analyses included behavioral data of 24 participants (mean age: 63.21 years; ranging from 50 until 78 years; 16 male and 8 female; 23 right-handed, one left-handed), of which 23 had complementary EEG data (n = 10 with cortical EEG and LFP recordings and n = 13 with cortical EEG only). A detailed overview on the included participant's clinical and demographic specifications is given in Supplementary Table ST1 (Appendix).

2.2 Task

The task combined elements of a Posner motor response cueing task (Posner, 1980; Rushworth et al., 1997), which induces response preparation through probabilistic response cues, and the arrow version of an Eriksen flanker task (Eriksen & Eriksen, 1974), allowing for a combined assessment of response reprogramming and flanker-related conflict resolution

(Figure 1). This task was implemented using the Presentation® software (Version 18.0; Neurobehavioral Systems, Inc., Berkeley, CA).

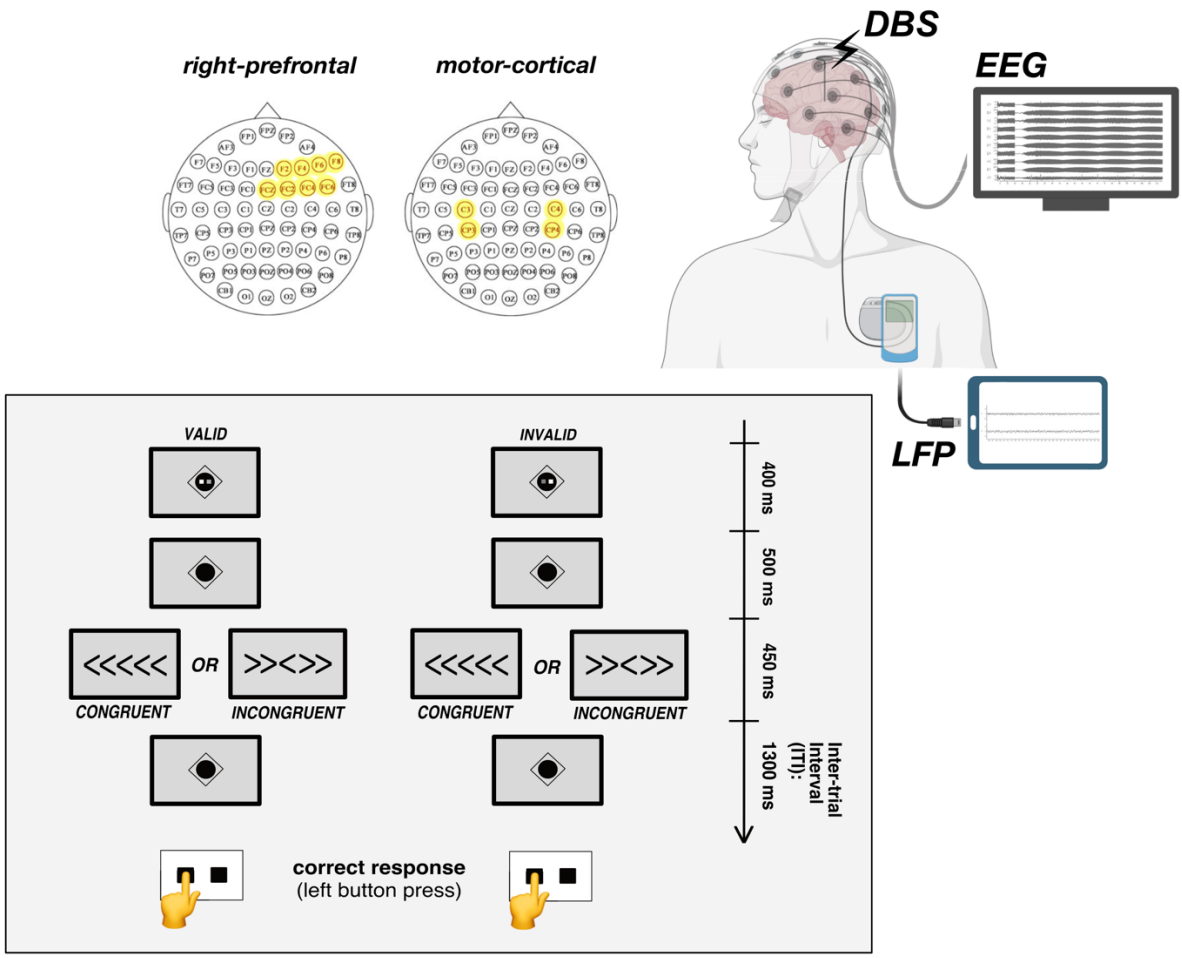

Fig.1 Top left: topography depicting the right-prefrontal channels (F2, F4, F6, F8, FCz, FC2, FC4, FC6) and motor-cortical channels (C3, CP3, C4, CP4) for our cortical regions of interest. Top right: EEG/LFP recording set-up. Participants were equipped with a 63-channel EEG cap that recorded cortical EEG signals (at 1000 Hz) during the task. In case participants were implanted with sensing-enabled Percept PC implanted pulse generators (Medtronic, Inc., Minneapolis, USA), the communicator (depicted in blue on top of the implanted pulse generator) transmitted STN LFP signals to the tablet, enabling continuous signal recordings (at 250 Hz) surrounding the selected contacts of the left and right hemispheric sensing leads (this image was created with tools from biorender.com; last accessed: June 2025). Bottom: Response cueing/conflict task. Each trial initially showed a motor response cue for 400 ms, displaying two squares representing the response keys. The white square indicated the cued response side. In valid trials, this cue correctly predicted the upcoming target response; in invalid trials, it pointed to the opposite side. This was followed by a fixation diamond, after which the target appeared for 450 ms. The cue-target interval was jittered and centered around 500 ms, in order to prevent anticipatory responses. The target was a central chevron-type arrow pointing left or right, requiring a corresponding index finger response of the left or right button. Flanking distractor arrows were presented on either side, pointing either in the same direction

(congruent) or the opposite direction (incongruent). A fixation point was shown during the inter-trial interval (jittered according to the cue-target interval), during which responses were still accepted. Each trial lasted for 2650 ms

Task structure

The task comprised 10 blocks of 62 trials each (~30 min. total). The blocks were separated by self-paced breaks and varied in the proportions of valid vs. invalid cues and congruent vs. incongruent targets, to modulate expectations. A 2 x 2 manipulation of cue validity proportion (VP; 50%/77% valid trials) and target congruency proportion (CP; 30%/70% congruent trials) specified four distinct block types. Each block type - defined by these proportions - was presented multiple times in a pseudorandomized order (resulting in 10 blocks total: 3 x 77% VP/70% CP; 3 x 77% VP/30% CP; 2 x 50% VP/ 70% CP; 50% VP/ 30% CP). Blocks of the same type did not follow each other consecutively. There were two different versions of block sequences, which were pseudorandomized across participants and "ON" and "OFF" sessions. Each block sequence version contained the same overall trial sequence, however, the trial sequences between blocks differed. This structure follows standard practices in probabilistic learning studies (e.g., Iglesias et al., 2013). Trial sequences within blocks were also pseudorandomized. A more detailed description of the block design is presented in Supplementary Fig. SF1 and SF2 (Appendix).

Across the entire task sequence, 50% of trials were congruent and 50% were incongruent, while around 66% of trials were valid and 34% invalid. Within each condition, left- and right-hand responses were evenly distributed.

Before each block, participants were informed whether the upcoming trials would be mostly congruent or incongruent (per Derosiere et al., 2018; Duque et al., 2016), while the cue validity proportions were inferred during the block (per Kuhns et al., 2017).

2.3 Procedure

Participants performed the described response cueing/conflict task (Figure 1) twice (two sessions), once with stimulation ON and once with stimulation OFF, while on their regular Parkinson's disease medication. They were seated comfortably in front of a computer screen on which the task was displayed. The experiment required bimanual responses with button

presses using left or right index fingers, which they rested on adjacent keys of a response pad. A prolonged break (~ 25 min.) was included in between sessions to allow for rest and a wash-out period for stimulation conditions. The order of performing the task with stimulation ON or OFF was counterbalanced across participants.

Upon arrival with activated DBS (stimulation settings: Supplementary Table ST2; Appendix), participants underwent a series of neuropsychiatric and Parkinson's disease-related assessments. Following these evaluations, participants received task instructions and completed a brief training session (~ 5 min.; training blocks are described in the Supplementary Material of the Appendix) while DBS remained on. All participants met the inclusion criteria based on their assessment scores, summarized in Supplementary Table ST1 (Appendix).

EEG/LFP recordings

The STN LFP data were streamed from the Percept PC implanted pulse generator (Medtronic, Inc.) via a communicator, which transmitted signals to the programmer tablet (Figure 1). In order to enable bipolar montage sensing of the LFPs, contacts above and below the clinical stimulation electrodes were selected, therefore centering voltage recordings onto the clinically relevant contact. In case the clinical stimulation contact included the upper- or lowermost contact, the stimulation was shifted accordingly. For non-Percept participants, DBS was delivered using each participant's routine clinical settings and active contacts.

EEG data were recorded using a 63-channel cap (signal amplification with BrainVision amplifiers; Brain Products GmbH, Germany), at a 1000 Hz sampling rate. Signals were filtered online with a 1 Hz high-pass and 100 Hz low-pass filter. The reference channel was at Cz, and the ground electrode was placed at FPz. In case LFPs were recorded alongside the cortical EEG, they were sampled at 250 Hz, which was the maximum available sampling rate, and filtered online between 1 Hz and 100 Hz. In order to synchronize EEG and LFP signals, the "power cycling" method was applied (Soh et al., 2025), for which DBS was briefly (~3 s) activated (during "OFF" sessions) or inactivated (for "ON" sessions). This introduced a distinct, simultaneous artifact in both EEG and LFP signals. These patterns were used for the offline temporal alignment of the two datasets.

2.4 Data analysis

Behavior

Only trials with correct responses were included in RT analyses. Anticipatory responses (100 ms and below) were excluded. For accuracy analyses, due to potential freezing episodes, only incorrect responses were treated as errors. Accuracy therefore represents a percentage of incorrect button presses of the total correct and incorrect responses.

We aimed to examine the effects of *validity* (valid/invalid), *congruency* (congruent/incongruent), *validity proportion* (77% or 50%), *congruency proportion* (70% or 30%), *stimulation* (ON/OFF) and their putative interactions on behavioral performance across conditions. To this end, we fitted linear mixed-effects models (LMEs) with the described fixed effects (and putative interactions), as well as a subject-specific random intercept. Model selection for RTs and accuracy was based on Bayesian Information Criterion (BIC) as well as the model's log likelihood in a stepwise reduction of the full model and performed in accordance with the principle of marginality (Nelder, 1977). Post hoc paired t-tests, Bonferroni-corrected for multiple comparisons, were used to detect differences in condition-levels for significant interactions. All behavioral analyses were conducted using MATLAB (The MathWorks Inc. (2023). MATLAB version: 9.13.0 (R2023b), Natick, Massachusetts: The MathWorks Inc. https://www.mathworks.com).

EEG/LFP data

Alignment

All electrophysiological data were processed using MATLAB (The MathWorks Inc. (2023). MATLAB version: 9.13.0 (R2023b), Natick, Massachusetts: The MathWorks Inc. https://www.mathworks.com; EEGLAB (Delorme & Makeig, 2004) and FieldTrip (Oostenveld et al., 2011)) custom scripts as well as the Spike2 software (Cambridge Electronic Design; RRID: SCR_000903). Clear-cut artifacts, as introduced with the "power cycling" method (Soh et al., 2025), were precisely detectable throughout cortical EEG recordings and used as a time reference point to determine the length of the recording between the start and end artifacts. The corresponding LFP artifact features were present as two peaks (one related to switch-ON and one to switch-OFF), of which the base prior and adjacent to the switch-OFF peak was

aligned with the EEG reference point. Soh et al. (2025) used the same alignment technique ("power cycling"), focusing on a transient single LFP spike marker related to the switch-ON artifact. We additionally tested this feature as a reference and obtained similar precision than with the switch-OFF marker. However, as certain recordings contained ambiguous switch-ON spikes, we decided to use the switch-OFF features as a reference.

Both LFP and EEG channel data were imported into Spike2 for facilitated artifact visualization and comparison across channels. Artifact onset and offset timestamps were extracted and used in a custom MATLAB script to segment and synchronize the recordings. LFP signals were upsampled to match the EEG sampling rate (1000 Hz), generating a unified, time-aligned dataset. Event markers from the aligned EEG recording were extended to LFP channels and used to link the data to task events.

Preprocessing

For combined EEG/LFP files, all channels were high-pass filtered above 1 Hz, while cortical EEG channels were additionally low-pass filtered at 40 Hz. Subsequently, channels with insufficient signal were detected and rejected automatically, based on cortical EEG channels. Afterwards, the cortical EEG data were re-referenced to the common average (Cz channel). In a next step, both EEG and LFP channels were downsampled to 500 Hz. The resampled data were subsequently epoched based on the cue event marker (-1 until 4 sec. around the cue). Furthermore, epochs with insufficient signal were automatically rejected based on data from the cortical EEG. Next, an independent component analysis (ICA) was performed on the cortical EEG channels to identify and remove stereotypical non-neural components, which were automatically rejected based on IC Label classifications. Recordings without LFP data followed the same procedure (without alignment step).

Time-frequency decomposition of EEG and LFP data was performed using the filter-Hilbert method, applying infinite impulse response (IIR) filters with 2 Hz bandwidth. Additionally, epoch power was normalized by conducting a mean power subtraction per frequency and per epoch. Subsequently, the epochs' power was z-scored using the mean and standard deviation of each epoch. Furthermore, the normalized epoch power was re-epoched

to encompass a temporal window of interest from -0.1 to 1 sec. around the target presentation and from -0.8 to 0.2 sec. relative to the response event, and was resampled to 100 Hz.

Our research questions focused on the beta-band, which can be divided into low (~13–20 Hz) and high (~21–35 Hz) sub-bands that may exhibit functional differences (e.g., Nougaret et al., 2024). In the context of Parkinson's disease, synchronization within the lower sub-band has been shown to correlate most sensitively with motor impairment (e.g., Neumann et al., 2016), highlighting its clinical relevance. Moreover, in tasks involving inhibition, flexibility and conflict, particularly the lower sub-band has been outlined as signaling increased control demands (Daniel et al., 2023; Pierrieau et al., 2025). Consequently, we included only the lower beta range (13–20 Hz) in our analyses. For simplicity, however, we hereafter still refer to it as "beta-band".

In order to investigate the lower beta sub-band, power from 13 to 20 Hz was averaged across conditions for each region of interest and time window (centered on target or response). The regions of interest entailed a motor-cortical region (channels C3, CP3, C4, CP4), a right-prefrontal region (channels F2, F4, F6, F8, FCz, FC2, FC4, FC6) and the STN (left and right channel). Only correct trials were included in this average, with RTs exceeding 100 ms (matching the criteria for correct trials in the behavioral RT analysis). Grand averages across participants were computed for each condition, channel and time window. Additionally, beta-power was averaged across a more confined window within the target-locked period, spanning 0 to 200 ms from target presentation. This reflects the initial "pause" reaction (beta peak ~150 ms; Wessel & Aron, 2017). Within the response-locked window, beta averages from 400 to 100 ms pre-response were calculated. Prior research has identified this as a critical window for beta-mediated response formation (e.g., Cohen & Donner, 2013; Kilavik et al., 2013), which we analyze as the "retune" stage. Given the pronounced RT differences between stimulation conditions in our study, we decided to define the "retune window" according to response-locked data, in order to minimize overlap with movement-related activity inherent in target-locked data. Averages were calculated for each condition and region of interest per participant and across participants.

Analysis of control-related beta dynamics

To identify control dynamics in the beta-band relating to our response cueing/conflict task, we conducted a linear mixed-effects (LME) analysis to predict beta averages within our two predefined post-target windows: 0 to 200 ms after target presentation ("pause window") and 400 to 100 ms before response ("retune window"). This was investigated for motor-cortical, right-prefrontal and STN regions.

The LME model incorporated *validity, congruency*, and *stimulation* along with their interactions as fixed effects, and included a random intercept for each subject to account for inter-individual variability (*BetaPower ~ Stimulation*Validity*Congruency + (1 |Subject)*). Given the absence of significant interactions with stimulation and our block-level factors (*validity* and *congruency proportion*) in our behavioral data, we decided to enhance parsimony by excluding these factors from any LMEs relating to electrophysiological data.

Post hoc, we performed an additional LME for the STN, as the planned LME showed marginal condition-specific beta effects that we aimed to delineate further. To explore a more transient time window of significance, the LME was performed across each time point of the "pause window" and the "retune window". Subsequently, the p-values were FDR-corrected to address the issue of multiple comparisons.

Informed by our data of right-prefrontal activation, this post hoc LME analysis was also performed more selectively at the FC2 channel (part of the right-prefrontal cluster), in order to investigate a narrower representation of the reprogramming-related beta desynchronization ("retune window"). The resulting p-values were FDR-corrected.

Investigating the relationship between beta and behavior

To examine the influence of trial-wise beta power on behavioral performance, we employed LME models that included mean STN beta power of our response-related "retune window" (400 to 100 ms pre-response) to predict RTs and response accuracy (correct vs. incorrect) per trial.

For RT analyses, only correct trials with RTs exceeding 100 ms were included, consistent with our behavioral criteria for correct trials. Accuracy analyses encompassed all correct and incorrect trials (excluding missed trials).

Each LME model (for accuracy: generalized linear mixed-effects model (GLME) with binomial distribution and logit link function to predict binary outcomes) incorporated *validity*, *congruency*, *stimulation*, and *beta power* as fixed effects, alongside their interactions. To account for inter-individual variability, subject was included as a random intercept. Additionally, random slopes for *validity*, *congruency*, *stimulation*, and *beta power* were included to account for variability in predictor effects across subjects (*RT (or accuracy) ~ BetaPower*Stimulation*Validity*Congruency + (1 + BetaPower + Stimulation + Validity + Congruency |Subject)*). This approach helps to reduce inflated statistical power that is common to large datasets, to provide more accurate and generalizable results (e.g., Matuschek et al., 2017). Post hoc linear hypothesis tests were used to compare the slopes between levels of predictors, based on the fixed-effects estimates from the LME and GLME models.

4. Results

4. 1 Behavior

Reaction time

Our LME analyses revealed significant main effects of both *validity* (β = 14.22, SE: 5.83, $p < .05$) and *congruency* (β = 94.35, SE: 8.24, $p < .001$) on RTs. Specifically, participants exhibited slower responses on incongruent compared to congruent and on invalid compared to valid trials, reflecting the expected reprogramming and conflict costs (Figure 2, A & B). The analysis did not reveal any interactions between the validity and congruency effects.

Stimulation condition also significantly influenced RTs. Participants responded faster when stimulation was active (β = 78.55, SE: 5.83, $p < .001$), aligning with the well-described motor facilitation effects of DBS. Regarding the modulation of anticipatory control, *congruency proportion* influenced the congruency effect for RTs as expected, leading to

larger congruency effects in blocks with a lower proportion of incongruent trials (i.e., unexpected conflict; β = 49.23, SE: 11.65, $p < .001$; paired t-test: $t(23) = -6.58$, $p < 0.001$; depicted in Supplementary Fig. SF3 (left), Appendix). In contrast to the congruency effect, the validity effect was not modulated by expectations (*validity proportion*).

Accuracy

Likewise to RTs, our LME analyses on accuracy resulted in main effects of *validity* (β = -3.70, SE = 0.69, $p < .001$) and *congruency* (β = -8.50, SE = 1.19, $p < .001$). As hypothesized, higher error rates were observed in invalid as opposed to valid and incongruent compared to congruent trials (Figure 2, C & D). Again, *validity* and *congruency* did not interact.

Regarding stimulation, accuracy was modulated in relation to trial congruency: a significant interaction between *congruency* and *stimulation* (β = 3.15, SE = 1.37, $p < .05$) revealed that the congruency effect on accuracy was amplified during DBS ON, with reduced errors on congruent trials but increased errors on incongruent trials (paired t-test: $t(23) = -3.37$, $p < 0.01$; Figure 2, D). Importantly, overall accuracy did not differ significantly between stimulation conditions when averaging across trial types (DBS ON: 90.58 ± 10.13%, DBS OFF: 90.09 ± 9.68% accuracy).

Similar to RTs, *congruency proportion* interacted with *congruency* for accuracy, such that blocks with a high congruency proportion (unexpected conflict resolution) elicited larger congruency effects (β = -3.57, SE = 1.37, $p < .01$; paired t-test: $t(23) = -4.59$, $p < 0.001$; as shown in Supplementary Fig. SF3 (right), Appendix).

In contrast to the accuracy congruency effect, the validity effect was not influenced by stimulation or expectations (*validity proportion*).

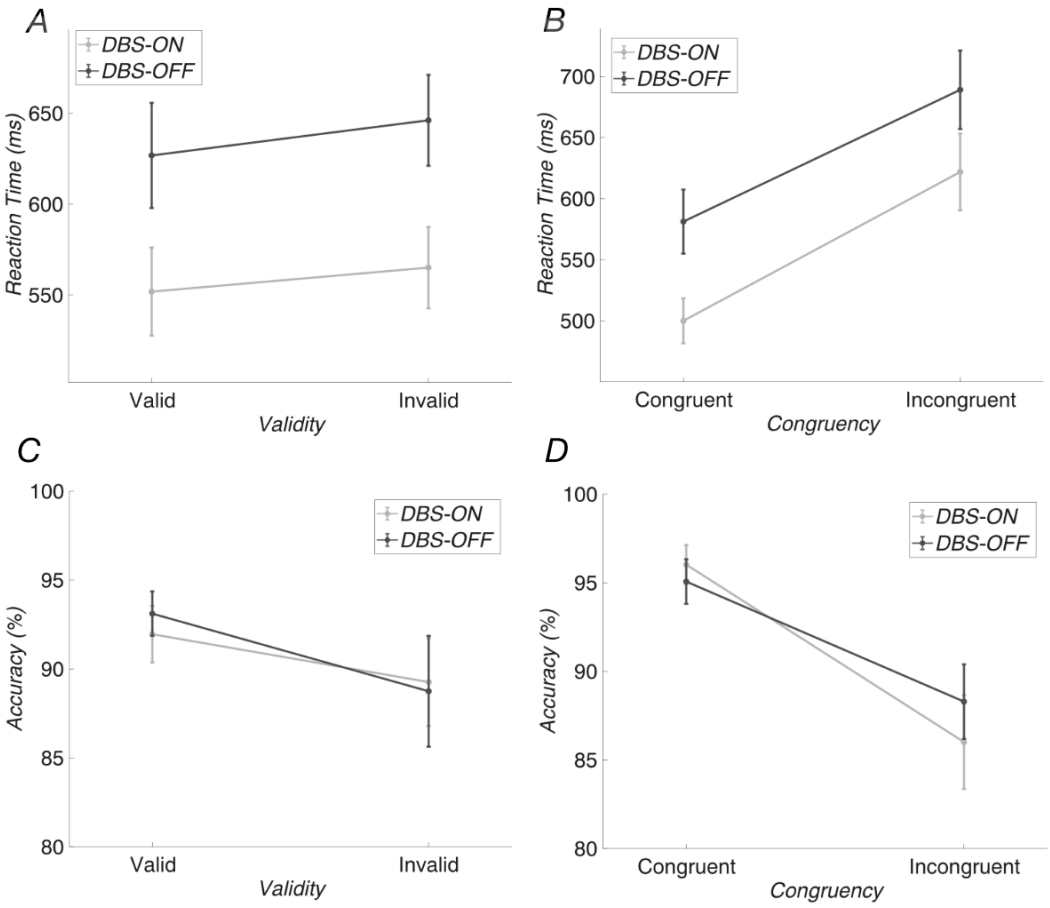

Fig. 2 A: RT validity effects for DBS-ON (light grey) and DBS-OFF (dark grey), showing slower responses for invalid trials (reprogramming) than valid trials (β = 14.22, SE: 5.83, $p < .05$) in both ON and OFF conditions. Stimulation shows a general speeding effect on responses (β = 78.55, SE: 5.83, $p < .001$). B: The RT congruency effect is apparent in slower responses for incongruent (conflict) compared to congruent trials (β = 94.35, SE: 8.24, $p < .001$) and is generally larger than the validity effect (see A). While stimulation leads to generally shorter RTs (β = 78.55, SE: 5.83, $p < .001$), there is no significant difference between RT congruency effects between DBS-ON (light grey) and DBS-OFF (dark grey). C: Depicted is the validity effect regarding accuracy, apparent as a significant accuracy decrease in invalid compared to valid conditions (β = -3.70, SE = 0.69, $p < .001$), for DBS-ON (light grey) and DBS-OFF (dark grey). D: Similarly, the congruency effect is visible as significantly lower accuracy scores in incongruent compared to congruent trials (β = -8.50, SE = 1.19, $p < .001$), which was more pronounced in DBS-ON (light grey) than DBS-OFF (dark grey). Accordingly, *congruency* interacted significantly with *stimulation* (β = 3.15, SE = 1.37, $p < .05$), presented as a larger difference (steeper slope) between incongruent and congruent accuracy scores when DBS was ON (light grey; paired t-test: $t(23) = -3.37$, $p < 0.01$), i.e., lower accuracy in incongruent and higher accuracy in congruent trials

4.2 Electrophysiological results

Target-locked beta power

Right-prefrontal beta synchronization

Our LME analysis of beta power in the "pause window" revealed a significant interaction between congruency and stimulation (β = 0.039, SE = 0.019, $p < .05$) at right-prefrontal regions, showing the expected increase of inhibitory beta synchronization upon conflict presentation. This was observed exclusively when stimulation was inactive (Figure 3).

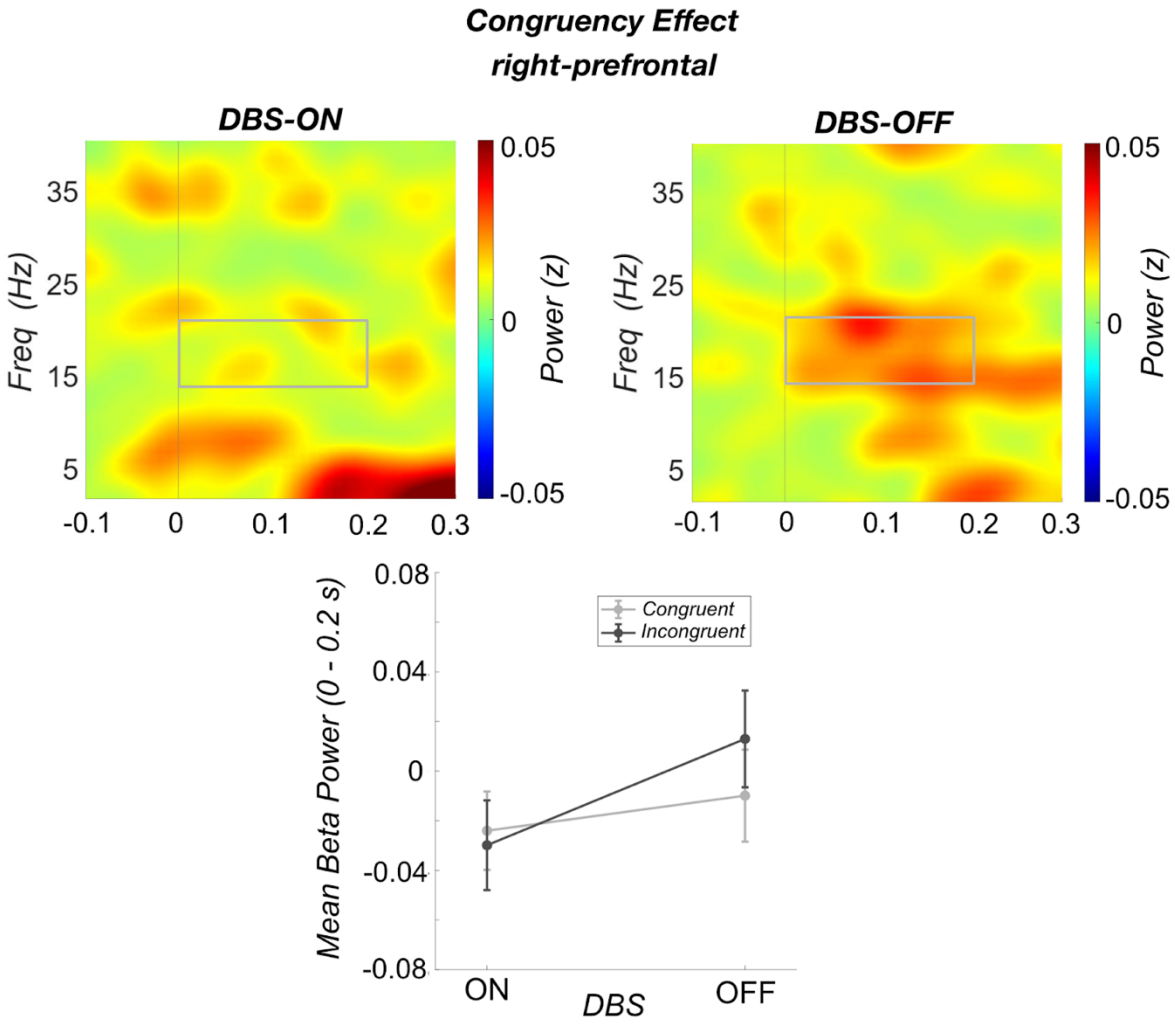

Fig. 3 Top: visualization of target-locked power differences ("pause window") between incongruent (conflict) and congruent trials for DBS-ON (left) and DBS-OFF (right) at right-prefrontal regions, which highlights the significant *congruency-by-stimulation* interaction. Increased beta synchronization between 0 and 0.2 sec. (grey square: window of interest) appeared only when stimulation was inactive. Bottom: line-graph visualization of the

congruency-by-stimulation interaction, showing average beta power (0 to 0.2 sec.) increases when trials were incongruent and stimulation was turned OFF

Response-locked beta power

Right-prefrontal and motor-cortical beta desynchronization

Motor-cortical and right-prefrontal regions revealed a significant main effect of *congruency* in our LME analysis for the "retune window" (motor-cortical region: β = -0.046, SE = 0.016, $p < .01$; right-prefrontal region: β = -0.048, SE = 0.014, $p < .001$). Incongruent trials exhibited a more pronounced beta desynchronization compared to congruent trials, in line with increased flexible control demands (see Figure 4).

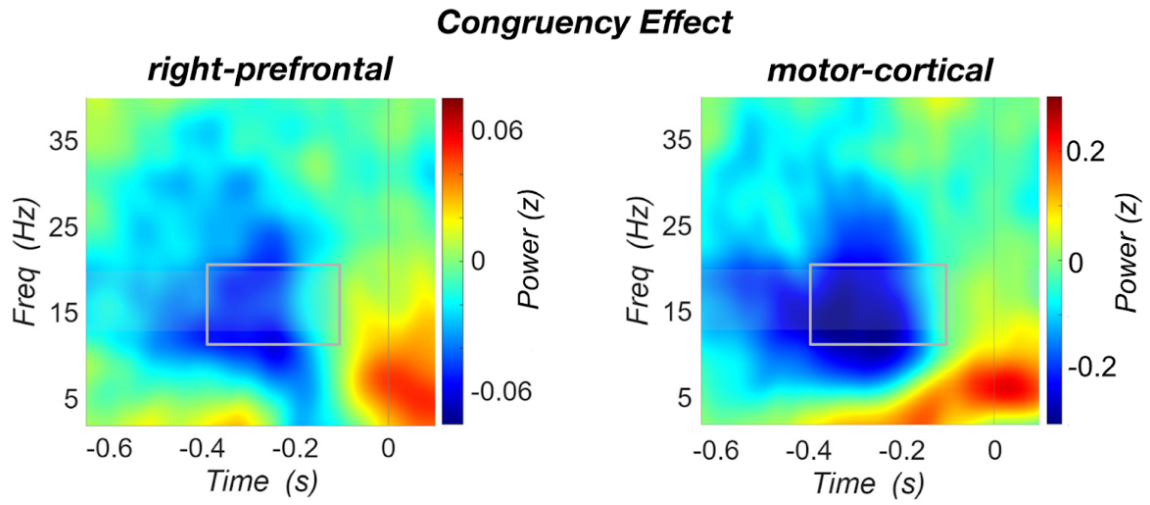

Fig. 4 Response-locked power differences ("retune window") between incongruent (conflict) and congruent trials at right-prefrontal (left) and motor-cortical (right) regions, showing enhanced beta desynchronization for incongruent trials. The grey square depicts our window of interest (-0.4 to -0.1 sec. pre-response and 13-20 Hz)

While no significant main effect of validity appeared in the planned analysis, right-prefrontal patterns pointed to a narrower region of interest that we explored post hoc, including only the FC2 channel. A time-sensitive calculation across each timepoint of our "retune window" revealed a significant *validity-by-stimulation* interaction at this channel, present between 350 to 235 ms pre-response (range: β = 0.064 to 0.078, SE = 0.032 to 0.033, p = 0.021 to 0.048, FDR-corrected) with enhanced beta desynchronization for invalid compared to valid trials (in line with increased flexible control demands in invalid trials). This

effect appeared exclusively when stimulation was inactive (Supplementary Fig. SF4, Appendix).

Beta desynchronization at the STN

The planned STN LME analysis of beta power in the "retune window" showed only marginal effects. Given the decreased number of observations at our STN channels, we conducted a more sensitive post hoc LME analysis at each time point of the "retune window". This revealed a significant congruency effect from 185 to 175 ms before response (β = -0.085, SE = 0.043, $p < .05$, FDR-corrected), which pointed into the same direction as the cortical regions: more pronounced beta desynchronization for incongruent compared to congruent trials (Figure 5). Additionally, there was a main effect of *stimulation*, appearing between 295-255 ms (range: β = –0.092 to –0.074, SE =0.035 to 0.040, p = 0.011 to 0.048, FDR-corrected) and between 185-95 ms pre-response (range: β = -0.120 to -0.082, SE = 0.039 to 0.047, p = 0.0034 to 0.045, FDR-corrected). This stimulation effect coincided with the congruency effect and depicted generally enhanced beta desynchronization when DBS was OFF (Supplementary Fig. SF5, Appendix).

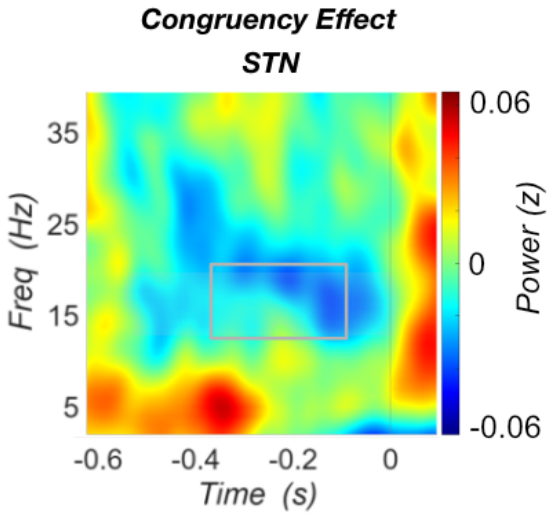

Fig. 5 STN response-locked power differences between incongruent (conflict) and congruent trials. The grey square indicates the window of interest: beta power (13-20 Hz) and the "retune" time window (-0.4 to -0.1 sec. pre-response), presenting amplified beta desynchronization in incongruent trials

RTs and error rates are connected to response-locked beta power at the STN

Our LME analysis revealed a significant interaction between trial-wise STN beta power and stimulation status for predicting RTs (β = - 23.60, SE = 11.62, $p < .05$). Post hoc analyses of separated conditions showed that the "speeding" effect of increased beta power was only significant when stimulation was inactive (β = -33.58, SE = 11.62, $p < .05$). The association of beta power and RTs with inactive stimulation is illustrated in Figure 6 (left).

Regarding accuracy, beta power interacted significantly with *validity* and *congruency* to predict error probability (β = 2.26, SE = 0.71, $p < 0.01$). A post hoc evaluation of separate conditions showed that in trials requiring both response reprogramming and conflict resolution (i.e., invalid-incongruent trials), increased beta power predicted higher error rates (β = 0.69, SE = 0.22, $p < 0.01$). In contrast, response reprogramming alone, i.e., the invalid-congruent condition, showed a significant negative association of beta power with error probability (β = -1.21, SE = 0.34, $p < .001$). The difference between invalid-incongruent and invalid-congruent trials was significant ($p < .001$, Bonferroni-corrected). In contrast, valid-congruent trials, which do not require flexible response adaptations, and valid-incongruent trials, which require solely conflict resolution, showed no significant association of beta power with error rates. These results underscore the particular importance of beta dynamics in situations with amplified demand for flexible response adaptations. The relationship between beta power, the significant trial conditions and predicted error rate is visualized in Figure 6. (right).

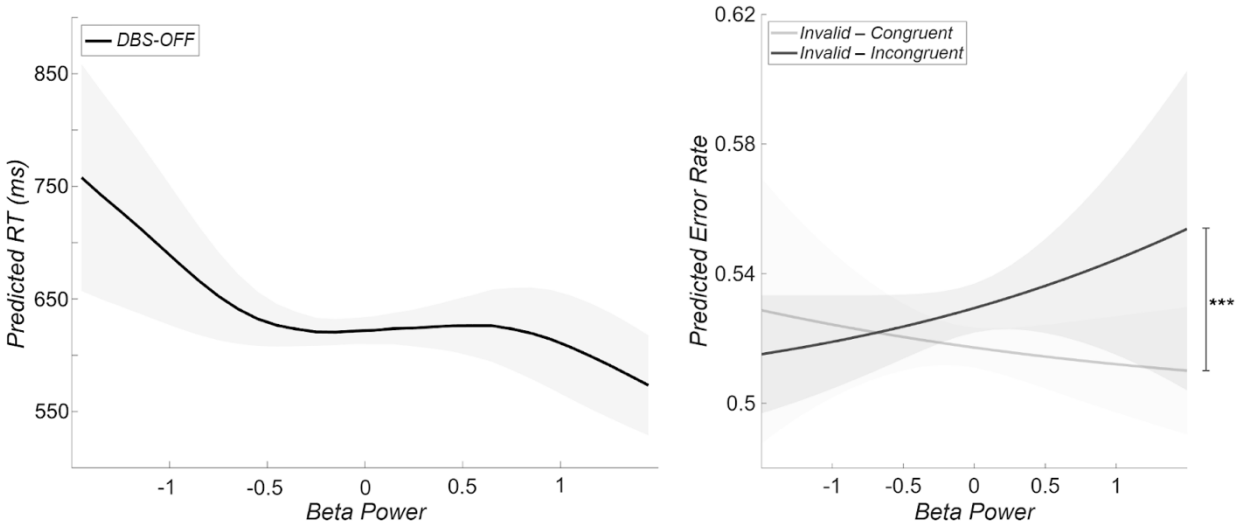

Fig. 6 Left: predicted RTs for the significant DBS OFF condition (y-axis) were plotted against STN beta power (x-axis) by sorting trials into 30 equal-sized bins based on predicted beta magnitude, in order to adequately represent dynamic patterns across the large number of trial observations. The figure displays the negative association of RTs with increasing beta power (slower responses with decreased beta power, particularly at low magnitudes; β = -33.58, SE = 11.62, $p < .05$). Within each bin, the mean model-predicted RT was computed and smoothed using a Gaussian kernel (window size = 15) to show central patterns (excluding random effects). The shaded regions depict 95% confidence intervals, as estimated from the predicted distribution. The z-scored beta values in this figure are restricted to a range between -1.5 and 1.5, showing the central distribution to enhance interpretability. Right: predicted error rates for significant condition effects. Slopes for invalid-congruent (reprogramming: light grey) and invalid-incongruent (reprogramming and conflict resolution: dark grey) trials were derived from the fixed effects (*validity*, *congruency* and *beta power*) of a generalized linear mixed-effects model using a logistic link function and excluding random effects to illustrate average trends across participants. They were computed separately for the different effect levels. Confidence intervals (95%) were calculated by converting the predicted log-odds and their bounds into error rate probabilities using the logistic function. Invalid-congruent (β = -1.21, SE = 0.34, $p < .001$) and invalid-incongruent conditions (β = 0.69, SE = 0.22, $p < 0.01$) differed significantly in their relationship with beta ($p < .001$), showing a positive association for invalid-incongruent trials (increased beta power predicts higher error probability) and a negative association for invalid-congruent trials (increased beta power decreases error probability). Depicted are again only the z-scored beta values ranging from -1.5 to 1.5, to reduce the visual influence of values at the distribution's tail.

5. Discussion

In this combined EEG-LFP study in people with Parkinson's disease receiving STN DBS, we aimed to delineate two response control mechanisms - response reprogramming and conflict

resolution - by investigating their putatively shared mechanisms within fronto-subthalamic pathways. Specifically, we focused on beta dynamics as a proposed general mechanism that governs cognitive-behavioral inhibition and flexibility (e.g., Wessel & Anderson, 2024).

On a behavioral level, we observed performance costs for both response reprogramming and conflict resolution (increased RTs and error rates), and a DBS-effect on conflict resolution (increased error rates). EEG recordings showed control-related beta dynamics reflecting a reactive "pause" and subsequent "retuning" of responses. Specifically, we found an initial conflict-related beta synchronization at right-prefrontal regions when stimulation was inactive, relating to the inhibitory "pause". Subsequently, a pronounced beta desynchronization appeared at motor-cortical and right-prefrontal regions for conflict resolution (independent of stimulation), while reprogramming-related desynchronization localized to a more confined right-prefrontal site during this time window (when stimulation was inactive). The STN showed similarly enhanced beta desynchronization during conflict resolution as present in the cortical EEG (also unaffected by stimulation) and no significant beta modulation during reprogramming. Furthermore, higher STN beta power predicted faster RTs when stimulation was inactive, and increased error rates when response reprogramming and conflict resolution coincided.

In line with recent literature (e.g., Wessel & Anderson, 2024), our data suggest that beta dynamics not only affect motor-related processes but rather serve a domain-general control function in fronto-subthalamic pathways, integrating cognitive-behavioral demands for flexible response regulation and adaptation.

5.1 Behavioral costs of reprogramming and conflict resolution with DBS

Generally, participants exhibited significantly faster RTs when stimulation was ON, aligning with the expected improvement in motor execution. In contrast, we found no general stimulation effect on accuracy, indicating that DBS did not affect correct responding per se.

Invalid trials, demanding response reprogramming, were associated with increased control demands for the cancellation of the prepared and programming of an alternative response. In line with this, we found the expected higher error rates and RTs when a response

cue was invalid compared to valid, reflecting the "validity effect". Conflict resolution, required in incongruent trials, is also related to increased control demands to inhibit distracting flanker arrows. Accordingly, we found the expected increase in error rates and RTs for incongruent trials compared to congruent trials, also described as the "congruency effect". These behavioral patterns are consistent with findings from healthy participants performing the same task (Sauter et al., 2024), as well as prior studies on motor response cueing (e.g., Kuhns et al., 2017) and flanker conflict tasks (e.g., Derosiere et al., 2018). However, we observed no significant interaction between the validity and congruency effects on behavioral outcomes. This contrasts with findings from Sauter et al. (2024), where such an interaction was observed in young, healthy participants using the same task. The discrepancy may be attributed to differences in the investigated samples, mainly because our cohort consisted of elderly people with Parkinson's disease. Furthermore, the congruency effect was notably dominant over the validity effect in this population. We can think of two plausible reasons for this finding. Firstly, a stronger susceptibility to flanker interference may be attributed to general deficits in inhibitory control mechanisms, which are commonly affected in Parkinson's disease. A study by Wylie et al. (2009), for example, compared the flanker congruency effect in people with Parkinson's disease (on their regular medication) and controls and found that the Parkinson's disease group exhibited larger congruency effects. Secondly, recent research indicates general motor preparation deficits in people with Parkinson's disease compared to healthy controls, which is unaffected by DBS state (Wilhelm et al., 2024). Attenuated response preparation would decrease reprogramming costs for invalid trials, leading to smaller validity effects. Accordingly, we found no influence of stimulation on the behavioral validity effect. Moreover, the validity effect did not adapt to anticipatory control variations (validity proportion).

In contrast, anticipatory control regarding conflict (congruency proportion) influenced the congruency effect as hypothesized, showing larger conflict costs and congruency effects when incongruent trials were unexpected. This aligns with prior findings suggesting that unexpected conflict demands increased reliance on reactive control, thereby amplifying conflict interference effects (e.g., Braver, 2012; Duque et al., 2016). It should be noted that some alternative accounts propose that conflict adaptation effects may partly reflect lower-

level learning effects (e.g., J. R. Schmidt, 2019), rather than top-down control. Potentially, the lack of an expectational modulation on the validity effect (validity proportion) may hint at dissociative anticipatory control mechanisms regarding reprogramming and conflict expectations. This may also relate to the task design, as people with Parkinson's disease have shown reduced updating capacities (Salmi et al., 2020). While they were externally informed about the frequency of upcoming conflict, this may have promoted stable strategic adjustments even if probability learning was impaired. In contrast, the frequency of invalid trials had to be inferred implicitly through trial-by-trial updating. As we focused on the target-response period for our neural results, these implications warrant further investigations that can differentiate correlates of anticipatory control between response and conflict expectations and their modulation by Parkinson's disease pathogenesis and DBS.

Next to these findings, our results revealed that stimulation interacted with accuracy, with significantly larger congruency effects observed when stimulation was active. This was characterized by increased errors in incongruent trials, consistent with literature suggesting that stimulation may enhance impulsivity and impair the suppression of automated or prepotent responses, leading to difficulties in conflict resolution (e.g., Frank et al., 2007).

5.2 Beta dynamics of reactive control

We focused on beta-related synchronization and desynchronization (peaks and troughs) relating to reactive control during reprogramming and conflict resolution, which was analyzed in two distinct time windows. For one, we investigated beta averages around 150 ms after target presentation, which is associated with reactive inhibition during a global "pause" (Hervault & Wessel, 2025; Wessel & Aron, 2017). This broad inhibition is commonly linked to right-prefrontal and STN beta synchronization (e.g., Daniel et al., 2023; Wessel, 2020).

We observed this signature at right-prefrontal regions when conflict was presented and stimulation was inactive. This demonstrates on the one hand, that this inhibitory beta-signature, originally proposed for outright motor inhibition (e.g. Aron et al., 2007), is similarly related to conflict-related inhibition, which supports a domain-general role of beta in inhibitory control processes (e.g., Wessel & Anderson, 2024). Furthermore, stimulation of the STN interfered with this inhibitory beta synchronization, which may relate to the increased

error rates observed in incongruent trials and the general notion of reduced inhibitory control under stimulation (e.g. Frank et al., 2007). We did not find a beta-related conflict signature in the STN, which may be partly attributed to the reduced sample size at the STN. Furthermore, invalid trials (reprogramming) did not elicit the expected beta synchronization during this time window in our regions of interest. However, as discussed in the previous section, impaired motor preparation in Parkinson's disease may lead to reduced inhibitory demand when the prepared response needs to be cancelled (invalid trials) (Wilhelm et al., 2024). This could explain the missing inhibitory beta signature.

In our second time window, we analyzed beta averages during the response "retune" stage, around 200 ms before responding. This relates to a window of selective response adaptations (Hervault & Wessel, 2025), during which amplified beta desynchronization was for example observed during conflict resolution (Brittain et al., 2012). Consistent with prior research, we anticipated pronounced beta desynchronization during top-down processing in this time window, relating to reprogramming (invalid trials) and conflict resolution (incongruent trials) in our task. Beta desynchronization is thought to allow enhanced flexibility for response adaptations (e.g., R. Schmidt et al., 2019). As hypothesized, our analysis revealed a significantly amplified beta desynchronization during conflict resolution at right-prefrontal, motor-cortical and STN regions. Notably, this effect was present only shortly at the STN, as revealed in a post hoc analysis. Given the smaller sample size for STN recordings compared to cortical EEG data, this could again be attributed to reduced statistical power. The same post hoc analysis also revealed an effect of stimulation concurrently to the congruency effect, which lasted for more than 100 ms. This stimulation effect was characterized by stronger beta desynchronization when stimulation was OFF, which could be explained by a generally attenuated beta dynamic (flatter peaks as well as troughs) when stimulation is ON. As DBS suppresses beta power in a general manner (e.g. Kühn et al., 2006), it may leave less flexibility to adapt to contextual demand despite reducing overall inhibition (e.g. Little & Brown, 2014).

In contrast to conflict resolution, reprogramming did not elicit characteristic beta desynchronization at our regions of interest. To explore a more confined right-prefrontal localization, we conducted a time-sensitive post hoc analysis on the FC2 channel. In fact, this channel exhibited a significant *validity-by-stimulation* interaction for beta power, with

amplified beta desynchronization for invalid compared to valid trials, but exclusively when stimulation was inactive. This is in contrast to the desynchronization effects for conflict resolution during the "retune window", which were insensitive to stimulation. It is likely that during this time window, reprogramming and conflict resolution require distinct control processes, which relate to a new response activation for reprogramming and sustained inhibition for conflict (Bestmann & Duque, 2016). These processes may be differently affected by stimulation. Further research is needed to elucidate the timing and signature of reprogramming stages in greater detail.

5.3 Behavioral performance is predicted by pre-response STN beta power

We explored whether control-related STN beta dynamics during the "retune window" may be reflected in behavioral outcomes. For prediction of RTs, our analysis revealed a significant interaction between beta power and stimulation, which related to the OFF condition. In detail, increased beta power correlated with faster RTs when DBS was inactive, which is in line with heightened readiness and lowered flexibility reported for higher beta levels (e.g., Pierrieau et al., 2025). Lower beta power during DBS-OFF was accordingly associated with slower RTs. This is in line with a recent study by Pierrieau et al. (2025), which proposes that beta desynchronization relates to motor flexibility, predicting RTs in relation to the task's performance parameters. Consequently, the relationship of RTs and beta power during the "retune" window would be context-dependent. In our case, increased adaptation demands upon reprogramming or conflict were related to stronger desynchronization, which appears to be complemented with slower RTs to prevent premature responses. Pierrieau et al. (2025) focused on cortical beta dynamics, while Herz et al. (2023) found similar associations at the STN, with lower beta power relating to greater performance-related adjustments. Our findings corroborate the importance of STN beta in performance-related response tuning. Stimulation seems to flatten beta band dynamics (e.g., Kühn et al., 2006), which could explain the specificity to the OFF state.

With regard to error rates, our analysis revealed a significant three-way interaction between *validity, congruency*, and *beta power*. Notably, in valid-congruent trials - where neither response reprogramming nor conflict resolution was required - and valid-incongruent

trials - necessitating conflict resolution alone - error rates were not significantly affected by beta dynamics. However, in case reprogramming and conflict control demands coincided (invalid-incongruent trials), beta power at the STN was associated with increased errors. This is in line with a reduced capacity for flexible response adaptations at higher beta levels (e.g., Pierrieau et al., 2025). In contrast, invalid-congruent trials, i.e., trials requiring only reprogramming, beta power showed a significant negative association with error probability (protective effect). However, this entails further considerations. With regard to our analysis of beta desynchronization in invalid trials, we observed a reprogramming-related desynchronization only when stimulation was OFF. At the STN, stimulation generally attenuated beta dynamics, leading to higher beta power in this time window when stimulation was ON compared to OFF. Speculatively, since desynchronization of STN beta in this time window is therefore associated with the OFF condition (where the beta "validity effect" was present), the finding that lower beta power in invalid-congruent trials predicts increased errors may simply hinge on its association with the OFF condition, where reprogramming costs may have been higher. Taken together, these results emphasize the shared reliance of reprogramming and conflict-related control processes on STN beta dynamics, especially in case of multiple control demands.

5.4 Clinical context and implications

Beta dynamics have emerged as critical biomarkers for tailoring Parkinson's disease treatments, particularly in the development of adaptive DBS systems. Unlike continuous stimulation, adaptive DBS adjusts in real-time to motor control demands, reducing side effects and conserving energy (e.g., Priori et al., 2013)

Thus far, beta activity has predominantly been used to track motor symptoms of Parkinson's disease. Our results show that beta dynamics, both cortically and in the STN, are critically involved in cognitive as well as executive functions. This raises the question whether cognitive functions may be influenced by adaptive DBS protocols that use beta power as the predominant input signal. Future studies might want to address this both from a basic research perspective and from a clinical point of view.

6. Limitations

Participants completed the sessions on their regular dopaminergic medication, in order to facilitate task engagement and minimize side effects during the extended testing period. While medication may aid in isolating the effects of DBS, it could have influenced our data due to fluctuations in dopamine levels over time. However, we expect that randomization sufficiently balanced these effects across participants. Future studies could consider assessing participants both with and without medication and with a matched group of healthy controls, to better disentangle the individual effects of pharmacological treatment and DBS on the current results, as well as that of Parkinson's disease pathology itself.

Another limitation is the reduced number of observations regarding the STN data. Further studies could replicate these effects in a larger sample and conduct coherence analyses to gain a more comprehensive understanding of the robustness, directionality and interdependence of our reported findings.

7. Conclusions

In sum, our findings support the account that fronto-subthalamic beta dynamics constitute a general control process that governs flexibility and inhibition during response reprogramming and conflict resolution. Nonetheless, while these processes seem to rely on the same beta functions, a dominant congruency effect and variations in their manifestation suggest that the same control architecture was deployed in partially distinct ways, relating to different demands for response adjustments. Accordingly, DBS affected reprogramming and conflict signatures at different time points.

Moreover, pre-response beta power at the STN predicted behavioral outcome, showing reduced flexibility in relation to higher beta power, which manifested in faster RTs and higher error rates. This relationship with error rates was exclusively found when reprogramming and conflict resolution coincided, thus when the demand for flexible response adaptations was elevated. These results contribute to a growing understanding of how the STN flexibly supports control processes across domains in concert with shared beta dynamics.

8. References

Appleby, B. S., Duggan, P. S., Regenberg, A., & Rabins, P. V. (2007). Psychiatric and neuropsychiatric adverse events associated with deep brain stimulation: A meta-analysis of ten years' experience: Psychiatric and Neuropsychiatric Adverse Events. Movement Disorders, 22(12), 1722–1728. https://doi.org/10.1002/mds.21551

Aron, A. R., Behrens, T. E., Smith, S., Frank, M. J., & Poldrack, R. A. (2007). Triangulating a Cognitive Control Network Using Diffusion-Weighted Magnetic Resonance Imaging (MRI) and Functional MRI. Journal of Neuroscience, 27(14), 3743–3752. https://doi.org/10.1523/JNEUROSCI.0519-07.2007

Beck, A. T., Ward, C. H., Mendelson, M., Mock, J., & Erbauch, J. (2011). Beck Depression Inventory [Dataset]. https://doi.org/10.1037/t00741-000

Bestmann, S., & Duque, J. (2016). Transcranial Magnetic Stimulation: Decomposing the Processes Underlying Action Preparation. The Neuroscientist, 22(4), 392–405. https://doi.org/10.1177/1073858415592594

Bestmann, S., Harrison, L. M., Blankenburg, F., Mars, R. B., Haggard, P., Friston, K. J., & Rothwell, J. C. (2008). Influence of Uncertainty and Surprise on Human Corticospinal Excitability during Preparation for Action. Current Biology, 18(10), 775–780. https://doi.org/10.1016/j.cub.2008.04.051

Bonnevie, T., & Zaghloul, K. A. (2019). The Subthalamic Nucleus: Unravelling New Roles and Mechanisms in the Control of Action. The Neuroscientist, 25(1), 48–64. https://doi.org/10.1177/1073858418763594

Braem, S., Bugg, J. M., Schmidt, J. R., Crump, M. J. C., Weissman, D. H., Notebaert, W., & Egner, T. (2019). Measuring Adaptive Control in Conflict Tasks. Trends in Cognitive Sciences, 23(9), 769–783. https://doi.org/10.1016/j.tics.2019.07.002

Braver, T. S. (2012). The variable nature of cognitive control: A dual mechanisms framework. Trends in Cognitive Sciences, 16(2), 106–113. https://doi.org/10.1016/j.tics.2011.12.010

Brittain, J.-S., Watkins, K. E., Joundi, R. A., Ray, N. J., Holland, P., Green, A. L., Aziz, T. Z., & Jenkinson, N. (2012). A Role for the Subthalamic Nucleus in Response Inhibition during Conflict. The Journal of Neuroscience, 32(39), 13396–13401. https://doi.org/10.1523/JNEUROSCI.2259-12.2012

Brown, P. (2003). Oscillatory nature of human basal ganglia activity: Relationship to the pathophysiology of Parkinson's disease. Movement Disorders, 18(4), 357–363. https://doi.org/10.1002/mds.10358

Chandrasekaran, C., Bray, I. E., & Shenoy, K. V. (2019). Frequency Shifts and Depth Dependence of Premotor Beta Band Activity during Perceptual Decision-Making. The Journal of Neuroscience, 39(8), 1420–1435. https://doi.org/10.1523/JNEUROSCI.1066-18.2018

Chen, W., de Hemptinne, C., Miller, A. M., Leibbrand, M., Little, S. J., Lim, D. A., Larson, P. S., & Starr, P. A. (2020). Prefrontal-Subthalamic Hyperdirect Pathway Modulates Movement Inhibition in Humans. Neuron, 106(4), 579-588.e3. https://doi.org/10.1016/j.neuron.2020.02.012

Chen, X., Scangos, K. W., & Stuphorn, V. (2010). Supplementary motor area exerts proactive and reactive control of arm movements. The Journal of Neuroscience: The Official Journal of the Society for Neuroscience, 30(44), 14657–14675. https://doi.org/10.1523/JNEUROSCI.2669-10.2010

Chikermane, M., Weerdmeester, L., Rajamani, N., Köhler, R. M., Merk, T., Vanhoecke, J., Horn, A., & Neumann, W. J. (2024). Cortical beta oscillations map to shared brain networks modulated by dopamine. eLife, 13, RP97184. https://doi.org/10.7554/eLife.97184.3

Cohen, M. X., & Donner, T. H. (2013). Midfrontal conflict-related theta-band power reflects neural oscillations that predict behavior. Journal of Neurophysiology, 110(12), 2752–2763. https://doi.org/10.1152/jn.00479.2013

Daniel, P. L., Bonaiuto, J. J., Bestmann, S., Aron, A. R., & Little, S. (2023). High precision magnetoencephalography reveals increased right-inferior frontal gyrus beta power during response conflict. Cortex, 158, 127–136. https://doi.org/10.1016/j.cortex.2022.10.007

Delorme, A., & Makeig, S. (2004). EEGLAB: An open source toolbox for analysis of single-trial EEG dynamics including independent component analysis. Journal of Neuroscience Methods, 134(1), 9–21. https://doi.org/10.1016/j.jneumeth.2003.10.009

Derosiere, G., Klein, P.-A., Nozaradan, S., Zénon, A., Mouraux, A., & Duque, J. (2018). Visuomotor Correlates of Conflict Expectation in the Context of Motor Decisions. The Journal of Neuroscience, 38(44), 9486–9504. https://doi.org/10.1523/JNEUROSCI.0623-18.2018

Dubey, A., Markowitz, D. A., & Pesaran, B. (2023). Top-down control of exogenous attentional selection is mediated by beta coherence in prefrontal cortex. Neuron, 111(20), 3321-3334.e5. https://doi.org/10.1016/j.neuron.2023.06.025

Duque, J., Petitjean, C., & Swinnen, S. P. (2016). Effect of Aging on Motor Inhibition during Action Preparation under Sensory Conflict. Frontiers in Aging Neuroscience, 8. https://doi.org/10.3389/fnagi.2016.00322

Frank, M. J., Samanta, J., Moustafa, A. A., & Sherman, S. J. (2007). Hold your horses: Impulsivity, deep brain stimulation, and medication in parkinsonism. Science (New York, N.Y.), 318(5854), 1309–1312. https://doi.org/10.1126/science.1146157

Hammond, C., Bergman, H., & Brown, P. (2007). Pathological synchronization in Parkinson's disease: Networks, models and treatments. Trends in Neurosciences, 30(7), 357–364. https://doi.org/10.1016/j.tins.2007.05.004

Hervault, M., & Wessel, J. R. (2025). Common and Unique Neurophysiological Processes That Support the Stopping and Revising of Actions. The Journal of Neuroscience, 45(13), e1537242025. https://doi.org/10.1523/JNEUROSCI.1537-24.2025

Herz, D. M., Bange, M., Gonzalez-Escamilla, G., Auer, M., Ashkan, K., Fischer, P., Tan, H., Bogacz, R., Muthuraman, M., Groppa, S., & Brown, P. (2022). Dynamic control of decision and movement speed in the human basal ganglia. Nature Communications, 13(1), 7530. https://doi.org/10.1038/s41467-022-35121-8

Herz, D. M., Bange, M., Gonzalez-Escamilla, G., Auer, M., Muthuraman, M., Glaser, M., Bogacz, R., Pogosyan, A., Tan, H., Groppa, S., & Brown, P. (2023). Dynamic modulation of subthalamic nucleus activity facilitates adaptive behavior. PLOS Biology, 21(6), e3002140. https://doi.org/10.1371/journal.pbio.3002140

Iglesias, S., Mathys, C., Brodersen, K. H., Kasper, L., Piccirelli, M., DenOuden, H. E. M., & Stephan, K. E. (2013). Hierarchical Prediction Errors in Midbrain and Basal Forebrain during Sensory Learning. Neuron, 80(2), 519–530. https://doi.org/10.1016/j.neuron.2013.09.009

Iskhakova, L., Rappel, P., Deffains, M., Fonar, G., Marmor, O., Paz, R., Israel, Z., Eitan, R., & Bergman, H. (2021). Modulation of dopamine tone induces frequency shifts in cortico-basal ganglia beta oscillations. Nature Communications, 12(1). https://doi.org/10.1038/s41467-021-27375-5

Jahanshahi, M., Obeso, I., Rothwell, J. C., & Obeso, J. A. (2015). A fronto–striato–subthalamic–pallidal network for goal-directed and habitual inhibition. Nature Reviews Neuroscience, 16(12), 719–732. https://doi.org/10.1038/nrn4038

Kilavik, B. E., Zaepffel, M., Brovelli, A., MacKay, W. A., & Riehle, A. (2013). The ups and downs of beta oscillations in sensorimotor cortex. Experimental Neurology, 245, 15–26. https://doi.org/10.1016/j.expneurol.2012.09.014

Kuhns, A. B., Dombert, P. L., Mengotti, P., Fink, G. R., & Vossel, S. (2017). Spatial Attention, Motor Intention, and Bayesian Cue Predictability in the Human Brain. The Journal of Neuroscience, 37(21), 5334–5344. https://doi.org/10.1523/JNEUROSCI.3255-16.2017

Leventhal, D. K., Gage, G. J., Schmidt, R., Pettibone, J. R., Case, A. C., & Berke, J. D. (2012). Basal Ganglia Beta Oscillations Accompany Cue Utilization. Neuron, 73(3), 523–536. https://doi.org/10.1016/j.neuron.2011.11.032

Little, S., & Brown, P. (2014). The functional role of beta oscillations in Parkinson's disease. Parkinsonism & Related Disorders, 20, S44–S48. https://doi.org/10.1016/S1353-8020(13)70013-0

Mars, R. B., Piekema, C., Coles, M. G. H., Hulstijn, W., & Toni, I. (2007). On the programming and reprogramming of actions. Cerebral Cortex, 17(12), 2972–2979. https://doi.org/10.1093/cercor/bhm022

Matuschek, H., Kliegl, R., Vasishth, S., Baayen, H., & Bates, D. (2017). Balancing Type I error and power in linear mixed models. Journal of Memory and Language, 94, 305–315. https://doi.org/10.1016/j.jml.2017.01.001

Nasreddine, Z. S., Phillips, N. A., Bédirian, V., Charbonneau, S., Whitehead, V., Collin, I., Cummings, J. L., & Chertkow, H. (2014). Montreal Cognitive Assessment [Dataset]. https://doi.org/10.1037/t27279-000

Neumann, W., Degen, K., Schneider, G., Brücke, C., Huebl, J., Brown, P., & Kühn, A. A. (2016). Subthalamic synchronized oscillatory activity correlates with motor impairment in patients with Parkinson's disease. Movement Disorders, 31(11), 1748–1751. https://doi.org/10.1002/mds.26759

Nilsson, M. H., Hariz, G.-M., Wictorin, K., Miller, M., Forsgren, L., & Hagell, P. (2010). Development and testing of a self administered version of the Freezing of Gait Questionnaire. BMC Neurology, 10, 85. https://doi.org/10.1186/1471-2377-10-85

Niv, Y., Daw, N. D., Joel, D., & Dayan, P. (2007). Tonic dopamine: Opportunity costs and the control of response vigor. Psychopharmacology, 191(3), 507–520. https://doi.org/10.1007/s00213-006-0502-4

Nougaret, S., Fascianelli, V., Ravel, S., & Genovesio, A. (2021). Intrinsic timescales across the basal ganglia. Scientific Reports, 11(1), 21395. https://doi.org/10.1038/s41598-021-00512-2

Nougaret, S., López-Galdo, L., Caytan, E., Poitreau, J., Barthélemy, F. V., & Kilavik, B. E. (2024). Low and high beta rhythms have different motor cortical sources and distinct roles in movement control and spatiotemporal attention. PLOS Biology, 22(6), e3002670. https://doi.org/10.1371/journal.pbio.3002670

Oostenveld, R., Fries, P., Maris, E., & Schoffelen, J.-M. (2011). FieldTrip: Open Source Software for Advanced Analysis of MEG, EEG, and Invasive Electrophysiological Data. Computational Intelligence and Neuroscience, 2011, 1–9. https://doi.org/10.1155/2011/156869

Patton, J. H., Stanford, M. S., & Barratt, E. S. (2011). Barratt Impulsiveness Scale-11 [Dataset]. https://doi.org/10.1037/t05661-000

Pierrieau, E., Dussard, C., Plantey--Veux, A., Guerrini, C., Lau, B., Pillette, L., George, N., & Jeunet-Kelway, C. (2025). Changes in cortical beta power predict motor control flexibility, not vigor. Communications Biology, 8(1). https://doi.org/10.1038/s42003-025-08465-2

Priori, A., Foffani, G., Rossi, L., & Marceglia, S. (2013). Adaptive deep brain stimulation (aDBS) controlled by local field potential oscillations. Experimental Neurology, 245, 77–86. https://doi.org/10.1016/j.expneurol.2012.09.013

Ridderinkhof, K. R., Van Den Wildenberg, W. P. M., Segalowitz, S. J., & Carter, C. S. (2004). Neurocognitive mechanisms of cognitive control: The role of prefrontal cortex in action selection, response inhibition, performance monitoring, and reward-based learning. Brain and Cognition, 56(2), 129–140. https://doi.org/10.1016/j.bandc.2004.09.016

Rosenbaum, D. A., & Kornblum, S. (1982). A priming method for investigating the selection of motor responses. Acta Psychologica, 51(3), 223–243. https://doi.org/10.1016/0001-6918(82)90036-1

Rushworth, M. F. S., Ellison, A., & Walsh, V. (2001). Complementary localization and lateralization of orienting and motor attention. Nature Neuroscience, 4(6), 656–661. https://doi.org/10.1038/88492

Rushworth, M. F. S., Nixon, P. D., Renowden, S., Wade, D. T., & Passingham, R. E. (1997). The left parietal cortex and motor attention. Neuropsychologia, 35(9), 1261–1273.

Salmi, J., Ritakallio, L., Fellman, D., Ellfolk, U., Rinne, J. O., & Laine, M. (2020). Disentangling the Role of Working Memory in Parkinson's Disease. Frontiers in Aging Neuroscience, 12. https://doi.org/10.3389/fnagi.2020.572037

Sauter, A. E., Zabicki, A., Schüller, T., Baldermann, J. C., Fink, G. R., Mengotti, P., & Vossel, S. (2024). Response and conflict expectations shape motor responses interactively. Experimental Brain Research, 242(11), 2599–2612. https://doi.org/10.1007/s00221-024-06920-w

Schmidt, J. R. (2019). Evidence against conflict monitoring and adaptation: An updated review. Psychonomic Bulletin & Review, 26(3), 753–771. https://doi.org/10.3758/s13423-018-1520-z

Schmidt, R., Herrojo Ruiz, M., Kilavik, B. E., Lundqvist, M., Starr, P. A., & Aron, A. R. (2019). Beta Oscillations in Working Memory, Executive Control of Movement and Thought, and Sensorimotor Function. The Journal of Neuroscience, 39(42), 8231–8238. https://doi.org/10.1523/JNEUROSCI.1163-19.2019

Soh, C., Hervault, M., Rohl, A. H., Greenlee, J. D. W., & Wessel, J. R. (2025). Precisely-timed outpatient recordings of subcortical local field potentials from wireless streaming-capable deep-brain stimulators: A method and toolbox. Journal of Neuroscience Methods, 418, 110448. https://doi.org/10.1016/j.jneumeth.2025.110448

Spitzer, B., & Haegens, S. (2017). Beyond the Status Quo: A Role for Beta Oscillations in Endogenous Content (Re)Activation. Eneuro, 4(4), ENEURO.0170-17.2017. https://doi.org/10.1523/ENEURO.0170-17.2017

Tan, H., Wade, C., & Brown, P. (2016). Post-Movement Beta Activity in Sensorimotor Cortex Indexes Confidence in the Estimations from Internal Models. The Journal of Neuroscience, 36(5), 1516–1528. https://doi.org/10.1523/JNEUROSCI.3204-15.2016

Weintraub, D., Mamikonyan, E., Papay, K., Shea, J. A., Xie, S. X., & Siderowf, A. (2012). Questionnaire for impulsive-compulsive disorders in Parkinson's Disease-Rating Scale: Quip-RS. Movement Disorders, 27(2), 242–247. https://doi.org/10.1002/mds.24023

Wessel, J. R., & Anderson, M. C. (2024). Neural mechanisms of domain-general inhibitory control. Trends in Cognitive Sciences, 28(2), 124–143. https://doi.org/10.1016/j.tics.2023.09.008

Wessel, J. R., Diesburg, D. A., Chalkley, N. H., & Greenlee, J. D. W. (2022). A causal role for the human subthalamic nucleus in non-selective cortico-motor inhibition. Current Biology, 32(17), 3785-3791.e3. https://doi.org/10.1016/j.cub.2022.06.067

Wessel, J. R., Waller, D. A., & Greenlee, J. D. (2019). Non-selective inhibition of inappropriate motor-tendencies during response-conflict by a fronto-subthalamic mechanism. eLife, 8, e42959. https://doi.org/10.7554/eLife.42959

Wilhelm, E., Derosiere, G., Quoilin, C., Cakiroglu, I., Paço, S., Raftopoulos, C., Nuttin, B., & Duque, J. (2024). Subthalamic DBS does not restore deficits in corticospinal suppression during movement preparation in

Parkinson's disease. Clinical Neurophysiology, 165, 107–116. https://doi.org/10.1016/j.clinph.2024.06.002

Wilhelm, E., Quoilin, C., Derosiere, G., Paço, S., Jeanjean, A., & Duque, J. (2022). Corticospinal Suppression Underlying Intact Movement Preparation Fades in Parkinson's Disease. Movement Disorders, 37(12), 2396–2406. https://doi.org/10.1002/mds.29214

Wylie, S. A., Van Den Wildenberg, W. P. M., Ridderinkhof, K. R., Bashore, T. R., Powell, V. D., Manning, C. A., & Wooten, G. F. (2009). The effect of Parkinson's disease on interference control during action selection. Neuropsychologia, 47(1), 145–157. https://doi.org/10.1016/j.neuropsychologia.2008.08.001

5. General Discussion

5.1 Summary of empirical findings

We conducted three empirical studies that employed the same novel task to explore the relationship between expectation-dependent response reprogramming and conflict resolution. We aimed to find behavioral, imaging, and electrophysiological correlates of the underlying control processes, putatively revealing shared mechanisms and a bottleneck effect. The first two studies were carried out in young, healthy participants, while the third study included people with Parkinson's disease receiving DBS of the STN, thus allowing us to extend our perspective to pathological control functions and neuromodulatory influences.

The novel task integrated response cues and flanker conflict, with varying frequency of invalid cues (validity proportion) and incongruent flankers (congruency proportion) to manipulate expectations of response reprogramming and conflict resolution. Invalid cues required inhibition of a prepotent response and programming of an alternative (inhibition and shifting), while incongruent flankers demanded conflict resolution (interference inhibition). Critically, invalid-incongruent trials allowed us to assess simultaneous control demands. These processes have thus far never been tested in such a comprehensive design.

Chapter 2: behavior in healthy participants

In our initial study, we employed the novel task in young, healthy participants (n = 31) and explored behavioral control costs in RTs and accuracy, as well as their putative interaction. Rather than strictly applying the additive factors' method (Sternberg, 1969), we interpreted disproportionate performance costs in trials combining response reprogramming and conflict resolution (invalid-incongruent) as indicative of overlapping or co-dependent control mechanisms.

Our results revealed the anticipated validity effect, showing behavioral reprogramming costs as increased RTs and error rates in invalid trials. Furthermore, we observed the expected congruency effect appearing as increased RTs and error rates during

conflict resolution in incongruent trials. Moreover, both effects varied with our block-wise trial frequencies, showing the hypothesized increase of validity and congruency effects when response and conflict expectations were violated (i.e., reprogramming or conflict resolution occurred rarely, thus unexpectedly). Furthermore, our results depicted an interaction between response reprogramming and conflict resolution, in both RTs and accuracy. Notably, the origin of this interaction deviated between behavioral measures: RTs were more strongly influenced by flanker interference when it occurred without reprogramming (valid-incongruent trials), while error rates were more susceptible to flanker interference when it coincided with reprogramming (invalid-incongruent trials). The latter increase in error rates for simultaneous control demands was further amplified when both reprogramming and conflict occurred unexpectedly. These findings hint at a shared underlying control process that entails a bottleneck for correct responses when reprogramming and conflict resolution coincide. Furthermore, this bottleneck effect appears to be attenuated when reprogramming and conflict resolution are expected (anticipatory control), and amplified when they occur unexpectedly.

Chapter 3: fMRI in healthy participants

The second study used fMRI in young, healthy participants (n = 26) to explore the core network activations underlying the task's control processes. Particularly, we anticipated shared engagement of core network regions within the cingulo-opercular network, complemented by more selective recruitment of fronto-parietal network regions. Furthermore, we expected fronto-parietal network activation in the left inferior parietal cortex during reprogramming, consistent with Rushworth et al. (2001b), as well as in frontal regions, such as the dlPFC, during conflict resolution (Cieslik et al., 2015).

Due to a programming error, analyses were limited to task blocks in which incongruent trials occurred rarely (unexpected conflict). Therefore, only response expectation (validity proportion) varied between blocks of the final dataset and was included as a condition in the analyses.

Again, our behavioral results revealed the expected validity and congruency effects in both RTs and accuracy. Similarly to the behavioral study, both measures showed a modulation

of the validity effect by anticipatory control, with larger validity effects for unexpected response reprogramming. Furthermore, reprogramming and conflict resolution interacted, but only regarding error rates. Similarly to the behavioral study (**Chapter 2**), this interaction showed that flanker interference had a stronger impact on error rates when occurring simultaneously with response reprogramming (invalid-incongruent trials), hinting at a bottleneck effect. Additionally, this effect was amplified when reprogramming was unexpected, which is in line with the behavioral study (**Chapter 2**).

At the whole-brain level, a validity contrast revealed activations for reprogramming (i.e., higher activity in invalid as compared to valid trials) in the anterior insula, the pre-SMA and the right dorsal premotor cortex. Notably, activations also included right temporoparietal regions, indicating that reprogramming may combine multiple processes, likely related to inhibition, shifting and updating (e.g., Bestmann & Duque, 2016; Isherwood et al., 2021). As hypothesized, activations included regions from the fronto-parietal (right dorsal premotor cortex) as well as the cingulo-opercular (e.g., bilateral frontal operculum cortex) networks.

The congruency contrast revealed activations of the cingulo-opercular network, with peak activations in the right insular cortex. The ACC, however, did not show any conflict-related activation. Nevertheless, this is in line with a meta-analysis by Isherwood et al. (2021) and emphasizes an inconsistent involvement of the ACC in conflict-related processes. As hypothesized, frontal regions of the fronto-parietal network, such as the precentral frontal gyrus, were also active during conflict resolution. Similarly to the validity contrast, peak activations were also detected in the pre-SMA.

In a conjunction analysis, consistently shared engagement for reprogramming and conflict resolution was detected in the pre-SMA, with extension into the SMA. Furthermore, a region-of-interest (ROI) analysis of condition-specific interactions (derived from a global null) revealed an interaction in the right precentral gyrus, in the vicinity to the junction with the inferior frontal gyrus. This region showed selective activation during trials with the highest control demands, i.e., unexpected reprogramming and simultaneous conflict resolution, hinting at a specific role of this region in particularly challenging conditions. Interestingly, a higher level of activation in this region increased error rates in this condition, which also showed general, disproportionate error increases on a behavioral level. This provides further

evidence for a bottleneck during elevated control demand. Next to this, the ROI analysis also revealed an interaction of reprogramming and conflict for activity in the right superior parietal lobule, showing highest activation in invalid-incongruent trials, thus also in association with high control demand. However, in contrast to the right precentral gyrus, activity in the right superior parietal lobule was not significantly modulated by expectations about reprogramming.

Chapter 4: EEG/LFPs in people with Parkinson's disease receiving STN DBS

The third study used EEG/LFP recordings in people with Parkinson's disease receiving DBS of the STN to investigate shared oscillatory mechanisms associated with the control demands in the response cueing/conflict task, and to investigate the contribution of the STN in sessions of active and of inactive stimulation. We hypothesized that DBS would modulate behavioral outcomes and attenuate beta-band dynamics, generally reducing inhibitory control (Appleby et al., 2007; Frank et al., 2007). Our hypothesis focused on the lower beta sub-band (~13-20 Hz), at right-prefrontal, motor-cortical and STN regions. Based on the two-stage model of reactive response control (Hervault & Wessel, 2025), we expected beta synchronization at right-prefrontal and STN regions immediately following the target, initiating global inhibition ("pause") when reprogramming and conflict resolution would be demanded (e.g., Daniel et al., 2023). Following this increase, we hypothesized enhanced beta desynchronization upon reprogramming and conflict resolution (e.g., Brittain et al., 2012), signaling a shift toward flexible response adaptation ("retune").

Behaviorally, we observed main effects of validity and congruency in RTs and accuracy, reflecting behavioral costs associated with reprogramming and conflict resolution, consistent with the studies in healthy participants (**Chapter 2 & 3**). However, in this study population with Parkinson's disease, validity and congruency effects did not show any behavioral interaction. In addition, only the congruency effect varied with expectations (congruency proportion), while the validity effect was unaffected by the frequency of invalid trials (validity proportion). Regarding the impact of DBS, active stimulation selectively amplified the congruency effect in error rates, suggesting impaired inhibition of conflict-related interference (as hypothesized), while the validity effect remained unchanged.

As expected, the electrophysiological results revealed increased beta synchronization upon conflict in right-prefrontal regions, directly following target presentation. Importantly, this was only apparent when stimulation was inactive. Furthermore, subsequent beta desynchronization was enhanced for conflict trials, appearing in right-prefrontal, motor-cortical, and STN regions, which was irrespective of stimulation. A post hoc analysis at a more constrained right-prefrontal location revealed enhanced beta desynchronization also for invalid trials (reprogramming). This was, in contrast to conflict resolution during this time window, only present when stimulation was inactive.

Beta dynamics at the STN were directly linked to behavior, as higher beta power at the STN during the "retune" stage predicted faster RTs, indicating response readiness and reduced flexibility. Additionally, higher STN beta power was associated with increased errors when reprogramming and conflict resolution coincided (invalid-incongruent trials), suggesting reduced adaptive capacities (bottleneck effect).

5.2 Theoretical implications

Overall, the behavioral, imaging, and electrophysiological evidence revealed shared control processes underlying response reprogramming and conflict resolution. At the same time, the expression of these processes varied with the level of control demand, which was modulated by expectations.

Before discussing our findings in the bigger picture, it is worth highlighting some aspects that may affect the translation of results from the Parkinson's disease study (**Chapter 4**). Firstly, people with Parkinson's disease have shown general impairments in motor preparation (Wilhelm et al., 2022), which could explain the smaller validity effect observed in this study (reduced reprogramming costs). Moreover, previous research indicates that congruency effects tend to be larger in people with Parkinson's disease than in healthy controls (Wylie et al., 2009), which might have further amplified a dominant congruency effect. Therefore, the control demands regarding reprogramming and conflict resolution in this group likely differed from those in healthy participants. Additionally, our electrophysiological analyses did not consider the expectational modulation, which limits comparisons in this regard. Finally, because the STN data are based on fewer participants than the cortical EEG

recordings, any absence of STN effects may simply reflect low statistical power, which needs to be determined in a larger cohort. Nonetheless, this study adds a novel layer to the findings from our studies in healthy participants (**Chapter 2 & 3**) and provides unique evidence of subcortical involvement, both through observations of DBS effects and direct STN recordings.

I will now turn to the theoretical implications of our findings in detail. First, I will review the neural signatures that were common to both reprogramming and conflict resolution, independent of whether they occurred together. Second, I will discuss how their simultaneous occurrence may have caused a processing bottleneck and how this was further amplified by violated expectations. Finally, I will incorporate these findings into a broader theoretical framework.

General cortical and subcortical mechanisms underlying reprogramming and conflict resolution

Behaviorally, control demands of response reprogramming and conflict resolution consistently appeared as increased RTs and error rates, reflecting expected costs of inhibition and adaptation. From a network perspective, our imaging results revealed engagement of both cingulo-opercular and fronto-parietal networks in these processes, in line with the dual-network model (Dosenbach, 2008). However, the results also highlighted the importance of other key control regions, especially regarding shared or interactive processes. This included shared activation in the pre-SMA during reprogramming and conflict resolution, including parts of the SMA.

The pre-SMA and the SMA are functionally interconnected, but considered to differ in their primary contribution to response control. While the pre-SMA has been mainly associated with top-down functions, such as controlled selection and switching, the SMA is rather connected to aspects related to response execution, such as motor planning and coordination (Nachev et al., 2008). Both regions have been attributed to core response control across inhibition, shifting and updating tasks in MRI meta-analyses (e.g., Isherwood et al., 2021; Rodríguez-Nieto et al., 2022), which fits with our result of their shared involvement across the investigated task processes. Notably, our MRI study only revealed results in cortical areas. This

may be due to difficulties in imaging subcortical structures such as the STN. The cortico-subcortical interplay was instead investigated in the Parkinson's disease EEG/LFP study.

Generally, our electrophysiological results indicate that reprogramming and conflict resolution rely, at least in part, on the STN as a critical component of the CBGTC pathways. For reprogramming, however, this evidence is less robust. Behaviorally, reprogramming was not affected by DBS. Furthermore, the enhanced beta dynamics that we expected during reprogramming were only observed post hoc at the FC2 (when stimulation was inactive), not at the STN. However, higher STN beta power prior to responding was associated with increased errors in invalid-incongruent trials (reprogramming and conflict resolution). This indicates that effective reprogramming under conflict depends on modulation of STN beta activity. This relates to a study by Herz et al. (2023), which showed that successful response adjustments are crucially governed by STN beta dynamics, with a negative association of higher beta power with performance. Again, the attenuated validity effect in our Parkinson's disease study population combined with low statistical power at the STN may explain the lack of further evidence regarding the STN's role in response reprogramming.

Conflict resolution, in contrast, showed a clear association with STN function. First of all, we found a behavioral modulation by DBS, revealing increased errors under active stimulation. This indicates that withholding automated responses depends crucially on the STN, which is supported by the literature (e.g., Frank et al., 2007). Furthermore, the initial right-lateralized beta synchronization upon conflict appeared exclusively when stimulation was inactive. Stimulation has been shown to interfere with motor stopping (e.g., Georgiev et al., 2016), which may extend to conflict-related inhibition and explain why this beta signature was only present without stimulation. In fact, right-prefrontal beta synchronization in this time window has been mainly related to inhibition of an anticipated response, as in outright motor inhibition or reprogramming (e.g., Daniel et al., 2023), rather than to inhibition of flanker interference. Our finding therefore provides further evidence for a domain-general role of beta in control processes relating to inhibition (Wessel & Anderson, 2024). At the STN, potentially owing to the reduced number of observations, we did not detect a significant effect during the same time window ("pause" stage). Just prior to the response ("retune" stage), however, we found a more pronounced beta desynchronization for conflict trials, at

motor-cortical, right-prefrontal and STN sites. Notably, this response-locked effect, although present at the STN, was not influenced by stimulation.

Taken together, reprogramming and conflict resolution seem to both rely on STN activity within CBGTC pathways. During the response adaptation stage ("retune"), we observed enhanced beta dynamics for reprogramming as well as conflict resolution. Importantly, DBS seemed to have a selective impact in this time window: while stimulation did not alter beta desynchronization during conflict, reprogramming only showed beta desynchronization when stimulation was inactive. These distinctions may relate to the type of response adaptations: conflict resolution likely requires sustained, gradual adjustments of activations while reprogramming demands initiation of an alternative response ("shifting") (e.g., Bestmann & Duque, 2016). According to our results, this gradual inhibition during conflict adaptation may be less dependent on targeted coordination, as it shows widespread effects that may be less affected by stimulation. In contrast, initiating an alternative response showed a clear localization and likely requires more specific coordination (Picazio et al., 2014), which appears to be affected by stimulation.

Importantly, given the focus on the beta-band, our results do not exclude that additional frequency bands (e.g., theta) in fronto-subthalamic pathways are modulated by stimulation and influence control processes during the "pause" and "retune" stages. Additionally, task-related EEG correlates of healthy controls may aid to generalize these results.

Anticipatory modulation

With varying frequencies of reprogramming and conflict, we modulated expectations of their occurrence to test influences of anticipatory control on the reactive process. Notably, there are important differences on how anticipatory modulations may shape reprogramming and conflict resolution, which I will delineate first to contextualize our findings.

Anticipatory control based on our response cue (relating to reprogramming) entails selective response preparation to prime either the left or right hand for a more efficient execution of the correct response (Bestmann & Duque, 2016). Varying response expectations, as modulated by the frequency of invalid cues, influence the strength of this preparation. The

block-wise validity proportion is implicitly learned in our task, similarly to related task designs (e.g., Kuhns et al., 2017). Preparation of selective unimanual responses has been related to interhemispheric inhibition targeted at the alternative response, which was shown to vary with expectations (e.g., Puri & Hinder, 2022). Correlates of response preparation are often associated with the SMA and motor-cortical regions (Cunnington et al., 2003). Chen et al. (2010), for instance, recorded single-unit and LFP signals from the primate SMA and demonstrated its involvement in anticipatory response preparation as well as reactive inhibition upon a stop signal. Its anticipatory control function was related to changes in spiking activity and power that tuned response readiness in relation to trial history, indicating an important function in updating and implicit learning. This function is pivotal to infer the validity proportions in different blocks of our novel task. A study by Welniarz et al. (2019) further corroborated the role of the SMA in anticipatory control, specifically in coordinating interhemispheric modulation during movement preparation.

Anticipation of conflict, in contrast, has been associated with adjustments of top-down attentional processes, which may be less response-selective (Derosiere et al., 2018). Furthermore, the participants were explicitly informed about the frequency of conflict (high or low congruency proportion) in the upcoming block (e.g., Derosiere et al., 2018), which contrasts the implicit learning of the validity proportion. Consequently, conflict expectation may induce strategic control mechanisms even if learning mechanisms or motor preparation were impaired. Anticipatory control of conflict is also associated with the pre-SMA and SMA, similarly to response preparation (Nachev et al., 2008).

Our behavioral results show that in healthy participants (**Chapter 2 & 3**), anticipatory control can attenuate increased RTs and error rates that are related to reactive reprogramming and conflict resolution. In people with Parkinson's disease, this effect was exclusively found for conflict and not for response expectations. Given that motor preparation and related suppression of cortico-spinal excitability appears to be generally impaired in Parkinson's disease (Wilhelm et al., 2022), our findings indicate that conflict expectation operates through a mechanism less dependent on pronounced suppression of cortico-spinal excitability. Furthermore, people with Parkinson's disease have shown decreased updating abilities (e.g., Salmi et al., 2020). Since participants were explicitly informed regarding the

upcoming conflict frequency, this may have led to stable strategic adjustments without trial-wise updating. In **Chapter 4** (EEG/LFP Parkinson's disease study), the anticipatory modulation was only considered for the behavioral analysis. Additionally, we did not focus our analysis on the electrophysiological activity directly post cue nor measure cortico-spinal excitability, which could have provided additional insight to this matter. Further studies are needed to explore the mechanistic difference between response preparation and conflict adjustments further.

Given that the pre-SMA/SMA showed common activity for reprogramming and conflict resolution (**Chapter 3**), it would be of interest to explore their contribution to the related anticipatory control mechanisms, potentially serving as a global preparatory hub. Generally, the literature and our current results support the view that the pre-SMA/SMA are key sites of functional convergence across control processes.

Bottleneck effects of reprogramming and conflict resolution

Next to identifying general correlates of reprogramming and conflict resolution, our central objective was to identify their interactions. We expected these to manifest as bottleneck effects in invalid-incongruent trials, reflecting processing limitations and disproportionate performance costs when control demands coincided.

Overall, our behavioral results on error rates point to such a bottleneck. We observed disproportionate error increases for invalid-incongruent trials for the studies presented in **Chapter 2** and **3** (healthy participants). This interaction was not observed in people with Parkinson's disease; however, we attribute this to the aforementioned population-differences. Nonetheless, an interaction was found in this population at the level of STN pre-response beta power. Higher beta power predicted increased errors exclusively when reprogramming and conflict resolution coincided. This underlines not only the importance of STN pre-response beta in response adaptation but points to an elevated demand, potentially a bottleneck effect, for mediating flexibility in invalid-incongruent trials.

In other words, inhibiting conflicting flanker activations next to processes of inhibiting a prepared response and switching to an alternative (reprogramming) appear to compromise each other. Based on our data, we cannot conclusively determine whether this bottleneck involves all underlying processes or whether only specific aspects rely on the same resource.

Nonetheless, our evidence points at a bottleneck during adaptations in the "retune" stage. Firstly, correct responses in invalid-incongruent trials appear to depend on beta power during that stage, which may suggest limitations for flexible adaptations. Potentially, the initiation of a new response (reprogramming) and sustained adjustments of flanker activations cannot be carried out in parallel. Secondly, an interaction between reprogramming and conflict resolution was found in the right superior parietal lobule (fMRI study in **Chapter 3**; strongest engagement in invalid-incongruent trials), which is mainly associated with updating and reallocation of attention (e.g., Corbetta & Shulman, 2002; Piguet et al., 2013; Shulman et al., 2009). This would fit with a bottleneck of adaptations and switching during the "retune" stage rather than during outright inhibition (e.g., Rodríguez-Nieto et al., 2022). Trautwein et al. (2016) similarly observed a bottleneck effect relating to shifting and flanker-related conflict resolution, which was in their case related to attentional shifting after invalid spatial cues.

The specificity of the bottleneck to error rates and not RTs could owe to various explanations. Firstly, strategic prioritization of speed over accuracy can lead to elevated error rates without corresponding RT changes. Supporting this, Draheim et al. (2021) argued that RTs alone may insufficiently capture performance in flanker tasks due to individual speed-accuracy trade-offs that affect response thresholds (e.g., Katsimpokis et al., 2020). Second, brain regions differ in how they contribute to the urgency and evidence accumulation of a response (e.g., Thura et al., 2022). Accordingly, depending on the time period and region that is affected by the bottleneck, it may impair correct response selection without delaying the commitment to respond, leading to fast but inaccurate responses. Finally, a high percentage of errors in the invalid-incongruent trials decreases the number of trials that are included in the RT analyses, which in turn increases variability in the RT data.

Anticipatory modulation

Our findings suggest that control demands of invalid-incongruent trials (reprogramming and conflict resolution) are amplified when the trial occurs unexpectedly. For one, we found disproportionate error rate increases in the studies with healthy participants (**Chapter 2 & 3**) when reprogramming or conflict occurred unexpectedly. Moreover, in our fMRI study, which only analyzed variation in response expectations, the right precentral gyrus close to the junction with the IFG was selectively activated for invalid-incongruent trials when

reprogramming was unexpected. This activation also correlated with error rates in this condition, showing increased errors with stronger activation.

Aron et al. (2007) had previously described a core response inhibition (or "stopping") network, in which the right IFG detects and signals a stopping demand in coordination with the pre-SMA, which rapidly engages the STN through the hyperdirect pathway for implementation. However, reactive inhibition is increasingly recognized as a spectrum ranging from this "all-or-nothing" stopping process to more selective and graded modalities (e.g., Wessel & Aron, 2017), as for instance in the aforementioned "pause-then-retune" model of reactive control (Hervault & Wessel, 2025). For instance, signatures of the initial global "pause," such as beta synchronization, have been shown to adapt to different stopping probabilities (expectations) (Benis et al., 2014; Jahfari et al., 2012). Furthermore, the right IFG has also been linked to salience detection, which extends its role from stopping signal to a reactive "circuit-breaker" in case of unexpected events (Corbetta & Shulman, 2002). This is also coherent with our findings from the fMRI study, according to which a region related to the right IFG was not merely engaged in response inhibition but selectively activated when violated expectations amplified the control demand of invalid-incongruent trials. Similar evidence relates to a study by Daniel et al. (2023), which investigated the role of the right IFG, the left IFG and the pre-SMA in response reprogramming and reported increased beta (lower beta sub-band) and theta activity for reprogramming in all three areas. This referred to a time period starting from target onset; thus, these results likely correspond to the initial inhibition ("pause") of the prepotent response. When control demand was elevated in this study (higher trial-wise perceptual ambiguity), exclusively the right IFG showed increased beta activity, indicating a selective, beta-dependent involvement during particularly challenging conditions. This fits with the selective engagement in our most challenging condition in the fMRI study and points to an "emergency" process that is triggered "on demand". Nonetheless, its positive correlation with error rates points to a maladaptive effect, or potentially a protective effect that is not reflected in immediate accuracy. However, Daniel et al. (2023) found no correlation of error rates and right IFG engagement during conflict, thus the role of selective right IFG engagement during challenging situations requires further investigations. The right IFG may act on decision parameters such as thresholds and drift rate

(e.g., Bond et al., 2023), or generally enhance interareal coordination (R. Schmidt et al., 2019; Schmidt & Berke, 2017), with heterogeneous behavioral effects depending on task requirements. In any circumstance, such an "emergency" process may come at a cost. Studies have shown cross-domain effects of beta-mediated inhibition, such that motor inhibition can result in unwanted memory inhibition (e.g., Chiu & Egner, 2015), and surprise events can disrupt cognitive processes through motor inhibitory signatures (Wessel et al., 2016). Conceivably, these are cases in which inhibition was highly reactive and global, explaining the lack of selectivity for the targeted process. Accordingly, control employment needs to be flexibly scaled to the demand, in order to prevent unnecessary interference (e.g., Cai et al., 2011).

In sum, our results highlight the influence of anticipatory modulation in scaling reactive control demands. Defining the thresholds and incentives of different control levels is an interesting topic for future research.

Broader Implications and open questions

Core control-networks

On a network level, we observed both fronto-parietal and cingulo-opercular network activations during reprogramming and conflict resolution, supporting their mutual role in core control processes, as proposed by the dual-network model (Dosenbach et al., 2008). However, shared or interactive engagement was related to regions that are usually not considered principal regions of the fronto-parietal or cingulo-opercular networks. The pre-SMA/SMA showed the most consistent shared activity across conditions, in line with their proposed role as core regions in all executive functions (updating, shifting, and inhibition) (Rodríguez-Nieto et al., 2022), as well as in anticipatory and reactive control (Chen et al., 2010; Nachev et al., 2008).

Furthermore, we found an interaction in the right superior parietal lobule, potentially reflecting a bottleneck during response adaptation in relation to shifting and updating. Moreover, an area adjacent to the right IFG was selectively engaged when control demands were elevated by violated expectations, in line with its role in inhibition and top-down attentional control (Rodríguez-Nieto et al., 2022). Together, these patterns suggest that the

pre-SMA/SMA activity may underlie common, core control processes, while right superior parietal lobule and right IFG engagement reflects "on demand" recruitment.

Next to cortical control activity, our study in people with Parkinson's disease (**Chapter 4**) highlighted the contribution of fronto-subthalamic pathways to both reprogramming and conflict resolution. Future work may provide more comprehensive links of STN dynamics to the observed cortical network activity during these processes, in order to reveal their interdependencies. Another open question relates to the precise nature of the bottleneck effect observed here. It likely arises from partially overlapping response adaptations during reprogramming and conflict resolution, but this requires a finer temporal and mechanistic dissection.

Oscillatory correlates of core control processes

In addition to exploring network associations, we examined control processes through oscillatory activity to gain a more profound understanding on their implementation. As outlined in the introduction, neither purely functional nor temporal categorizations seem to fully capture the integrated nature of cognitive control. A process related to inhibition, which Miyake and Friedman (2012) described as a core module in all executive functions, appears central in our results. A common inhibitory marker is oscillatory activity in the beta-band (Wessel & Anderson, 2024), which was involved in both reprogramming and conflict resolution, aligning with views that beta dynamics govern cognitive-behavioral flexibility in a domain-general way (Chikermane et al., 2024; Wessel & Anderson, 2024).

Beyond executive functions, the beta-band's association with dopaminergic signaling, which shapes value and motivation, suggests an additional role in goal formation processes (Chikermane et al., 2024), which we did not investigate in the scope of this thesis. From a clinical perspective, insights into beta functions are particularly relevant for Parkinson's disease, as beta dynamics are a sensitive marker of Parkinsonian motor impairments (Neumann et al., 2016) and used to inform adaptive DBS systems. Understanding the broader implications of beta function could enhance therapeutic efficacy. In people with Parkinson's disease, we found preliminary evidence for a beta-related bottleneck effect at the STN when demands for flexible response adaptations coincided. Further investigations in a healthy

population would be needed to elucidate this further. Overall, beta dynamics appear to shape cognitive-behavioral control at its core.

5.3 Limitations

Task design

One limitation in our task design is the small number of trials in blocks with rare invalid-incongruent trials. Moreover, the manipulation of trial proportions resulted in heterogeneous trial counts and thus variance across conditions, which may have compromised comparability. While increasing the number of trials in the rarest condition could have improved this imbalance, it would have substantially lengthened the experiment. Based on participant feedback during piloting, we decided against extending the task duration, to avoid decreases in attention. Owing again to time constraints, our task did not entail a neutral condition to perform detailed analyses of cueing- and flanker-related costs and benefits. Another limitation concerns the cue, which for one indicates the likely response and at the same time contains a latent perceptual indication of the target display (arrow presentation). However, our behavioral results show that the cue affected task performance in the expected direction, revealing enhanced performance for valid cues and reprogramming costs for invalid cues (i.e., significant validity effects). Nonetheless, we cannot dissect a potential contribution of visual anticipation from effects relating purely to motor preparation, particularly considering the integrative nature of control processes highlighted in our results. Future studies may extend the task design to avoid this shortcoming and perhaps divide the length of the experiment into multiple sessions.

fMRI study (Chapter 3)

In the fMRI study, a programming error prevented the correct presentation of the prior information of blocks with frequent incongruent trials (i.e., when conflict was expected). At the start of each block, participants were shown on-screen instructions telling them whether most upcoming trials would be congruent or incongruent (following the approach of Derosiere et al. (2018)). However, due to the programming error, participants were always told that the blocks would mainly contain congruent trials (i.e., conflict was unexpected), which was

incorrect for half of the blocks. An additional analysis comparing our behavioral study (**Chapter 2**) (in which instructions were always correct) with our fMRI study (**Chapter 3**) showed that this error in fact influenced the congruency effect. To address this, we included only the trials for which the instructions had matched the actual block type, i.e., the blocks for which conflict was unexpected. Still, the remaining results were consistent with the behavioral study (**Chapter 2**), which supports the reliability of the observed behavioral and neural effects despite a smaller number of analyzed blocks.

EEG/LFP study (Chapter 4)

The results of the behavioral and fMRI studies are based on a healthy, young population (**Chapter 2 & 3**), which complicates comparisons to the electrophysiological findings in people with Parkinson's disease. Future studies including matched healthy controls and testing people with Parkinson's disease both on and off medication could help disentangle the effects of age, pharmacological treatment, DBS, and Parkinson's disease pathology itself.

Additionally, the task in the Parkinson's disease study (**Chapter 4**) differed slightly from the one originally used in our behavioral study (healthy participants; **Chapter 2**). It did not include null trials but used a jittered cue-target interval to prevent temporal anticipation, which shortened the task for the people with Parkinson's disease, who had to complete two sessions (ON/OFF DBS). Additionally, we used 10 blocks instead of 12 to further decrease the length of the experiment. This slightly increased the overall proportion of valid trials, which could have influenced the results compared to the behavioral study (**Chapter 2**). However, in this case, we would have expected an increased reliance on the cue, leading to stronger validity effects. Instead, the results showed decreased validity effects, likely reflecting the general impairment in motor preparation in people with Parkinson's disease (Wilhelm et al., 2022).

Another limitation concerns the small number of observations regarding our LFP recordings, which was due to a smaller patient cohort with an implanted Percept PC implanted pulse generator (Medtronic, Inc.). Furthermore, because EEG and LFP signals were synchronized offline and the LFP recordings lacked direct event markers, there was some

uncertainty about the precise event timing. Additionally, occasional errors in employing the "power cycling" method (transient activation/inactivation of stimulation for synchronization) led to fewer dependable timestamps in the affected files, thus decreasing alignment reliability. Subsequent cross-correlations analyses of event-related beta desynchronization between EEG and LFP channels helped validate overall signal coherence, but some uncertainty remained. As a result, we did not perform time-sensitive coherence analyses of fronto-subthalamic interactions. Future studies with larger samples or more consistent synchronization techniques could address this issue and provide deeper insight into the directionality and broader network mechanisms behind our findings.

A major challenge in combined EEG/LFP recordings with DBS is managing stimulation-induced artifacts and signal distortions (e.g., sub-harmonics), as well as intrinsic LFP noise. During active stimulation, LFP recordings are monopolar, with the implanted pulse generator case coupled to the system. Because the implanted pulse generator is in the vicinity of the heart, the cardiac dipole introduces electrocardiogram (ECG) artifacts into the signal. When stimulation is OFF, sensing is bipolar and independent of the implanted pulse generator case, thus ECG artifacts do not appear, as we observed in our data. This difference can distort ON/OFF comparisons, especially at low frequencies. Recent studies recommend using a "pseudo"-OFF mode, keeping stimulation at a negligible amplitude to continue monopolar sensing (Stam et al., 2023). While we did not record in pseudo-OFF mode, we focused on a beta sub-band (13–20 Hz), which is higher in frequency than ECGs (~1 Hz). However, we cannot completely rule out the possibility that ECG artifacts influenced our results. Therefore, we carefully inspected data files throughout the processing steps to capture their peculiarities.

5.4 Conclusion

This thesis combined behavioral, imaging, and electrophysiological evidence to explore shared mechanisms of response control within reprogramming and conflict resolution, in both healthy individuals and people with Parkinson's disease receiving STN DBS. Furthermore, we varied expectations of these processes to investigate how they are modulated by anticipatory control. This multimodal approach allowed for a nuanced understanding of how main

anticipatory and reactive control functions interact and whether they draw on shared resources.

The empirical findings of this thesis consistently support the idea that response control is not a set of isolated functions but rather an emergent property of dynamic interactions between cortical and subcortical systems, which share basic processes and are fine-tuned by demand, which can be modulated by expectations (Gratton et al., 2018).

Along these lines, the pre-SMA/SMA was consistently activated across control modalities, while activity of the right superior parietal lobule and right IFG was more selective to increased demands. Next to this, beta-band dynamics emerged as a domain-general marker of control, aligning with evidence that beta regulates information processing at the core by mediating cognitive-behavioral inhibition and flexibility (Chikermane et al., 2024; Wessel & Anderson, 2024). Moreover, our results showed that beta-mediated flexibility directly influenced behavioral performance via the STN, as previously demonstrated for cortical regions (Pierrieau et al., 2025), which highlights subcortical contributions alongside our findings on cortical activities. Additionally, active STN DBS attenuated control-related beta dynamics particularly during global response inhibition and selective reprogramming, which further implies that STN-dependent coordination is involved in these processes.

A bottleneck effect for increased control demands appeared as disproportionate error increases in healthy participants. Further indications related to limited capacities for flexible response adaptations via STN beta, as well as to interactions in the right superior parietal cortex and a region relating to the right IFG. Crucially, the bottleneck effect was amplified when response adjustments had to be carried out unexpectedly, demonstrating again an important control-tuning by anticipatory mechanisms. Interestingly, our results implied maladaptive response preparation but not conflict anticipation in relation to Parkinson's disease pathology, indicating divergent anticipatory control mechanisms in these processes.

From a broader perspective, these insights highlight the evolutionary refinement of response control processes for adaptive behavior in complex environments. Unlike organisms such as bacteria that can also adapt, human society benefits neural architectures that support internal models, long-term strategies, and abstraction (Badre & Nee, 2018). Understanding

interconnected control functions across healthy and clinical populations offers critical insights into human cognition and its shortcomings. Across psychiatric conditions and neurological disorders such as Parkinson's disease, impairments in cognitive control are linked to disrupted network functions (e.g., Badre, 2025). Recent advances of interventional approaches, such as targeted training or neuromodulation, can partially restore or modulate these control pathways (e.g., Koster et al., 2017; Sigcha et al., 2023). Enhancing our understanding of their neural substrates is thus essential to not only inform theoretical models but also underpin future therapeutic strategies.

6. References

Aarts, E., Roelofs, A., & Van Turennout, M. (2008). Anticipatory Activity in Anterior Cingulate Cortex Can Be Independent of Conflict and Error Likelihood. The Journal of Neuroscience, 28(18), 4671–4678. https://doi.org/10.1523/JNEUROSCI.4400-07.2008

Albin, R. L., Young, A. B., & Penney, J. B. (1989). The functional anatomy of basal ganglia disorders. Trends in Neurosciences, 12(10), 366–375. https://doi.org/10.1016/0166-2236(89)90074-X

Alkemade, A., Schnitzler, A., & Forstmann, B. U. (2015). Topographic organization of the human and non-human primate subthalamic nucleus. Brain Structure and Function, 220(6), 3075–3086. https://doi.org/10.1007/s00429-015-1047-2

Appleby, B. S., Duggan, P. S., Regenberg, A., & Rabins, P. V. (2007). Psychiatric and neuropsychiatric adverse events associated with deep brain stimulation: A meta-analysis of ten years' experience: Psychiatric and Neuropsychiatric Adverse Events. Movement Disorders, 22(12), 1722–1728. https://doi.org/10.1002/mds.21551

Arnold Anteraper, S., Guell, X., Whitfield-Gabrieli, S., Triantafyllou, C., Mattfeld, A. T., Gabrieli, J. D., & Geddes, M. R. (2018). Resting-State Functional Connectivity of the Subthalamic Nucleus to Limbic, Associative, and Motor Networks. Brain Connectivity, 8(1), 22–32. https://doi.org/10.1089/brain.2017.0535

Aron, A. R. (2011). From Reactive to Proactive and Selective Control: Developing a Richer Model for Stopping Inappropriate Responses. Biological Psychiatry, 69(12), e55–e68. https://doi.org/10.1016/j.biopsych.2010.07.024

Aron, A. R., Behrens, T. E., Smith, S., Frank, M. J., & Poldrack, R. A. (2007). Triangulating a Cognitive Control Network Using Diffusion-Weighted Magnetic Resonance Imaging (MRI) and Functional MRI. Journal of Neuroscience, 27(14), 3743–3752. https://doi.org/10.1523/JNEUROSCI.0519-07.2007

Aron, A. R., & Verbruggen, F. (2008). Stop the Presses: Dissociating a Selective From a Global Mechanism for Stopping. Psychological Science, 19(11), 1146–1153. https://doi.org/10.1111/j.1467-9280.2008.02216.x

Asanowicz, D., Kotlewska, I., & Panek, B. (2022). Neural Underpinnings of Proactive and Preemptive Adjustments of Action Control. Journal of Cognitive Neuroscience, 34(9), 1590–1615. https://doi.org/10.1162/jocn_a_01884

Badre, D. (2025). Cognitive Control. Annual Review of Psychology, 76(1), 167–195. https://doi.org/10.1146/annurev-psych-022024-103901

Badre, D., & Nee, D. E. (2018). Frontal Cortex and the Hierarchical Control of Behavior. Trends in Cognitive Sciences, 22(2), 170–188. https://doi.org/10.1016/j.tics.2017.11.005

Balbinot, G., Milosevic, M., Morshead, C. M., Iwasa, S. N., Zariffa, J., Milosevic, L., Valiante, T. A., Hoffer, J. A., & Popovic, M. R. (2025). The mechanisms of electrical neuromodulation. The Journal of Physiology, 603(2), 247–284. https://doi.org/10.1113/JP286205

Benis, D., David, O., Lachaux, J.-P., Seigneuret, E., Krack, P., Fraix, V., Chabardès, S., & Bastin, J. (2014). Subthalamic nucleus activity dissociates proactive and reactive inhibition in patients with Parkinson's disease. NeuroImage, 91, 273–281. https://doi.org/10.1016/j.neuroimage.2013.10.070

Bestmann, S., & Duque, J. (2016). Transcranial Magnetic Stimulation: Decomposing the Processes Underlying Action Preparation. The Neuroscientist, 22(4), 392–405. https://doi.org/10.1177/1073858415592594

Bestmann, S., Harrison, L. M., Blankenburg, F., Mars, R. B., Haggard, P., Friston, K. J., & Rothwell, J. C. (2008). Influence of uncertainty and surprise on human corticospinal excitability during preparation for action. Current Biology: CB, 18(10), 775–780. https://doi.org/10.1016/j.cub.2008.04.051

Bogacz, R., & Gurney, K. (2007). The Basal Ganglia and Cortex Implement Optimal Decision Making Between Alternative Actions. Neural Computation, 19(2), 442–477. https://doi.org/10.1162/neco.2007.19.2.442

Bond, K., Rasero, J., Madan, R., Bahuguna, J., Rubin, J., & Verstynen, T. (2023). Competing neural representations of choice shape evidence accumulation in humans. eLife, 12. https://doi.org/10.7554/elife.85223

Botvinick, M. M., Braver, T. S., Barch, D. M., Carter, C. S., & Cohen, J. D. (2001). Conflict monitoring and cognitive control. Psychological Review, 108(3), 624–652. https://doi.org/10.1037/0033-295X.108.3.624

Braak, H., Ghebremedhin, E., Rüb, U., Bratzke, H., & Del Tredici, K. (2004). Stages in the development of Parkinson's disease-related pathology. Cell and Tissue Research, 318(1), 121–134. https://doi.org/10.1007/s00441-004-0956-9

Braem, S., Bugg, J. M., Schmidt, J. R., Crump, M. J. C., Weissman, D. H., Notebaert, W., & Egner, T. (2019). Measuring Adaptive Control in Conflict Tasks. Trends in Cognitive Sciences, 23(9), 769–783. https://doi.org/10.1016/j.tics.2019.07.002

Braver, T. S. (2012). The variable nature of cognitive control: A dual mechanisms framework. Trends in Cognitive Sciences, 16(2), 106–113. https://doi.org/10.1016/j.tics.2011.12.010

Brittain, J.-S., & Brown, P. (2014a). Oscillations and the basal ganglia: Motor control and beyond. NeuroImage, 85, 637–647. https://doi.org/10.1016/j.neuroimage.2013.05.084

Brittain, J.-S., & Brown, P. (2014b). Oscillations and the basal ganglia: Motor control and beyond. NeuroImage, 85, 637–647. https://doi.org/10.1016/j.neuroimage.2013.05.084

Brittain, J.-S., Watkins, K. E., Joundi, R. A., Ray, N. J., Holland, P., Green, A. L., Aziz, T. Z., & Jenkinson, N. (2012). A Role for the Subthalamic Nucleus in Response Inhibition during Conflict. The Journal of Neuroscience, 32(39), 13396–13401. https://doi.org/10.1523/JNEUROSCI.2259-12.2012

Brown, P. (2003). Oscillatory nature of human basal ganglia activity: Relationship to the pathophysiology of Parkinson's disease. Movement Disorders, 18(4), 357–363. https://doi.org/10.1002/mds.10358

Buzsáki, G., Anastassiou, C. A., & Koch, C. (2012). The origin of extracellular fields and currents—EEG, ECoG, LFP and spikes. Nature Reviews Neuroscience, 13(6), 407–420. https://doi.org/10.1038/nrn3241

Buzsáki, G., & Draguhn, A. (2004). Neuronal Oscillations in Cortical Networks. Science, 304(5679), 1926–1929. https://doi.org/10.1126/science.1099745

Cai, W., Oldenkamp, C. L., & Aron, A. R. (2011). A Proactive Mechanism for Selective Suppression of Response Tendencies. The Journal of Neuroscience, 31(16), 5965–5969. https://doi.org/10.1523/JNEUROSCI.6292-10.2011

Cameron, M. A., Al Abed, A., Buskila, Y., Dokos, S., Lovell, N. H., & Morley, J. W. (2017). Differential effect of brief electrical stimulation on voltage-gated potassium channels. Journal of Neurophysiology, 117(5), 2014–2024. https://doi.org/10.1152/jn.00915.2016

Cavallo, A., & Neumann, W. (2024). Dopaminergic reinforcement in the motor system: Implications for Parkinson's disease and deep brain stimulation. European Journal of Neuroscience, 59(3), 457–472. https://doi.org/10.1111/ejn.16222

Cavanagh, J. F., & Frank, M. J. (2014). Frontal theta as a mechanism for cognitive control. Trends in Cognitive Sciences, 18(8), 414–421. https://doi.org/10.1016/j.tics.2014.04.012

Cavanagh, J. F., Wiecki, T. V., Cohen, M. X., Figueroa, C. M., Samanta, J., Sherman, S. J., & Frank, M. J. (2011). Subthalamic nucleus stimulation reverses mediofrontal influence over decision threshold. Nature Neuroscience, 14(11), 1462–1467. https://doi.org/10.1038/nn.2925

Chaudhuri, K. R., & Schapira, A. H. (2009). Non-motor symptoms of Parkinson's disease: Dopaminergic pathophysiology and treatment. The Lancet Neurology, 8(5), 464–474. https://doi.org/10.1016/S1474-4422(09)70068-7

Chaudhuri, K. R., Yates, L., & Martinez-Martin, P. (2005). The non-motor symptom complex of Parkinson's disease: A comprehensive assessment is essential. Current Neurology and Neuroscience Reports, 5(4), 275–283. https://doi.org/10.1007/s11910-005-0072-6

Chen, X., Scangos, K. W., & Stuphorn, V. (2010). Supplementary motor area exerts proactive and reactive control of arm movements. The Journal of Neuroscience: The Official Journal of the Society for Neuroscience, 30(44), 14657–14675. https://doi.org/10.1523/JNEUROSCI.2669-10.2010

Chikermane, M., Weerdmeester, L., Rajamani, N., Köhler, R. M., Merk, T., Vanhoecke, J., Horn, A., & Neumann, W. J. (2024). Cortical beta oscillations map to shared brain networks modulated by dopamine. eLife, 13, RP97184. https://doi.org/10.7554/eLife.97184.3

Chiu, Y.-C., & Egner, T. (2015). Inhibition-Induced Forgetting Results from Resource Competition between Response Inhibition and Memory Encoding Processes. Journal of Neuroscience, 35(34), 11936–11945. https://doi.org/10.1523/JNEUROSCI.0519-15.2015

Cieslik, E. C., Mueller, V. I., Eickhoff, C. R., Langner, R., & Eickhoff, S. B. (2015). Three key regions for supervisory attentional control: Evidence from neuroimaging meta-analyses. Neuroscience & Biobehavioral Reviews, 48, 22–34. https://doi.org/10.1016/j.neubiorev.2014.11.003

Cisek, P. (2007). Cortical mechanisms of action selection: The affordance competition hypothesis. Philosophical Transactions of the Royal Society of London. Series B, Biological Sciences, 362(1485), 1585–1599. https://doi.org/10.1098/rstb.2007.2054

Cisek, P., & Kalaska, J. F. (2010). Neural Mechanisms for Interacting with a World Full of Action Choices. Annual Review of Neuroscience, 33(1), 269–298. https://doi.org/10.1146/annurev.neuro.051508.135409

Cools, R. (2001). Mechanisms of cognitive set flexibility in Parkinson's disease. Brain, 124(12), 2503–2512. https://doi.org/10.1093/brain/124.12.2503

Cools, R. (2006). Dopaminergic modulation of cognitive function-implications for l-DOPA treatment in Parkinson's disease. Neuroscience & Biobehavioral Reviews, 30(1), 1–23. https://doi.org/10.1016/j.neubiorev.2005.03.024

Corbetta, M., & Shulman, G. L. (2002). Control of goal-directed and stimulus-driven attention in the brain. Nature Reviews Neuroscience, 3(3), 201–215. https://doi.org/10.1038/nrn755

Cunnington, R., Windischberger, C., Deecke, L., & Moser, E. (2003). The preparation and readiness for voluntary movement: A high-field event-related fMRI study of the Bereitschafts-BOLD response. NeuroImage, 20(1), 404–412. https://doi.org/10.1016/s1053-8119(03)00291-x

Daniel, P. L., Bonaiuto, J. J., Bestmann, S., Aron, A. R., & Little, S. (2023). High precision magnetoencephalography reveals increased right-inferior frontal gyrus beta power during response conflict. Cortex, 158, 127–136. https://doi.org/10.1016/j.cortex.2022.10.007

Davis, T., & Poldrack, R. A. (2013). Measuring neural representations with fMRI: Practices and pitfalls. Annals of the New York Academy of Sciences, 1296(1), 108–134. https://doi.org/10.1111/nyas.12156

DeLong, M. R. (1990). Primate models of movement disorders of basal ganglia origin. Trends in Neurosciences, 13(7), 281–285. https://doi.org/10.1016/0166-2236(90)90110-v

Derosiere, G., Klein, P.-A., Nozaradan, S., Zénon, A., Mouraux, A., & Duque, J. (2018). Visuomotor Correlates of Conflict Expectation in the Context of Motor Decisions. The Journal of Neuroscience, 38(44), 9486–9504. https://doi.org/10.1523/JNEUROSCI.0623-18.2018

Desimone, R., & Duncan, J. (1995). Neural Mechanisms of Selective Visual Attention. Annual Review of Neuroscience, 18(1), 193–222. https://doi.org/10.1146/annurev.ne.18.030195.001205

Donohue, S. E., Wendelken, C., & Bunge, S. A. (2008). Neural Correlates of Preparation for Action Selection as a Function of Specific Task Demands. Journal of Cognitive Neuroscience, 20(4), 694–706. https://doi.org/10.1162/jocn.2008.20042

Dosenbach, N. U. F., Fair, D. A., Cohen, A. L., Schlaggar, B. L., & Petersen, S. E. (2008). A dual-networks architecture of top-down control. Trends in Cognitive Sciences, 12(3), 99–105. https://doi.org/10.1016/j.tics.2008.01.001

Dosenbach, N. U. F., Fair, D. A., Miezin, F. M., Cohen, A. L., Wenger, K. K., Dosenbach, R. A. T., Fox, M. D., Snyder, A. Z., Vincent, J. L., Raichle, M. E., Schlaggar, B. L., & Petersen, S. E. (2007). Distinct brain

networks for adaptive and stable task control in humans. Proceedings of the National Academy of Sciences, 104(26), 11073–11078. https://doi.org/10.1073/pnas.0704320104

Dosenbach, N. U. F., Visscher, K. M., Palmer, E. D., Miezin, F. M., Wenger, K. K., Kang, H. C., Burgund, E. D., Grimes, A. L., Schlaggar, B. L., & Petersen, S. E. (2006). A Core System for the Implementation of Task Sets. Neuron, 50(5), 799–812. https://doi.org/10.1016/j.neuron.2006.04.031

Draheim, C., Tsukahara, J. S., Martin, J. D., Mashburn, C. A., & Engle, R. W. (2021). A toolbox approach to improving the measurement of attention control. Journal of Experimental Psychology: General, 150(2), 242–275. https://doi.org/10.1037/xge0000783

Drummond, N. M., & Chen, R. (2020). Deep brain stimulation and recordings: Insights into the contributions of subthalamic nucleus in cognition. NeuroImage, 222(July). https://doi.org/10.1016/j.neuroimage.2020.117300

Dubey, A., Markowitz, D. A., & Pesaran, B. (2023). Top-down control of exogenous attentional selection is mediated by beta coherence in prefrontal cortex. Neuron, 111(20), 3321-3334.e5. https://doi.org/10.1016/j.neuron.2023.06.025

Duque, J., & Ivry, R. B. (2009). Role of Corticospinal Suppression during Motor Preparation. Cerebral Cortex, 19(9), 2013–2024. https://doi.org/10.1093/cercor/bhn230

Duque, J., Labruna, L., Verset, S., Olivier, E., & Ivry, R. B. (2012). Dissociating the role of prefrontal and premotor cortices in controlling inhibitory mechanisms during motor preparation. The Journal of Neuroscience: The Official Journal of the Society for Neuroscience, 32(3), 806–816. https://doi.org/10.1523/JNEUROSCI.4299-12.2012

Duque, J., Olivier, E., & Rushworth, M. (2013). Top–Down Inhibitory Control Exerted by the Medial Frontal Cortex during Action Selection under Conflict. Journal of Cognitive Neuroscience, 25(10), 1634–1648. https://doi.org/10.1162/jocn_a_00421

Duque, J., Petitjean, C., & Swinnen, S. P. (2016). Effect of Aging on Motor Inhibition during Action Preparation under Sensory Conflict. Frontiers in Aging Neuroscience, 8. https://doi.org/10.3389/fnagi.2016.00322

Dux, P. E., Ivanoff, J., Asplund, C. L., & Marois, R. (2006). Isolation of a central bottleneck of information processing with time-resolved FMRI. Neuron, 52(6), 1109–1120. https://doi.org/10.1016/j.neuron.2006.11.009

Egner, T., & Hirsch, J. (2005). Cognitive control mechanisms resolve conflict through cortical amplification of task-relevant information. Nature Neuroscience, 8(12), 1784–1790. https://doi.org/10.1038/nn1594

Engel, A. K., Moll, C. K. E., Fried, I., & Ojemann, G. A. (2005). Invasive recordings from the human brain: Clinical insights and beyond. Nature Reviews Neuroscience, 6(1), 35–47. https://doi.org/10.1038/nrn1585

Eriksen, B. A., & Eriksen, C. W. (1974). Effects of noise letters upon the identification of a target letter in a nonsearch task. Perception & Psychophysics, 16(1), 143–149. https://doi.org/10.3758/BF03203267

Eusebio, A., Pogosyan, A., Wang, S., Averbeck, B., Gaynor, L. D., Cantiniaux, S., Witjas, T., Limousin, P., Azulay, J.-P., & Brown, P. (2009). Resonance in subthalamo-cortical circuits in Parkinson's disease. Brain: A Journal of Neurology, 132(Pt 8), 2139–2150. https://doi.org/10.1093/brain/awp079

Fan, J., Byrne, J., Worden, M. S., Guise, K. G., McCandliss, B. D., Fossella, J., & Posner, M. I. (2007). The Relation of Brain Oscillations to Attentional Networks. Journal of Neuroscience, 27(23), 6197–6206. https://doi.org/10.1523/JNEUROSCI.1833-07.2007

Fan, J., Flombaum, J. I., McCandliss, B. D., Thomas, K. M., & Posner, M. I. (2003). Cognitive and Brain Consequences of Conflict. NeuroImage, 18(1), 42–57. https://doi.org/10.1006/nimg.2002.1319

Fan, J., Kolster, R., Ghajar, J., Suh, M., Knight, R. T., Sarkar, R., & McCandliss, B. D. (2007). Response Anticipation and Response Conflict: An Event-Related Potential and Functional Magnetic Resonance Imaging Study. Journal of Neuroscience, 27(9), 2272–2282. https://doi.org/10.1523/JNEUROSCI.3470-06.2007

Fan, J., McCandliss, B. D., Sommer, T., Raz, A., & Posner, M. I. (2002). Testing the Efficiency and Independence of Attentional Networks. Journal of Cognitive Neuroscience, 14(3), 340–347. https://doi.org/10.1162/089892902317361886

Fan, J., Mccandliss, B., Fossella, J., Flombaum, J., & Posner, M. (2005). The activation of attentional networks. NeuroImage, 26(2), 471–479. https://doi.org/10.1016/j.neuroimage.2005.02.004

Fasano, A., Romito, L. M., Daniele, A., Piano, C., Zinno, M., Bentivoglio, A. R., & Albanese, A. (2010). Motor and cognitive outcome in patients with Parkinson's disease 8 years after subthalamic implants. Brain, 133(9), 2664–2676. https://doi.org/10.1093/brain/awq221

Feldmann, L. K., Lofredi, R., Neumann, W.-J., Al-Fatly, B., Roediger, J., Bahners, B. H., Nikolov, P., Denison, T., Saryyeva, A., Krauss, J. K., Faust, K., Florin, E., Schnitzler, A., Schneider, G.-H., & Kühn, A. A. (2022). Toward therapeutic electrophysiology: Beta-band suppression as a biomarker in chronic local field potential recordings. Npj Parkinson's Disease, 8(1), 44. https://doi.org/10.1038/s41531-022-00301-2

Frank, M. J., Samanta, J., Moustafa, A. A., & Sherman, S. J. (2007). Hold your horses: Impulsivity, deep brain stimulation, and medication in parkinsonism. Science (New York, N.Y.), 318(5854), 1309–1312. https://doi.org/10.1126/science.1146157

Friston, K. J., Holmes, A. P., Price, C. J., Büchel, C., & Worsley, K. J. (1999). Multisubject fMRI Studies and Conjunction Analyses. NeuroImage, 10(4), 385–396. https://doi.org/10.1006/nimg.1999.0484

Friston, K. J., Penny, W. D., & Glaser, D. E. (2005). Conjunction revisited. *NeuroImage*, *25*(3), 661–667. https://doi.org/10.1016/j.neuroimage.2005.01.013

Galea, J. M., Bestmann, S., Beigi, M., Jahanshahi, M., & Rothwell, J. C. (2012). Action Reprogramming in Parkinson's Disease: Response to Prediction Error Is Modulated by Levels of Dopamine. The Journal of Neuroscience, 32(2), 542–550. https://doi.org/10.1523/jneurosci.3621-11.2012

Georgiev, D., Dirnberger, G., Wilkinson, L., Limousin, P., & Jahanshahi, M. (2016). In Parkinson's disease on a probabilistic Go/NoGo task deep brain stimulation of the subthalamic nucleus only interferes with withholding of the most prepotent responses. Experimental Brain Research, 234(4), 1133–1143. https://doi.org/10.1007/s00221-015-4531-2

Gratton, G., Coles, M. G. H., & Donchin, E. (1992). Optimizing the use of information: Strategic control of activation of responses. Journal of Experimental Psychology: General, 121(4), 480–506. https://doi.org/10.1037/0096-3445.121.4.480

Gratton, G., Cooper, P., Fabiani, M., Carter, C. S., & Karayanidis, F. (2018). Dynamics of cognitive control: Theoretical bases, paradigms, and a view for the future. Psychophysiology, 55(3). https://doi.org/10.1111/psyp.13016

Haber, S. N. (2003). The primate basal ganglia: Parallel and integrative networks. Journal of Chemical Neuroanatomy, 26(4), 317–330. https://doi.org/10.1016/j.jchemneu.2003.10.003

Haegens, S., Nácher, V., Hernández, A., Luna, R., Jensen, O., & Romo, R. (2011). Beta oscillations in the monkey sensorimotor network reflect somatosensory decision making. Proceedings of the National Academy of Sciences, 108(26), 10708–10713. https://doi.org/10.1073/pnas.1107297108

Haenschel, C., Baldeweg, T., Croft, R. J., Whittington, M., & Gruzelier, J. (2000). Gamma and beta frequency oscillations in response to novel auditory stimuli: A comparison of human electroencephalogram (EEG) data with in vitro models. Proceedings of the National Academy of Sciences, 97(13), 7645–7650. https://doi.org/10.1073/pnas.120162397

Hammond, C., Bergman, H., & Brown, P. (2007). Pathological synchronization in Parkinson's disease: Networks, models and treatments. Trends in Neurosciences, 30(7), 357–364. https://doi.org/10.1016/j.tins.2007.05.004

Hannah, R., Cavanagh, S. E., Tremblay, S., Simeoni, S., & Rothwell, J. C. (2018). Selective Suppression of Local Interneuron Circuits in Human Motor Cortex Contributes to Movement Preparation. The Journal of Neuroscience, 38(5), 1264–1276. https://doi.org/10.1523/JNEUROSCI.2869-17.2017

Hariz, M., & Blomstedt, P. (2022). Deep brain stimulation for Parkinson's disease. Journal of Internal Medicine, 292(5), 764–778. https://doi.org/10.1111/joim.13541

Haynes, W. I. A., & Haber, S. N. (2013). The Organization of Prefrontal-Subthalamic Inputs in Primates Provides an Anatomical Substrate for Both Functional Specificity and Integration: Implications for Basal Ganglia Models and Deep Brain Stimulation. Journal of Neuroscience, 33(11), 4804–4814. https://doi.org/10.1523/JNEUROSCI.4674-12.2013

Helfrich, R. F., & Knight, R. T. (2016). Oscillatory Dynamics of Prefrontal Cognitive Control. Trends in Cognitive Sciences, 20(12), 916–930. https://doi.org/10.1016/j.tics.2016.09.007

Hervault, M., & Wessel, J. R. (2025). Common and Unique Neurophysiological Processes That Support the Stopping and Revising of Actions. The Journal of Neuroscience, 45(13), e1537242025. https://doi.org/10.1523/JNEUROSCI.1537-24.2025

Herz, D. M., Bange, M., Gonzalez-Escamilla, G., Auer, M., Muthuraman, M., Glaser, M., Bogacz, R., Pogosyan, A., Tan, H., Groppa, S., & Brown, P. (2023). Dynamic modulation of subthalamic nucleus activity facilitates adaptive behavior. PLOS Biology, 21(6), e3002140. https://doi.org/10.1371/journal.pbio.3002140

Herz, D. M., Little, S., Pedrosa, D. J., Tinkhauser, G., Cheeran, B., Foltynie, T., Bogacz, R., & Brown, P. (2018). Mechanisms Underlying Decision-Making as Revealed by Deep-Brain Stimulation in Patients with Parkinson's Disease. Current Biology, 28(8), 1169-1178.e6. https://doi.org/10.1016/j.cub.2018.02.057

Huettel, S. A., Song, A. W., & McCarthy, G. (2004). *Functional magnetic resonance imaging.* Sinauer Associates, Publishers.

Hung, Y., Gaillard, S. L., Yarmak, P., & Arsalidou, M. (2018). Dissociations of cognitive inhibition, response inhibition, and emotional interference: Voxelwise ALE meta-analyses of fMRI studies. Human Brain Mapping, 39(10), 4065–4082. https://doi.org/10.1002/hbm.24232

Hwang, K., Bertolero, M. A., Liu, W. B., & D'Esposito, M. (2017). The Human Thalamus Is an Integrative Hub for Functional Brain Networks. The Journal of Neuroscience, 37(23), 5594–5607. https://doi.org/10.1523/JNEUROSCI.0067-17.2017

Isherwood, S. J. S., Keuken, M. C., Bazin, P. L., & Forstmann, B. U. (2021). Cortical and subcortical contributions to interference resolution and inhibition – An fMRI ALE meta-analysis. Neuroscience & Biobehavioral Reviews, 129, 245–260. https://doi.org/10.1016/j.neubiorev.2021.07.021

Jahanshahi, M., Obeso, I., Rothwell, J. C., & Obeso, J. A. (2015). A fronto–striato–subthalamic–pallidal network for goal-directed and habitual inhibition. Nature Reviews Neuroscience, 16(12), 719–732. https://doi.org/10.1038/nrn4038

Jahfari, S., Verbruggen, F., Frank, M. J., Waldorp, L. J., Colzato, L., Ridderinkhof, K. R., & Forstmann, B. U. (2012). How Preparation Changes the Need for Top–Down Control of the Basal Ganglia When Inhibiting Premature Actions. The Journal of Neuroscience, 32(32), 10870–10878. https://doi.org/10.1523/jneurosci.0902-12.2012

Jahfari, S., Waldorp, L., Van Den Wildenberg, W. P. M., Scholte, H. S., Ridderinkhof, K. R., & Forstmann, B. U. (2011). Effective Connectivity Reveals Important Roles for Both the Hyperdirect (Fronto-Subthalamic) and the Indirect (Fronto-Striatal-Pallidal) Fronto-Basal Ganglia Pathways during Response Inhibition. The Journal of Neuroscience, 31(18), 6891–6899. https://doi.org/10.1523/JNEUROSCI.5253-10.2011

Jensen, O., & Colgin, L. L. (2007). Cross-frequency coupling between neuronal oscillations. Trends in Cognitive Sciences, 11(7), 267–269. https://doi.org/10.1016/j.tics.2007.05.003

Jensen, O., & Mazaheri, A. (2010). Shaping Functional Architecture by Oscillatory Alpha Activity: Gating by Inhibition. Frontiers in Human Neuroscience, 4. https://doi.org/10.3389/fnhum.2010.00186

Joel, D., & Weiner, I. (2000). The connections of the dopaminergic system with the striatum in rats and primates: An analysis with respect to the functional and compartmental organization of the striatum. Neuroscience, 96(3), 451–474. https://doi.org/10.1016/s0306-4522(99)00575-8

Kalia, L. V., & Lang, A. E. (2015). Parkinson's disease. The Lancet, 386(9996), 896–912. https://doi.org/10.1016/S0140-6736(14)61393-3

Katsimpokis, D., Hawkins, G. E., & Van Maanen, L. (2020). Not all Speed-Accuracy Trade-Off Manipulations Have the Same Psychological Effect. Computational Brain & Behavior, 3(3), 252–268. https://doi.org/10.1007/s42113-020-00074-y

Kaufman, M. T., Churchland, M. M., Ryu, S. I., & Shenoy, K. V. (2014). Cortical activity in the null space: Permitting preparation without movement. Nature Neuroscience, 17(3), 440–448. https://doi.org/10.1038/nn.3643

Koessler, L., Maillard, L., Benhadid, A., Vignal, J. P., Felblinger, J., Vespignani, H., & Braun, M. (2009). Automated cortical projection of EEG sensors: Anatomical correlation via the international 10–10 system. NeuroImage, 46(1), 64–72. https://doi.org/10.1016/j.neuroimage.2009.02.006

Kornblum, S., Hasbroucq, T., & Osman, A. (1990). Dimensional overlap: Cognitive basis for stimulus-response compatibility--A model and taxonomy. Psychological Review, 97(2), 253–270. https://doi.org/10.1037/0033-295X.97.2.253

Koster, E. H. W., Hoorelbeke, K., Onraedt, T., Owens, M., & Derakshan, N. (2017). Cognitive control interventions for depression: A systematic review of findings from training studies. Clinical Psychology Review, 53, 79–92. https://doi.org/10.1016/j.cpr.2017.02.002

Kühn, A. A., Kupsch, A., Schneider, G., & Brown, P. (2006). Reduction in subthalamic 8–35 Hz oscillatory activity correlates with clinical improvement in Parkinson's disease. European Journal of Neuroscience, 23(7), 1956–1960. https://doi.org/10.1111/j.1460-9568.2006.04717.x

Kuhns, A. B., Dombert, P. L., Mengotti, P., Fink, G. R., & Vossel, S. (2017). Spatial Attention, Motor Intention, and Bayesian Cue Predictability in the Human Brain. The Journal of Neuroscience, 37(21), 5334–5344. https://doi.org/10.1523/JNEUROSCI.3255-16.2017

Lindquist, M. A., Meng Loh, J., Atlas, L. Y., & Wager, T. D. (2009). Modeling the hemodynamic response function in fMRI: Efficiency, bias and mis-modeling. NeuroImage, 45(1), S187–S198. https://doi.org/10.1016/j.neuroimage.2008.10.065

Little, S., & Brown, P. (2014). The functional role of beta oscillations in Parkinson's disease. Parkinsonism & Related Disorders, 20, S44–S48. https://doi.org/10.1016/S1353-8020(13)70013-0

Liu, X., Banich, M. T., Jacobson, B. L., & Tanabe, J. L. (2004). Common and distinct neural substrates of attentional control in an integrated Simon and spatial Stroop task as assessed by event-related fMRI. NeuroImage, 22(3), 1097–1106. https://doi.org/10.1016/j.neuroimage.2004.02.033

Lozano, A. M., & Lipsman, N. (2013). Probing and Regulating Dysfunctional Circuits Using Deep Brain Stimulation. Neuron, 77(3), 406–424. https://doi.org/10.1016/j.neuron.2013.01.020

Lozano, A. M., Lipsman, N., Bergman, H., Brown, P., Chabardes, S., Chang, J. W., Matthews, K., McIntyre, C. C., Schlaepfer, T. E., Schulder, M., Temel, Y., Volkmann, J., & Krauss, J. K. (2019). Deep brain stimulation: Current challenges and future directions. Nature Reviews. Neurology, 15(3), 148–160. https://doi.org/10.1038/s41582-018-0128-2

Marois, R., & Ivanoff, J. (2005). Capacity limits of information processing in the brain. Trends in Cognitive Sciences, 9(6), 296–305. https://doi.org/10.1016/j.tics.2005.04.010

McIntyre, C. C., & Hahn, P. J. (2010). Network perspectives on the mechanisms of deep brain stimulation. Neurobiology of Disease, 38(3), 329–337. https://doi.org/10.1016/j.nbd.2009.09.022

Miller, E. K., & Cohen, J. D. (2001). An Integrative Theory of Prefrontal Cortex Function. Annual Review of Neuroscience, 24(1), 167–202. https://doi.org/10.1146/annurev.neuro.24.1.167

Mink, J. W. (1996). THE BASAL GANGLIA: FOCUSED SELECTION AND INHIBITION OF COMPETING MOTOR PROGRAMS. Progress in Neurobiology, 50(4), 381–425. https://doi.org/10.1016/S0301-0082(96)00042-1

Miyake, A., & Friedman, N. P. (2012). The Nature and Organization of Individual Differences in Executive Functions: Four General Conclusions. Current Directions in Psychological Science, 21(1), 8–14. https://doi.org/10.1177/0963721411429458

Morris, H. R., Spillantini, M. G., Sue, C. M., & Williams-Gray, C. H. (2024). The pathogenesis of Parkinson's disease. The Lancet, 403(10423), 293–304. https://doi.org/10.1016/S0140-6736(23)01478-2

Nachev, P., Kennard, C., & Husain, M. (2008). Functional role of the supplementary and pre-supplementary motor areas. Nature Reviews Neuroscience, 9(11), 856–869. https://doi.org/10.1038/nrn2478

Nambu, A., Tokuno, H., & Takada, M. (2002). Functional significance of the cortico–subthalamo–pallidal 'hyperdirect' pathway. Neuroscience Research, 43(2), 111–117. https://doi.org/10.1016/S0168-0102(02)00027-5

Nee, D. E., Wager, T. D., & Jonides, J. (2007). Interference resolution: Insights from a meta-analysis of neuroimaging tasks. Cognitive, Affective, & Behavioral Neuroscience, 7(1), 1–17. https://doi.org/10.3758/CABN.7.1.1

Neubert, F.-X., Mars, R. B., Olivier, E., & Rushworth, M. F. S. (2011). Modulation of short intra-cortical inhibition during action reprogramming. Experimental Brain Research, 211(2), 265–276. https://doi.org/10.1007/s00221-011-2682-3

Neumann, W., Degen, K., Schneider, G., Brücke, C., Huebl, J., Brown, P., & Kühn, A. A. (2016). Subthalamic synchronized oscillatory activity correlates with motor impairment in patients with Parkinson's disease. Movement Disorders, 31(11), 1748–1751. https://doi.org/10.1002/mds.26759

Ni, Z., Gunraj, C., Nelson, A. J., Yeh, I.-J., Castillo, G., Hoque, T., & Chen, R. (2009). Two Phases of Interhemispheric Inhibition between Motor Related Cortical Areas and the Primary Motor Cortex in Human. Cerebral Cortex, 19(7), 1654–1665. https://doi.org/10.1093/cercor/bhn201

Nougaret, S., Fascianelli, V., Ravel, S., & Genovesio, A. (2021). Intrinsic timescales across the basal ganglia. Scientific Reports, 11(1), 21395. https://doi.org/10.1038/s41598-021-00512-2

Obeso, J. A., Rodriguez-Oroz, M. C., Rodriguez, M., Lanciego, J. L., Artieda, J., Gonzalo, N., & Olanow, C. W. (2000). Pathophysiology of the basal ganglia in Parkinson's disease. Trends in Neurosciences, 23, S8–S19. https://doi.org/10.1016/S1471-1931(00)00028-8

Oehrn, C. R., Cernera, S., Hammer, L. H., Shcherbakova, M., Yao, J., Hahn, A., Wang, S., Ostrem, J. L., Little, S., & Starr, P. A. (2024). Chronic adaptive deep brain stimulation versus conventional stimulation in Parkinson's disease: A blinded randomized feasibility trial. Nature Medicine, 30(11), 3345–3356. https://doi.org/10.1038/s41591-024-03196-z

Olanow, C. W., Kordower, J. H., Lang, A. E., & Obeso, J. A. (2009). Dopaminergic transplantation for parkinson's disease: Current status and future prospects. Annals of Neurology, 66(5), 591–596. https://doi.org/10.1002/ana.21778

Parent, A., & Hazrati, L.-N. (1995). Functional anatomy of the basal ganglia. I. The cortico-basal ganglia-thalamo-cortical loop. Brain Research Reviews, 20(1), 91–127. https://doi.org/10.1016/0165-0173(94)00007-C

Pashler, H. (1994). Dual-task interference in simple tasks: Data and theory. Psychological Bulletin, 116(2), 220–244. https://doi.org/10.1037/0033-2909.116.2.220

Patai, E. Z., Foltynie, T., Limousin, P., Akram, H., Zrinzo, L., Bogacz, R., & Litvak, V. (2022). Conflict Detection in a Sequential Decision Task Is Associated with Increased Cortico-Subthalamic Coherence and Prolonged

Subthalamic Oscillatory Response in the β Band. The Journal of Neuroscience, 42(23), 4681–4692. https://doi.org/10.1523/JNEUROSCI.0572-21.2022

Peterson, D. S., King, L. A., Cohen, R. G., & Horak, F. B. (2016). Cognitive Contributions to Freezing of Gait in Parkinson Disease: Implications for Physical Rehabilitation. Physical Therapy, 96(5), 659–670. https://doi.org/10.2522/ptj.20140603

Pfurtscheller, G. (2000). Chapter 26 Spatiotemporal ERD/ERS patterns during voluntary movement and motor imagery. In Supplements to Clinical Neurophysiology (Vol. 53, pp. 196–198). Elsevier. https://doi.org/10.1016/S1567-424X(09)70157-6

Pfurtscheller, G., & Lopes Da Silva, F. H. (1999). Event-related EEG/MEG synchronization and desynchronization: Basic principles. Clinical Neurophysiology, 110(11), 1842–1857. https://doi.org/10.1016/S1388-2457(99)00141-8

Picazio, S., Veniero, D., Ponzo, V., Caltagirone, C., Gross, J., Thut, G., & Koch, G. (2014). Prefrontal control over motor cortex cycles at beta frequency during movement inhibition. Current Biology: CB, 24(24), 2940–2945. https://doi.org/10.1016/j.cub.2014.10.043

Pierrieau, E., Dussard, C., Plantey--Veux, A., Guerrini, C., Lau, B., Pillette, L., George, N., & Jeunet-Kelway, C. (2025). Changes in cortical beta power predict motor control flexibility, not vigor. Communications Biology, 8(1). https://doi.org/10.1038/s42003-025-08465-2

Pieters, J. P. (1983). Sternberg's additive factor method and underlying psychological processes: Some theoretical considerations. Psychological Bulletin, 93(3), 411–426. https://doi.org/10.1037/0033-2909.93.3.411

Piguet, C., Sterpenich, V., Desseilles, M., Cojan, Y., Bertschy, G., & Vuilleumier, P. (2013). Neural substrates of cognitive switching and inhibition in a face processing task. NeuroImage, 82, 489–499. https://doi.org/10.1016/j.neuroimage.2013.06.015

Poldrack, R. (2006). Can cognitive processes be inferred from neuroimaging data? Trends in Cognitive Sciences, 10(2), 59–63. https://doi.org/10.1016/j.tics.2005.12.004

Posner, M. I. (1980). Orienting of Attention. Quarterly Journal of Experimental Psychology, 32(1), 3–25. https://doi.org/10.1080/00335558008248231

Prasad, A. A., & Wallén-Mackenzie, Å. (2024). Architecture of the subthalamic nucleus. Communications Biology, 7(1), 78. https://doi.org/10.1038/s42003-023-05691-4

Priori, A., Foffani, G., Rossi, L., & Marceglia, S. (2013). Adaptive deep brain stimulation (aDBS) controlled by local field potential oscillations. Experimental Neurology, 245, 77–86. https://doi.org/10.1016/j.expneurol.2012.09.013

Puri, R., & Hinder, M. R. (2022). Response bias reveals the role of interhemispheric inhibitory networks in movement preparation and execution. Neuropsychologia, 165, 108120. https://doi.org/10.1016/j.neuropsychologia.2021.108120

Redgrave, P., Prescott, T. J., & Gurney, K. (1999). The basal ganglia: A vertebrate solution to the selection problem? Neuroscience, 89(4), 1009–1023. https://doi.org/10.1016/S0306-4522(98)00319-4

Ridderinkhof, K. R., Van Den Wildenberg, W. P. M., Segalowitz, S. J., & Carter, C. S. (2004). Neurocognitive mechanisms of cognitive control: The role of prefrontal cortex in action selection, response inhibition, performance monitoring, and reward-based learning. Brain and Cognition, 56(2), 129–140. https://doi.org/10.1016/j.bandc.2004.09.016

Ritz, H., Leng, X., & Shenhav, A. (2022). Cognitive Control as a Multivariate Optimization Problem. Journal of Cognitive Neuroscience, 34(4), 569–591. https://doi.org/10.1162/jocn_a_01822

Rodríguez-Nieto, G., Seer, C., Sidlauskaite, J., Vleugels, L., Van Roy, A., Hardwick, R., & Swinnen, S. (2022). Inhibition, Shifting and Updating: Inter and intra-domain commonalities and differences from an executive functions activation likelihood estimation meta-analysis. NeuroImage, 264, 119665. https://doi.org/10.1016/j.neuroimage.2022.119665

Rosenbaum, D. A., & Kornblum, S. (1982). A priming method for investigating the selection of motor responses. Acta Psychologica, 51(3), 223–243. https://doi.org/10.1016/0001-6918(82)90036-1

Rushworth, M. F., Ellison, A., & Walsh, V. (2001a). Complementary localization and lateralization of orienting and motor attention. Nature Neuroscience, 4(6), 656–661. https://doi.org/10.1038/88492

Rushworth, M. F. S., Krams, M., & Passingham, R. E. (2001b). The Attentional Role of the Left Parietal Cortex: The Distinct Lateralization and Localization of Motor Attention in the Human Brain. Journal of Cognitive Neuroscience, 13(5), 698–710. https://doi.org/10.1162/089892901750363244

Rushworth, M. F. S., Nixon, P. D., Renowden, S., Wade, D. T., & Passingham, R. E. (1997). The left parietal cortex and motor attention. *Neuropsychologia*, *35*(9), 1261–1273.

Salmi, J., Ritakallio, L., Fellman, D., Ellfolk, U., Rinne, J. O., & Laine, M. (2020). Disentangling the Role of Working Memory in Parkinson's Disease. Frontiers in Aging Neuroscience, 12. https://doi.org/10.3389/fnagi.2020.572037

Sauter, A. E., Zabicki, A., Schüller, T., Baldermann, J. C., Fink, G. R., Mengotti, P., & Vossel, S. (2024). Response and conflict expectations shape motor responses interactively. Experimental Brain Research, 242(11), 2599–2612. https://doi.org/10.1007/s00221-024-06920-w

Schmidt, J. R. (2013). Questioning conflict adaptation: Proportion congruent and Gratton effects reconsidered. Psychonomic Bulletin & Review, 20(4), 615–630. https://doi.org/10.3758/s13423-012-0373-0

Schmidt, J. R. (2019). Evidence against conflict monitoring and adaptation: An updated review. Psychonomic Bulletin & Review, 26(3), 753–771. https://doi.org/10.3758/s13423-018-1520-z

Schmidt, J. R., & Besner, D. (2008). The Stroop effect: Why proportion congruent has nothing to do with congruency and everything to do with contingency. Journal of Experimental Psychology: Learning, Memory, and Cognition, 34(3), 514–523. https://doi.org/10.1037/0278-7393.34.3.514

Schmidt, R., & Berke, J. D. (2017). A Pause-then-Cancel model of stopping: Evidence from basal ganglia neurophysiology. Philosophical Transactions of the Royal Society B: Biological Sciences, 372(1718), 20160202. https://doi.org/10.1098/rstb.2016.0202

Schmidt, R., Herrojo Ruiz, M., Kilavik, B. E., Lundqvist, M., Starr, P. A., & Aron, A. R. (2019). Beta Oscillations in Working Memory, Executive Control of Movement and Thought, and Sensorimotor Function. The Journal of Neuroscience, 39(42), 8231–8238. https://doi.org/10.1523/JNEUROSCI.1163-19.2019

Schutter, D. J. L. G., & Knyazev, G. G. (2012). Cross-frequency coupling of brain oscillations in studying motivation and emotion. Motivation and Emotion, 36(1), 46–54. https://doi.org/10.1007/s11031-011-9237-6

Shulman, G. L., Astafiev, S. V., Franke, D., Pope, D. L. W., Snyder, A. Z., McAvoy, M. P., & Corbetta, M. (2009). Interaction of stimulus-driven reorienting and expectation in ventral and dorsal frontoparietal and basal ganglia-cortical networks. The Journal of Neuroscience: The Official Journal of the Society for Neuroscience, 29(14), 4392–4407. https://doi.org/10.1523/JNEUROSCI.5609-08.2009

Siebner, H. R., Hartwigsen, G., Kassuba, T., & Rothwell, J. C. (2009). How does transcranial magnetic stimulation modify neuronal activity in the brain? Implications for studies of cognition. Cortex, 45(9), 1035–1042. https://doi.org/10.1016/j.cortex.2009.02.007

Sigcha, L., Borzì, L., Amato, F., Rechichi, I., Ramos-Romero, C., Cárdenas, A., Gascó, L., & Olmo, G. (2023). Deep learning and wearable sensors for the diagnosis and monitoring of Parkinson's disease: A systematic review. Expert Systems with Applications, 229, 120541. https://doi.org/10.1016/j.eswa.2023.120541

Sigman, M., & Dehaene, S. (2008). Brain mechanisms of serial and parallel processing during dual-task performance. The Journal of Neuroscience: The Official Journal of the Society for Neuroscience, 28(30), 7585–7598. https://doi.org/10.1523/JNEUROSCI.0948-08.2008

Simon, J. R., & Rudell, A. P. (1967). Auditory S-R compatibility: The effect of an irrelevant cue on information processing. Journal of Applied Psychology, 51(3), 300–304. https://doi.org/10.1037/h0020586

Soh, C., Hervault, M., Chalkley, N. H., Moore, C. M., Rohl, A., Zhang, Q., Uc, E. Y., Greenlee, J. D. W., & Wessel, J. R. (2024). The human subthalamic nucleus transiently inhibits active attentional processes. Brain, 147(9), 3204–3215. https://doi.org/10.1093/brain/awae068

Soh, C., Hervault, M., Rohl, A. H., Greenlee, J. D. W., & Wessel, J. R. (2025). Precisely-timed outpatient recordings of subcortical local field potentials from wireless streaming-capable deep-brain stimulators: A method and toolbox. Journal of Neuroscience Methods, 418, 110448. https://doi.org/10.1016/j.jneumeth.2025.110448

Spitzer, B., & Haegens, S. (2017). Beyond the Status Quo: A Role for Beta Oscillations in Endogenous Content (Re)Activation. Eneuro, 4(4), ENEURO.0170-17.2017. https://doi.org/10.1523/ENEURO.0170-17.2017

Stafford, T., & Gurney, K. N. (2011). Additive Factors Do Not Imply Discrete Processing Stages: A Worked Example Using Models of the Stroop Task. Frontiers in Psychology, 2. https://doi.org/10.3389/fpsyg.2011.00287

Stam, M. J., Van Wijk, B. C. M., Sharma, P., Beudel, M., Piña-Fuentes, D. A., De Bie, R. M. A., Schuurman, P. R., Neumann, W.-J., & Buijink, A. W. G. (2023). A comparison of methods to suppress electrocardiographic artifacts in local field potential recordings. Clinical Neurophysiology, 146, 147–161. https://doi.org/10.1016/j.clinph.2022.11.011

Sternberg, S. (1969). The discovery of processing stages: Extensions of Donders' method. Acta Psychologica, 30, 276–315. https://doi.org/10.1016/0001-6918(69)90055-9

Strack, G., Kaufmann, C., Kehrer, S., Brandt, S., & Stürmer, B. (2013). Anticipatory Regulation of Action Control in a Simon Task: Behavioral, Electrophysiological, and fMRI Correlates. Frontiers in Psychology, 4. https://doi.org/10.3389/fpsyg.2013.00047

Stroop, J. R. (1935). Studies of interference in serial verbal reactions. Journal of Experimental Psychology, 18(6), 643–662. https://doi.org/10.1037/h0054651

Szczepanski, S. M., Crone, N. E., Kuperman, R. A., Auguste, K. I., Parvizi, J., & Knight, R. T. (2014). Dynamic Changes in Phase-Amplitude Coupling Facilitate Spatial Attention Control in Fronto-Parietal Cortex. PLoS Biology, 12(8), e1001936. https://doi.org/10.1371/journal.pbio.1001936

Thenaisie, Y., Palmisano, C., Canessa, A., Keulen, B. J., Capetian, P., Jiménez, M. C., Bally, J. F., Manferlotti, E., Beccaria, L., Zutt, R., Courtine, G., Bloch, J., Van Der Gaag, N. A., Hoffmann, C. F., Moraud, E. M., Isaias, I. U., & Contarino, M. F. (2021). Towards adaptive deep brain stimulation: Clinical and technical notes on a novel commercial device for chronic brain sensing. Journal of Neural Engineering, 18(4), 042002. https://doi.org/10.1088/1741-2552/ac1d5b

Thura, D., Cabana, J.-F., Feghaly, A., & Cisek, P. (2022). Integrated neural dynamics of sensorimotor decisions and actions. PLOS Biology, 20(12), e3001861. https://doi.org/10.1371/journal.pbio.3001861

Thura, D., & Cisek, P. (2014). Deliberation and Commitment in the Premotor and Primary Motor Cortex during Dynamic Decision Making. Neuron, 81(6), 1401–1416. https://doi.org/10.1016/j.neuron.2014.01.031

Trautwein, F.-M., Singer, T., & Kanske, P. (2016). Stimulus-Driven Reorienting Impairs Executive Control of Attention: Evidence for a Common Bottleneck in Anterior Insula. Cerebral Cortex, 26(11), 4136–4147. https://doi.org/10.1093/cercor/bhw225

Van Veen, V., Cohen, J. D., Botvinick, M. M., Stenger, V. A., & Carter, C. S. (2001). Anterior Cingulate Cortex, Conflict Monitoring, and Levels of Processing. NeuroImage, 14(6), 1302–1308. https://doi.org/10.1006/nimg.2001.0923

Volberg, G., & Thomaschke, R. (2017). Time-based expectations entail preparatory motor activity. Cortex, 92, 261–270. https://doi.org/10.1016/j.cortex.2017.04.019

Voloh, B., & Womelsdorf, T. (2018). Cell-Type Specific Burst Firing Interacts with Theta and Beta Activity in Prefrontal Cortex During Attention States. Cerebral Cortex, 28(12), 4348–4364. https://doi.org/10.1093/cercor/bhx287

Vossel, S., Mathys, C., Stephan, K. E., & Friston, K. J. (2015). Cortical Coupling Reflects Bayesian Belief Updating in the Deployment of Spatial Attention. The Journal of Neuroscience, 35(33), 11532–11542. https://doi.org/10.1523/JNEUROSCI.1382-15.2015

Welniarz, Q., Gallea, C., Lamy, J., Méneret, A., Popa, T., Valabregue, R., Béranger, B., Brochard, V., Flamand-Roze, C., Trouillard, O., Bonnet, C., Brüggemann, N., Bitoun, P., Degos, B., Hubsch, C., Hainque, E., Golmard, J., Vidailhet, M., Lehéricy, S., … Roze, E. (2019). The supplementary motor area modulates interhemispheric interactions during movement preparation. Human Brain Mapping, 40(7), 2125–2142. https://doi.org/10.1002/hbm.24512

Wessel, J. R. (2020). β-Bursts Reveal the Trial-to-Trial Dynamics of Movement Initiation and Cancellation. The Journal of Neuroscience, 40(2), 411–423. https://doi.org/10.1523/JNEUROSCI.1887-19.2019

Wessel, J. R., & Anderson, M. C. (2024). Neural mechanisms of domain-general inhibitory control. Trends in Cognitive Sciences, 28(2), 124–143. https://doi.org/10.1016/j.tics.2023.09.008

Wessel, J. R., & Aron, A. R. (2017). On the Globality of Motor Suppression: Unexpected Events and Their Influence on Behavior and Cognition. Neuron, 93(2), 259–280. https://doi.org/10.1016/j.neuron.2016.12.013

Wessel, J. R., Jenkinson, N., Brittain, J.-S., Voets, S. H. E. M., Aziz, T. Z., & Aron, A. R. (2016). Surprise disrupts cognition via a fronto-basal ganglia suppressive mechanism. Nature Communications, 7(1). https://doi.org/10.1038/ncomms11195

Wessel, J. R., Waller, D. A., & Greenlee, J. D. (2019). Non-selective inhibition of inappropriate motor-tendencies during response-conflict by a fronto-subthalamic mechanism. eLife, 8, e42959. https://doi.org/10.7554/eLife.42959

Whitmer, D., De Solages, C., Hill, B., Yu, H., Henderson, J. M., & Bronte-Stewart, H. (2012). High frequency deep brain stimulation attenuates subthalamic and cortical rhythms in Parkinson's disease. Frontiers in Human Neuroscience, 6. https://doi.org/10.3389/fnhum.2012.00155

Wichmann, T., & DeLong, M. R. (2006). Basal ganglia discharge abnormalities in Parkinson's disease. In P. Riederer, H. Reichmann, M. B. H. Youdim, & M. Gerlach (Eds.), Parkinson's Disease and Related Disorders (pp. 21–25). Springer Vienna. https://doi.org/10.1007/978-3-211-45295-0_5

Wilhelm, E., Derosiere, G., Quoilin, C., Cakiroglu, I., Paço, S., Raftopoulos, C., Nuttin, B., & Duque, J. (2024). Subthalamic DBS does not restore deficits in corticospinal suppression during movement preparation in Parkinson's disease. Clinical Neurophysiology, 165, 107–116. https://doi.org/10.1016/j.clinph.2024.06.002

Wilhelm, E., Quoilin, C., Derosiere, G., Paço, S., Jeanjean, A., & Duque, J. (2022). Corticospinal Suppression Underlying Intact Movement Preparation Fades in Parkinson's Disease. Movement Disorders, 37(12), 2396–2406. https://doi.org/10.1002/mds.29214

Witt, K., Daniels, C., Reiff, J., Krack, P., Volkmann, J., Pinsker, M. O., Krause, M., Tronnier, V., Kloss, M., Schnitzler, A., Wojtecki, L., Bötzel, K., Danek, A., Hilker, R., Sturm, V., Kupsch, A., Karner, E., & Deuschl, G. (2008). Neuropsychological and psychiatric changes after deep brain stimulation for Parkinson's disease: A randomised, multicentre study. The Lancet Neurology, 7(7), 605–614. https://doi.org/10.1016/S1474-4422(08)70114-5

Witt, K., Daniels, C., & Volkmann, J. (2012). Factors associated with neuropsychiatric side effects after STN-DBS in Parkinson's disease. Parkinsonism & Related Disorders, 18, S168–S170. https://doi.org/10.1016/S1353-8020(11)70052-9

Wühr, P., & Heuer, H. (2017). Response Preparation, Response Conflict, and the Effects of Irrelevant Flanker Stimuli. Advances in Cognitive Psychology, 13(1), 70–82. https://doi.org/10.5709/acp-0208-3

Wylie, S. A., Van Den Wildenberg, W. P. M., Ridderinkhof, K. R., Bashore, T. R., Powell, V. D., Manning, C. A., & Wooten, G. F. (2009). The effect of Parkinson's disease on interference control during action selection. Neuropsychologia, 47(1), 145–157. https://doi.org/10.1016/j.neuropsychologia.2008.08.001

Yin, Z., Zhu, G., Zhao, B., Bai, Y., Jiang, Y., Neumann, W.-J., Kühn, A. A., & Zhang, J. (2021). Local field potentials in Parkinson's disease: A frequency-based review. Neurobiology of Disease, 155, 105372. https://doi.org/10.1016/j.nbd.2021.105372

Yoon, H. H., Min, J., Hwang, E., Lee, C. J., Suh, J.-K. F., Hwang, O., & Jeon, S. R. (2016). Optogenetic Inhibition of the Subthalamic Nucleus Reduces Levodopa-Induced Dyskinesias in a Rat Model of Parkinson's Disease. Stereotactic and Functional Neurosurgery, 94(1), 41–53. https://doi.org/10.1159/000442891

Yu, C., Cassar, I. R., Sambangi, J., & Grill, W. M. (2020). Frequency-Specific Optogenetic Deep Brain Stimulation of Subthalamic Nucleus Improves Parkinsonian Motor Behaviors. The Journal of Neuroscience, 40(22), 4323–4334. https://doi.org/10.1523/jneurosci.3071-19.2020

Zavala, B. A., Jang, A. I., & Zaghloul, K. A. (2017). Human subthalamic nucleus activity during non-motor decision making. eLife, 6, e31007. https://doi.org/10.7554/eLife.31007

Zavala, B., Damera, S., Dong, J. W., Lungu, C., Brown, P., & Zaghloul, K. A. (2015). Human Subthalamic Nucleus Theta and Beta Oscillations Entrain Neuronal Firing During Sensorimotor Conflict. Cerebral Cortex, bhv244. https://doi.org/10.1093/cercor/bhv244

Zavala, B., Jang, A., Trotta, M., Lungu, C. I., Brown, P., & Zaghloul, K. A. (2018). Cognitive control involves theta power within trials and beta power across trials in the prefrontal-subthalamic network. Brain, 141(12), 3361–3376. https://doi.org/10.1093/brain/awy266

Zavala, B., Tan, H., Little, S., Ashkan, K., Green, A. L., Aziz, T., Foltynie, T., Zrinzo, L., Zaghloul, K., & Brown, P. (2016). Decisions Made with Less Evidence Involve Higher Levels of Corticosubthalamic Nucleus Theta Band Synchrony. Journal of Cognitive Neuroscience, 28(6), 811–825. https://doi.org/10.1162/jocn_a_00934

Zhang, R., Geng, X., & Lee, T. M. C. (2017). Large-scale functional neural network correlates of response inhibition: An fMRI meta-analysis. Brain Structure and Function, 222(9), 3973–3990. https://doi.org/10.1007/s00429-017-1443-x

7. Author Contributions

Chapter 2

Sauter, A. E., Zabicki, A., Schüller, T., Baldermann, J. C., Fink, G. R., Mengotti, P., & Vossel, S. (2024). Response and conflict expectations shape motor responses interactively. Experimental Brain Research, 242(11), 2599–2612. https://doi.org/10.1007/s00221-024-06920-w

Sauter, A. E.	Conceptualization, Data Analysis, Data Collection, Writing - original draft, review & editing
Zabicki, A.	Writing - review & editing
Schüller, T.	Conceptualization, Writing - review & editing
Baldermann, J. C.	Conceptualization, Writing - review & editing
Fink, G. R.	Conceptualization, Writing - review & editing
Mengotti, P.	Conceptualization, Data Analysis, Writing - review & editing
Vossel, S.	Conceptualization, Data Analysis, Project Administration, Writing - review & editing

Chapter 3

Sauter, A. E.	Conceptualization, Data Analysis, Data Collection, Writing - methods and preliminary results, review & editing
Bleser, A.	Data Collection
Burlon, E. Z.	Data Collection, Data Analysis
Zabicki, A.	Data Collection, Data Analysis
Schüller, T.	Conceptualization
Baldermann, J. C.	Conceptualization

Fink, G. R.	Conceptualization
Mengotti, P.	Conceptualization, Data Analysis
Vossel, S.	Conceptualization, Data Analysis, Project Administration, Writing - review & editing

Chapter 4

Sauter, A. E.	Conceptualization, Data Analysis, Data Collection, Writing – original draft, review & editing
Schüller, T.	Conceptualization, Data Analysis, Data Collection, Writing - review & editing
Mengotti, P.	Conceptualization
Barbe, M. T.	Conceptualization
Tan, H.	Data Analysis
Pogosyan, A.	Data Analysis
Zur Mühlen, K.	Data Analysis, Data Collection
Tecker, N.	Data Collection
Wehmeyer, L.	Data Analysis
Visser-Vandewalle, V.	Patient Care
Fink, G. R.	Conceptualization
Vossel, S.	Conceptualization, Data Analysis, Writing - review & editing
Baldermann, J. C.	Conceptualization, Data Analysis, Data Collection, Project Administration, Writing - review & editing

8. Appendix

Supplementary Material Chapter 2

Complementary Analysis of Inverse Efficiency

Considering the differential RT and accuracy patterns, we analyzed the inverse efficiency score (RT/accuracy) similarly, to assess combined performance. Overall, the results of this analysis mirror the accuracy effects.

Validity and Congruency Effects at Trial-Level

As for RT and accuracy alone, the analysis of inverse efficiency as a compound measure of both read-outs revealed significant main effects of *validity* ($F_{(1,30)} = 25.26$, $p < .001$, $\eta_p^2 = 0.46$) and congruency ($F_{(1,30)} = 157.13$, $p < .001$, $\eta_p^2 = 0.84$). Inverse efficiency scores were higher for invalid (506.41 ± 86.49 ms) in comparison to valid trials (427.55 ± 32.16 ms), as well as for incongruent (553.58 ± 79.87 ms) as compared to congruent (380.38 ± 35.75 ms) trials. Moreover, as in the separate analyses of RTs and accuracy, a significant two-way interaction between trial-wise *validity* and *congruency* was observed ($F_{(1,30)} = 12.37$, $p = .001$, $\eta_p^2 = 0.29$). For the inverse efficiency, larger congruency effects were observed in invalid (212.28 ± 135.41 ms) compared to valid trials (134.12 ± 33.97 ms), which points in the same direction as the accuracy analysis. Trial-level effects are visualized in Supplementary Figure SF1.

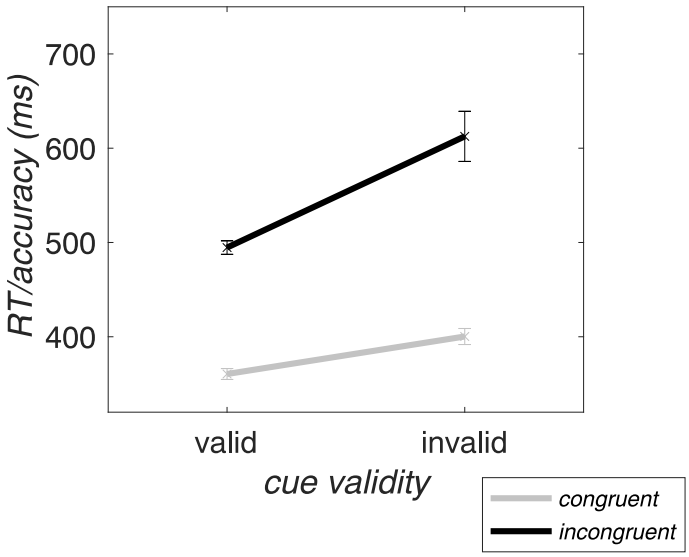

Supplementary Fig. SF1 Visualization of the inverse efficiency at the trial level, averaged over all block types. The congruency effect becomes visible as the difference between congruent (gray) and incongruent (black) lines, showing a more substantial increase in invalid compared to valid trials (depicted on the x-axis). Error bars display the standard error of the mean

Validity and Congruency Effects at Block-Level

The RM-ANOVA for inverse efficiency scores yielded a significant four-way interaction ($F_{(1,30)} = 9.17$, $p < .01$, $\eta_p^2 = 0.23$; Supplementary Figure SF4 C), likewise to the accuracy analysis. Every lower-order effect was also significant (please refer to Supplementary Table ST1 for a complete list of the RM-ANOVA outcome).

With focus on incongruent trials, inverse efficiency scores mirrored the accuracy scores (Supplementary Figure SF4 C) with the rare invalid (77% validity proportion)/rare incongruent (70% congruency proportion) trials presenting as the condition with disproportionally decreased performance compared to every other condition (as shown in slowest inverse efficiency scores: 788.16 ± 350.29 ms; every post-hoc paired samples t-test comparison with this condition was significant (all $p < .001$) after Bonferroni correction). This performance decrement is displayed again in Supplementary Figure SF2 regarding the congruency effect (inverse efficiency incongruent - congruent trials) that disproportionally increased for invalid trials within the rarely-invalid/rarely-incongruent block

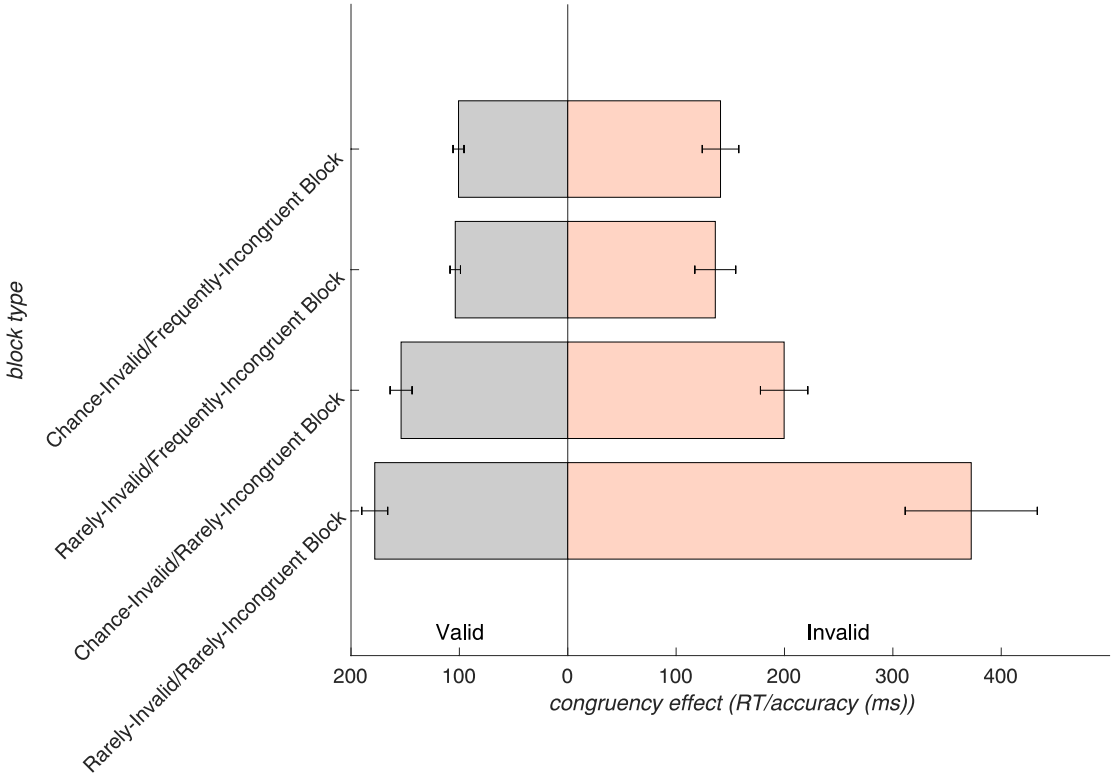

Supplementary Fig. SF2 Disproportionate increase of the congruency effect (inverse efficiency incongruent trials – congruent trials) for invalid trials within the rarely-invalid/rarely-incongruent block. The x-axis divides trial types between valid (grey bars) and invalid (orange bars). In addition, the y-axis shows the four different block types. Taken together, this graph visualizes how the congruency effect depends on block type and trial validity. The error bars indicate the standard errors of the mean

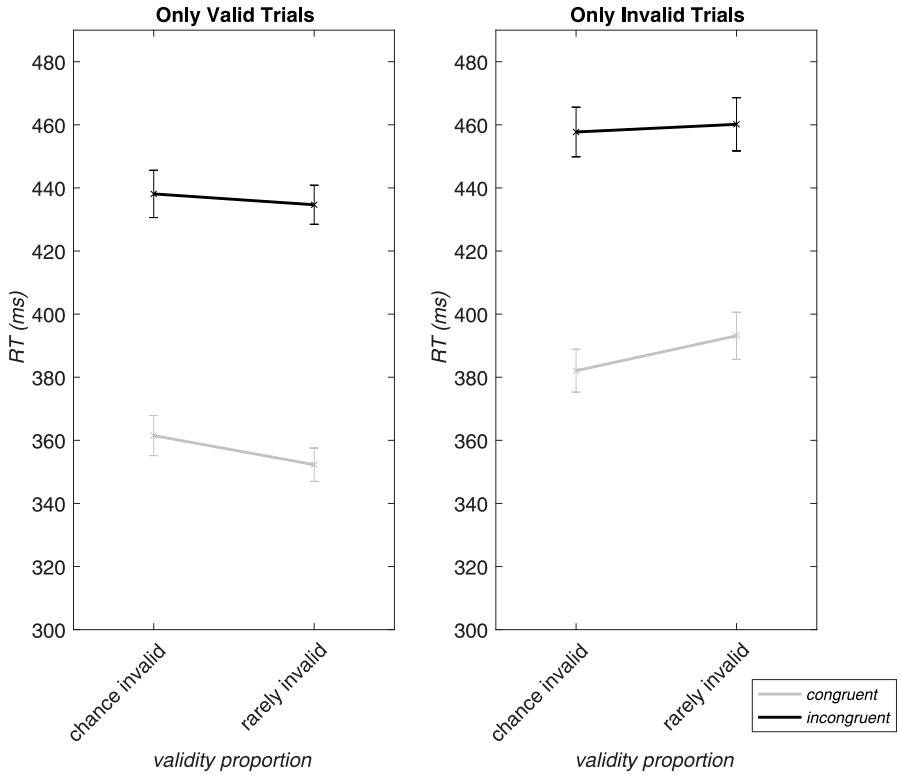

Supplementary Fig. SF3 Display of the RT congruency effect (RT incongruent – RT congruent trials) with respect to validity proportion in only valid (left side) or only invalid trials (right side). On the x-axis, the difference between chance invalid (50% validity proportion) and rarely invalid block types is shown. Congruent trials are shown in gray, and incongruent trials in black. When a primarily reliable response cue, as in the rarely invalid blocks, violated expectations (only invalid trials), the facilitation effect of congruent trials decreases compared to the chance-level response cue in chance invalid blocks. The opposite is visible in only valid trials: congruent trials benefit more from the flanker facilitation effect when response expectations with mostly reliable cues are not violated, compared to chance response cues

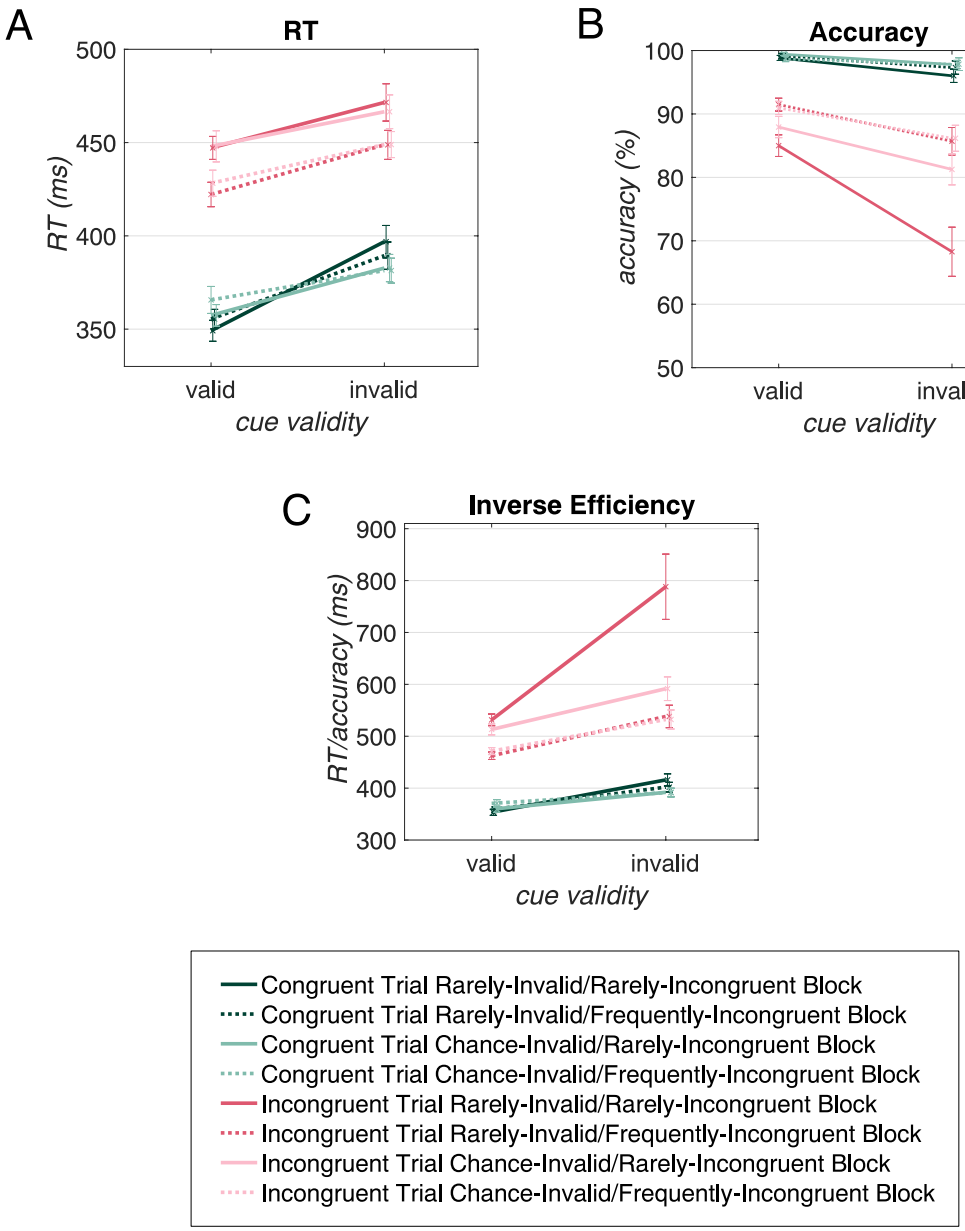

Supplementary Fig. SF4 Modulation of validity and congruency effects by response and conflict expectations. Line graphs show all sixteen conditions for each DV separately: (A) RTs, (B) accuracy, and (C) inverse efficiency (RT divided by accuracy). For (A), (B), (C): Incongruent trials are depicted in pink shades, while congruent trials are green-shaded. The x-axis is divided into valid and invalid trial types. Furthermore, the validity proportion is indicated by darker (rarely invalid block type: 77% validity proportion) and lighter (chance invalid block type: 50% validity proportion) color shadings. In addition, the congruency proportion of the respective block types is indicated by the line type: dotted lines represent frequently incongruent blocks (30% congruency proportion), while continuous lines represent rarely incongruent blocks (70% congruency proportion). Error bars depict the standard errors of the mean

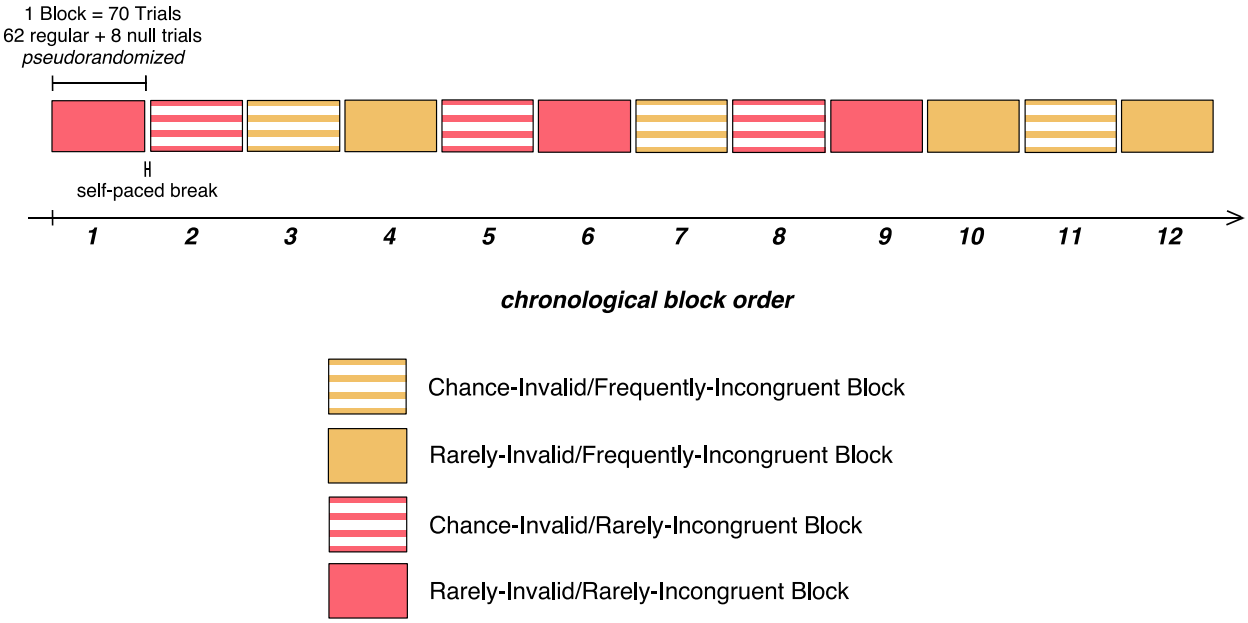

Supplementary Fig. SF5 Visualization of the response cueing/conflict task structure showing the consecutive order of blocks. Each of the four unique block types (depicted in different colors and patterns) occurred thrice during the task, each time with a unique pseudorandom trial sequence (the same across participants). Each block contained 70 trials, of which 62 were regular and 8 were null trials. In total, the task consisted of 840 trials (12 blocks x 70 trials), of which 96 trials were null trials. Self-paced breaks separated the blocks. The task lasted approximately 35 minutes in total

Supplementary Table ST1 Overview of RM-ANOVA results for RTs, accuracy, and inverse efficiency (RT divided by accuracy). Presented are F and p values and the partial eta squared for all main effects, two-way, three-way, and four-way interactions

	Main Effects	*2nd Order*	*3rd Order*	*4th Order*
RT	**Validity (val.):** $F_{(1,30)} = 37.68$, $p < .001$, $\eta_p^2 = 0.56$ **Congruency (con.):** $F_{(1,30)} = 737.88$, $p < .001$, $\eta_p^2 = 0.96$ **Validity proportion (VP):** $F_{(1,30)} = 0.02$, $p > 0.1$, $\eta_p^2 = 0.0005$ **Congruency proportion (CP):** $F_{(1,30)} = 29.83$, $p < .001$, $\eta_p^2 = 0.50$	**VP x CP:** $F_{(1,30)} = 3.90$, $p > .05$, $\eta_p^2 = 0.12$ **VP x Val.:** $F_{(1,30)} = 21.84$, $p < .001$, $\eta_p^2 = 0.42$ **VP x Con.:** $F_{(1,30)} = 0.68$, $p > .1$, $\eta_p^2 = 0.02$ **CP x Val.:** $F_{(1,30)} = 1.97$, $p > .1$, $\eta_p^2 = 0.06$ **CP x Con.:** $F_{(1,30)} = 82.20$, $p < .001$, $\eta_p^2 = 0.73$ **Val. x Con.:** $F_{(1,30)} = 7.51$, $p = .01$, $\eta_p^2 = 0.20$	**VP x CP x Val.:** $F_{(1,30)} = 0.21$, $p > .1$, $\eta_p^2 = 0.007$ **VP x CP x Con.:** $F_{(1,30)} = 0.03$, $p > .1$, $\eta_p^2 = 0.001$ **VP x Val. x Con.:** $F_{(1,30)} = 10.89$, $p < .01$, $\eta_p^2 = 0.27$ **CP x Val. x Con.:** $F_{(1,30)} = 6.20$, $p < .05$, $\eta_p^2 = 0.17$	**VP x CP x Val. x Con.:** $F_{(1,30)} = 0.15$, $p > .1$, $\eta_p^2 = 0.005$
Accuracy	**Val.:** $F_{(1,30)} = 21.24$, $p < .001$, $\eta_p^2 = 0.41$ **Con.:** $F_{(1,30)} = 108.53$, $p < .001$, $\eta_p^2 = 0.78$ **VP:** $F_{(1,30)} = 16.53$, $p < .001$, $\eta_p^2 = 0.36$ **CP:** $F_{(1,30)} = 39.45$, $p < .001$, $\eta_p^2 = 0.57$	**VP x CP:** $F_{(1,30)} = 32.96$, $p < .001$, $\eta_p^2 = 0.52$ **VP x Val.:** $F_{(1,30)} = 7.23$, $p < .05$, $\eta_p^2 = 0.19$ **VP x Con.:** $F_{(1,30)} = 11.09$, $p < .01$, $\eta_p^2 = 0.27$ **CP x Val.:** $F_{(1,30)} = 17.42$, $p < .001$, $\eta_p^2 = 0.37$ **CP x Con.:** $F_{(1,30)} = 43.82$, $p < .001$, $\eta_p^2 = 0.59$ **Val. x Con.:** $F_{(1,30)} = 22.48$, $p < .001$, $\eta_p^2 = 0.43$	**VP x CP x Val.:** $F_{(1,30)} = 7.93$, $p < .01$, $\eta_p^2 = 0.21$ **VP x CP x Con.:** $F_{(1,30)} = 15.81$, $p < .001$, $\eta_p^2 = 0.35$ **VP x Val. x Con.:** $F_{(1,30)} = 3.72$, $p > .05$, $\eta_p^2 = 0.11$ **CP x Val. x Con.:** $F_{(1,30)} = 9.86$, $p < .01$, $\eta_p^2 = 0.25$	**VP x CP x Val. x Con.:** $F_{(1,30)} = 7.11$, $p < .05$, $\eta_p^2 = 0.19$
Inverse Efficiency (RT divided by accuracy)	**Val.:** $F_{(1,30)} = 25.26$, $p < .001$, $\eta_p^2 = 0.46$ **Con.:** $F_{(1,30)} = 157.13$, $p < .001$, $\eta_p^2 = 0.84$ **VP:** $F_{(1,30)} = 12.72$, $p = .001$, $\eta_p^2 = 0.30$ **CP:** $F_{(1,30)} = 35.35$, $p < .001$, $\eta_p^2 = 0.54$	**VP x CP:** $F_{(1,30)} = 21.85$, $p < .001$, $\eta_p^2 = 0.42$ **VP x Val.:** $F_{(1,30)} = 15.46$, $p < .001$, $\eta_p^2 = 0.34$ **VP x Con.:** $F_{(1,30)} = 10.56$, $p < .01$, $\eta_p^2 = 0.26$ **CP x Val.:** $F_{(1,30)} = 15.22$, $p < .001$, $\eta_p^2 = 0.34$ **CP x Con.:** $F_{(1,30)} = 35.57$, $p < .001$, $\eta_p^2 = 0.54$ **Val. x Con.:** $F_{(1,30)} = 12.37$, $p = .001$, $\eta_p^2 = 0.29$	**VP x CP x Val.:** $F_{(1,30)} = 9.93$, $p < .01$, $\eta_p^2 = 0.25$ **VP x CP x Con.:** $F_{(1,30)} = 14.65$, $p < .001$, $\eta_p^2 = 0.33$ **VP x Val. x Con.:** $F_{(1,30)} = 5.06$, $p < .05$, $\eta_p^2 = 0.14$ **CP x Val. x Con.:** $F_{(1,30)} = 9.27$, $p < .01$, $\eta_p^2 = 0.24$	**VP x CP x Val. x Con.:** $F_{(1,30)} = 9.17$, $p < .01$, $\eta_p^2 = 0.23$

Supplementary Table ST2 Display of the RT RM-ANOVA results considering only RTs within 3 standard deviations from the individual mean RT. Presented are F and p values and the partial eta squared for all main effects, two-way, three-way, and four-way interactions

	Main Effects	*2nd Order*	*3rd Order*	*4th Order*
RT	**Validity (val.):** $F_{(1,30)} = 45.05$, $p < .001$, $\eta_p^2 = 0.60$ **Congruency (con.):** $F_{(1,30)} = 667.50$, $p < .001$, $\eta_p^2 = 0.96$ **Validity proportion (VP):** $F_{(1,30)} = 0.60$, $p > 0.1$, $\eta_p^2 = 0.02$ **Congruency proportion (CP):** $F_{(1,30)} = 24.63$, $p < .001$, $\eta_p^2 = 0.45$	**VP x CP:** $F_{(1,30)} = 5.55$, $p < .05$, $\eta_p^2 = 0.16$ **VP x Val.:** $F_{(1,30)} = 30.58$, $p < .001$, $\eta_p^2 = 0.51$ **VP x Con.:** $F_{(1,30)} = 0.98$, $p > .1$, $\eta_p^2 = 0.03$ **CP x Val.:** $F_{(1,30)} = 3.31$, $p > .05$, $\eta_p^2 = 0.10$ **CP x Con.:** $F_{(1,30)} = 74.60$, $p < .001$, $\eta_p^2 = 0.71$ **Val. x Con.:** $F_{(1,30)} = 11.41$, $p < .01$, $\eta_p^2 = 0.28$	**VP x CP x Val.:** $F_{(1,30)} = 0.81$, $p > .1$, $\eta_p^2 = 0.03$ **VP x CP x Con.:** $F_{(1,30)} = 0.36$, $p > .1$, $\eta_p^2 = 0.01$ **VP x Val. x Con.:** $F_{(1,30)} = 21.66$, $p < .001$, $\eta_p^2 = 0.42$ **CP x Val. x Con.:** $F_{(1,30)} = 5.16$, $p < .05$, $\eta_p^2 = 0.15$	**VP x CP x Val. x Con.:** $F_{(1,30)} = 0.57$, $p > .1$, $\eta_p^2 = 0.02$

Supplementary Table ST3 Mean (+ SD) values per condition, averaged over participants, for RTs, accuracy, and inverse efficiency (RT divided by accuracy). Block types are specified in the second column, and trial types are depicted in the first row

		Valid-Congruent	*Valid-Incongruent*	*Invalid-Congruent*	*Invalid-Incongruent*
RT	*Chance-Invalid Frequently-Incongruent*	365.66 ± 40.22 ms	428.22 ± 39.00 ms	381.39 ± 37.16 ms	448.93 ± 38.87 ms
	Rarely-Invalid Frequently-Incongruent	355.42 ± 28.90 ms	422.18 ± 36.58 ms	389.40 ± 40.71 ms	448.79 ± 43.29 ms
	Chance-Invalid Rarely-Incongruent	357.37 ± 32.23 ms	447.98 ± 46.45 ms	382.74 ± 40.75 ms	466.52 ± 50.37 ms
	Rarely-Invalid Rarely-Incongruent	349.14 ± 31.30 ms	447.16 ± 34.30 ms	396.88 ± 48.47 ms	471.52 ± 55.55 ms
Accuracy	*Chance-Invalid Frequently-Incongruent*	98.69 ± 1.40%	90.95 ± 9.32%	97.85 ± 3.62%	86.17 ± 13.59%
	Rarely-Invalid Frequently-Incongruent	99.16 ± 2.18%	91.48 ± 5.63%	97.31 ± 5.85%	85.70 ± 12.06%
	Chance-Invalid Rarely-Incongruent	99.46 ± 2.45%	87.93 ± 5.85%	97.80 ± 5.56%	81.26 ± 11.41%
	Rarely-Invalid Rarely-Incongruent	98.83 ± 2.21%	85.00 ± 9.48%	96.02 ± 5.86%	68.28 ± 21.56%
Inverse Efficiency (RT/accuracy)	*Chance-Invalid Frequently-Incongruent*	370.59 ± 39.98 ms	471.37 ± 37.47 ms	391.34 ± 47.29 ms	532.31 ± 101.91 ms
	Rarely-Invalid Frequently-Incongruent	358.59 ± 29.66 ms	462.40 ± 39.91 ms	401.95 ± 51.95 ms	538.19 ± 121.14 ms
	Chance-Invalid Rarely-Incongruent	359.37 ± 32.47 ms	513.16 ± 59.12 ms	391.93 ± 44.45 ms	591.60 ± 126.89 ms
	Rarely-Invalid Rarely-Incongruent	353.44 ± 32.84 ms	531.52 ± 63.02 ms	415.85 ± 64.89 ms	788.16 ± 350.29 ms

Supplementary Material Chapter 3

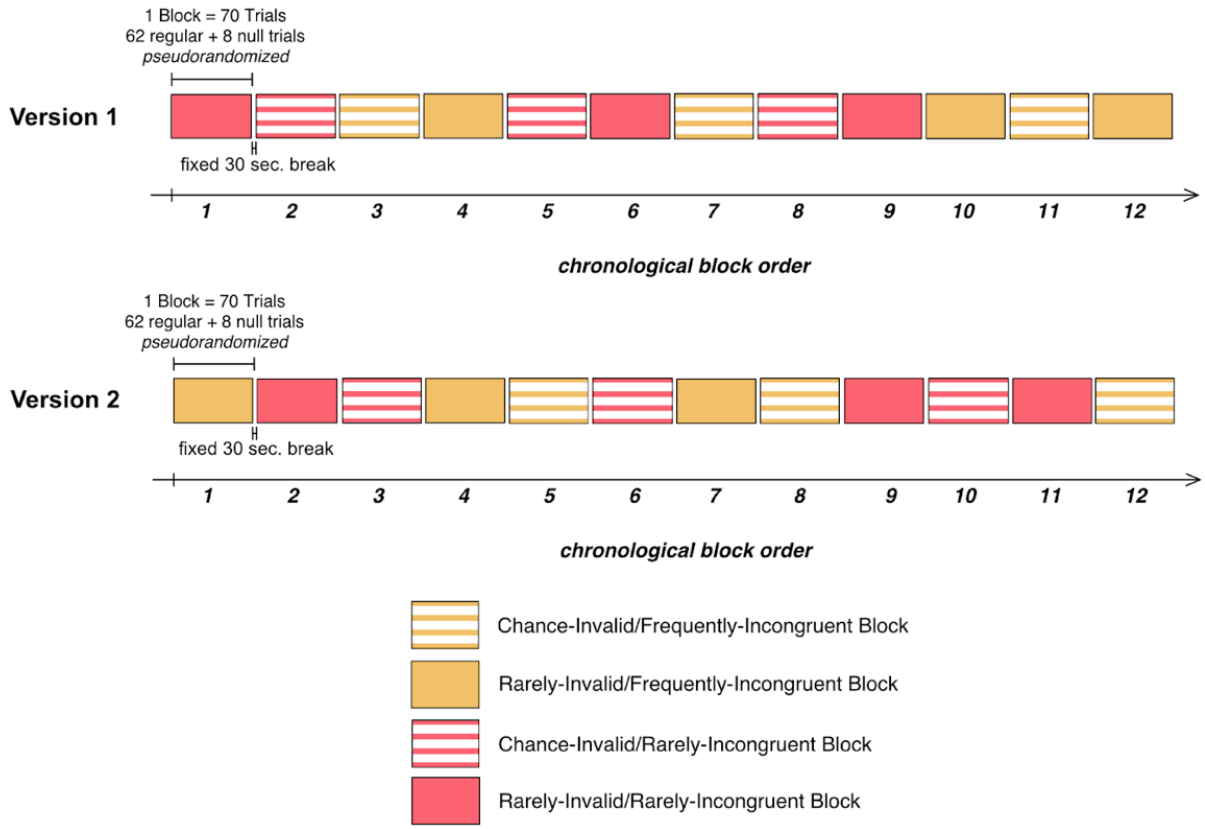

Supplementary Fig. SF1 Illustration of the response cueing/conflict task block structure employed in this study, displaying the sequence of blocks for the two task versions, which were counterbalanced across participants. Each of the four distinct block types (represented by red/orange color and stripes/fill) was presented thrice in both versions, each time featuring a unique pseudorandom trial sequence (identical within each version). Every block consisted of 70 trials, of which 8 were null trials, resulting in a total of 840 trials (12 blocks × 70 trials). The entire task lasted approximately 35 minutes and included fixed breaks of 30 seconds in between blocks

Supplementary Material Chapter 4

1. Methods

Training

Prior to the main experiment, participants completed a training session consisting of three blocks of 40 trials (~5 min. total), with self-paced breaks between blocks. The first two blocks featured only the central target arrow, helping participants familiarize themselves with the task's timing and structure. Block 1 used mostly valid cues (80%), while Block 2 balanced valid and invalid trials (50%). In Block 3, flanking distractor arrows were introduced, with a cue validity proportion of 80% and congruency proportion at chance level (50%). Trials were presented in a fixed, pseudorandom order without jittering the cue-target time-period. As in the main task, left- and right-hand responses were equally distributed across conditions.

2. Supplementary Figures

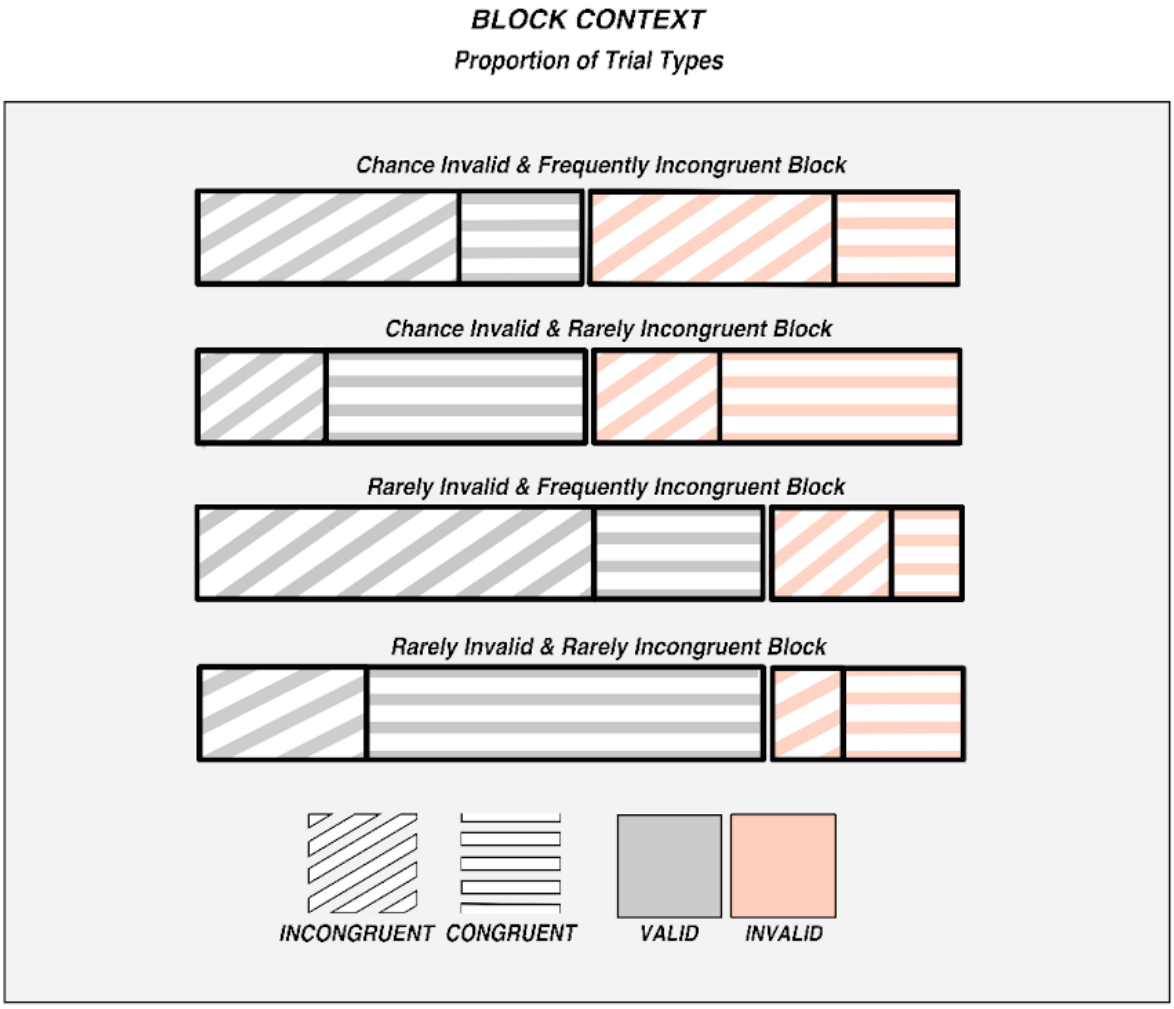

Supplementary Fig. SF1 Block context: schematic depiction of the four block types with varying ratios of valid to invalid trials (grey [50% or 77%] and orange colors [50% or 23%]) and congruent to incongruent trials (horizontal [30% or 70%] vs. diagonal stripes [30% or 70%])

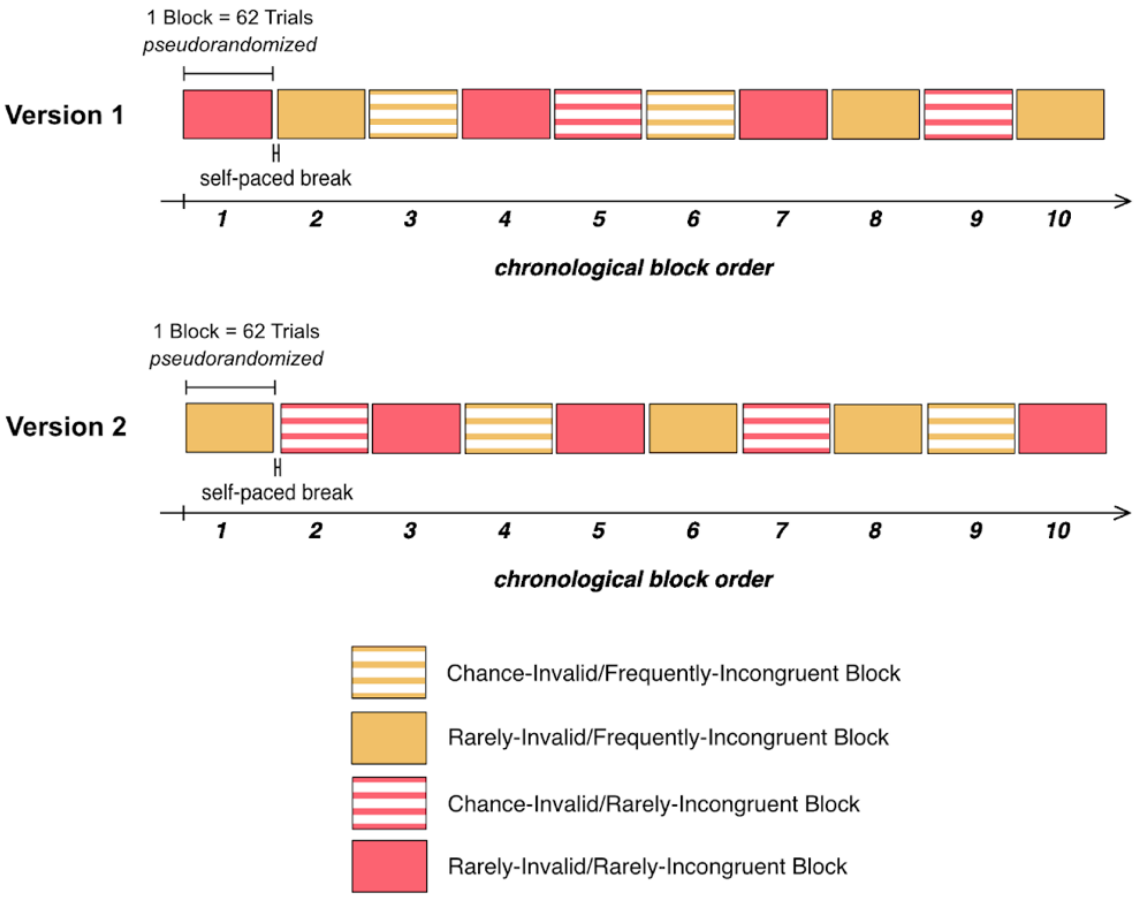

Supplementary Fig. SF2 This scheme depicts the response cueing/conflict task structure employed in this study, showing the consecutive order of blocks in two versions, which were counterbalanced between participant's stimulation conditions. Each of the four unique block types (depicted in different colors and patterns) was presented at least twice during the task, each time with a unique pseudorandom trial sequence (which was the same within a version). Each block contained 62 trials, which amounted to 620 trials in total (10 blocks x 62 trials). The whole task lasted for roughly 30 min. and included self-paced breaks in between blocks

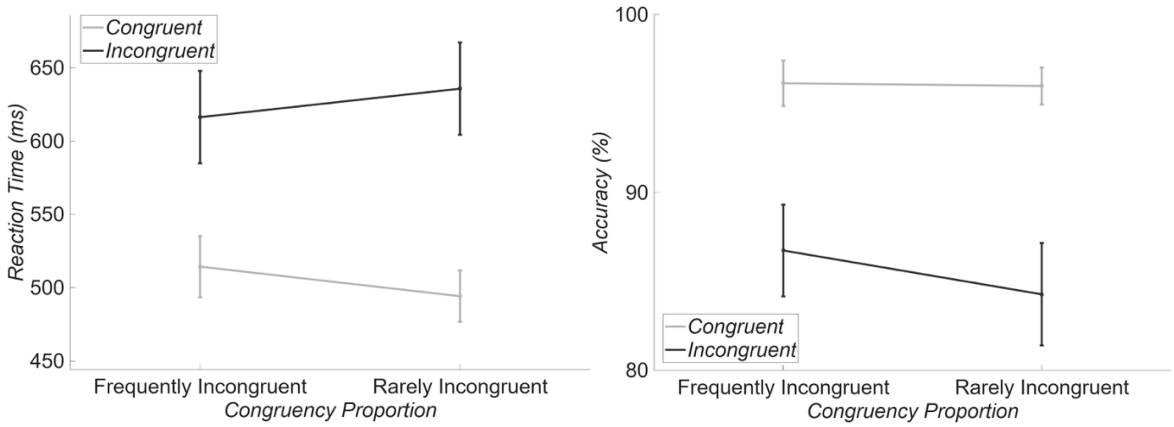

Supplementary Fig. SF3 Congruency effect as modulated by congruency proportion. Left: RTs of congruent (light grey) and incongruent (conflict; dark grey) trials, depicting the congruency effect as the difference between congruent and incongruent lines. The x-axis shows block-types with frequent incongruent trials (expected conflict) and rare incongruent trials (unexpected conflict). This visualizes the increase in the congruency effect when conflict is unexpected. Right: This graph depicts the congruency effect in the same way as the left side, however, for accuracy instead of RTs

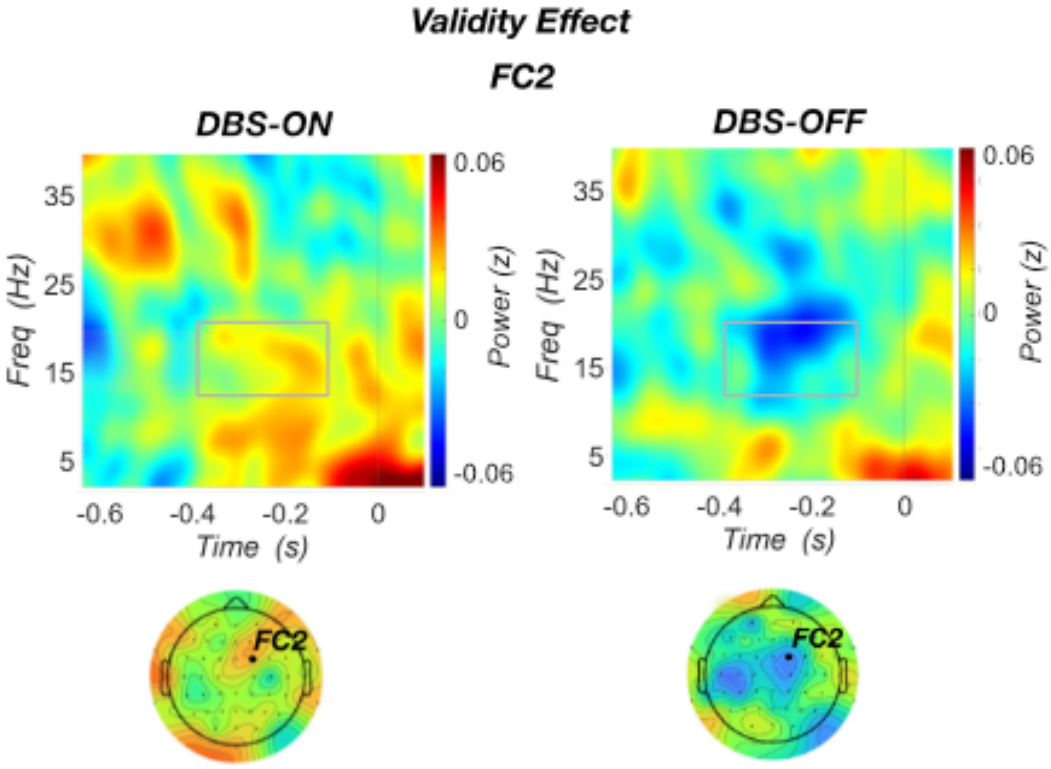

Supplementary Fig. SF4 Top: response-locked power differences between invalid (reprogramming) and valid trials at FC2, for DBS-ON (left) and DBS-OFF (right). The grey square depicts the time window of interest for the "retune" stage (-0.4 to -0.1 sec. from 13 to 20 Hz). The DBS-OFF condition shows beta desynchronization during this period, which is not visible when DBS is ON. Bottom: associated topographies show the scalp distribution of

average beta power in this window of interest, showing the concise localization of this effect around the FC2 electrode (DBS-OFF)

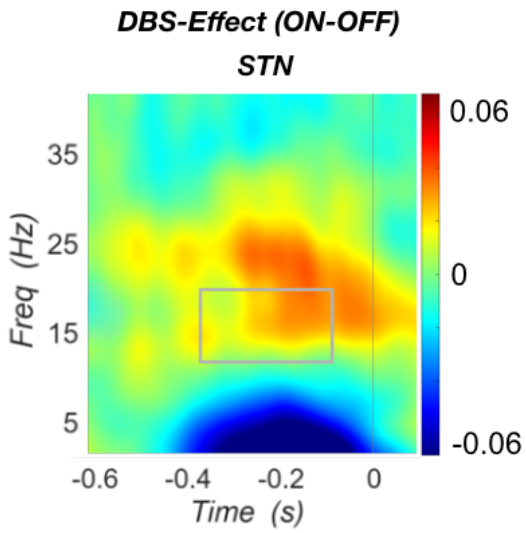

Supplementary Fig. SF5 Response-locked power differences at the STN, showing DBS-ON minus DBS-OFF values. The grey square depicts the window of interest during the "retune" stage, from -0.4 to -0.1 sec. and from 13 to 20 Hz. DBS-ON shows higher beta values than DBS-OFF in this window, i.e., enhanced beta desynchronization was present during DBS-OFF

3. Supplementary Tables

Supplementary Table ST1 Demographics and neuropsychiatric assessment scores of the study population represented in the data analyses. ID column: one asterisk (*) indicates that the participant had an implanted Percept PC device (Medtronic, Inc., Minneapolis, USA), thus LFP signals were recorded next to the cortical EEG. Two asterisks (**) mark the participant with behavioral data only (invalid EEG data due to missing event markers). LEDD: total L-dopa equivalent daily dose (dopaminergic medication). Questionnaires included the Beck Depression Inventory II (BDI-II) for depressive symptoms (Beck et al., 2011), the Montreal Cognitive Assessment (MoCA) to screen for cognitive impairment (Nasreddine et al., 2014), the Barratt Impulsiveness Scale (BIS-11) for general impulsivity (Patton et al., 2011), the Questionnaire for Impulsive-Compulsive Disorders in Parkinson's Disease (QUIP-PD) for PD-specific impulsivity traits (Weintraub et al., 2012), and the Freezing of Gait Questionnaire (FOG-Q) to assess freezing episodes and categorize PD subtypes (Nilsson et al., 2010)

ID	Age	Sex	Handedness	Disease Duration (years)	Time since DBS surgery (in months)	LEDD (mg)	UPDRS ON	UPDRS OFF	BDI-II	MoCA	BIS-11	QUIP-PD	FOG-Q
1	60	m	right	6	28	1015	2.5	6	12	25	64	21	11
3	58	m	right	11	7	350	8	21	6	29	65	4	0
5*	63	m	right	13	6	825	10,5	21	3	25	56	5	4
6	69	m	right	23	34	751,2	1	7.5	6	29	62	1	7
7*	67	w	right	17	26	300	6	7	17	29	59	16	17
8*	61	w	right	4	7	585	4.5	11.5	11	29	50	0	5
9*	61	m	right	16	24	575,75	8,5	15.5	11	26	68	36	17
10*	58	m	right	18	24	650	11,5	26	15	27	57	10	data unavailable
11	63	w	right	13	10 months (original surgery), 4 months since adjustment	300	9,5	23.5	25	24	69	2	17
12*	70	m	right	12	28	540	4,5	20	5	28	59	6	6
13**	56	m	right	6	5	520	5 / 3,5 (separate days)	13 / 13,5 (separate days)	6	27	59	1	3

14	66	m	right	18	9	665	7	27.5	14	25	58	31	10
15	61	w	right	8	4	121,2	4,5	10	2	27	54	0	6
16 *	68	m	right	20	21	785,6	4/6,5 (separate days)	16,5/18 (separate days)	4	26	53	3	1
17 *	53	w	right	10	10	225	3,5/2 (separate days)	17/20 (separate days)	7	21	59	40	2
18	50	w	right	9	14	147,2	2	23/20.5 (separate days)	26	24	63	13	10
19	78	m	right	7	9	1142,4	8,5	10.5	0	25.5	52	0	7
20	57	w	left	11	6	450	data unavailable	data unavailable	2	29	62	0	data unavailable
21	73	m	right	15	23	1358	4	10	11	24	61	0	12
22 *	66	m	right	15	26	404	6,5	15	3	28	57	1	14
23 *	71	m	right	5	6	52	7	10.5	1	30	52	3	0
24	68	m	right	18	24	data unavailable	3	11.5	data unavailable	23	61	data unavailable	0
25	60	m	right	6	24	855	9,5	14	data unavailable	data unavailable	data unavailable	data unavailable	data unavailable
27	60	w	right	6	47	342,4	3	10	9	30	59	0	1

Supplementary Table ST2 Clinical DBS settings of study population that was considered for the data analyses. ID column: numbers with one asterisk (*) denote that the participant was implanted with a Percept PC device (Medtronic, Inc., Minneapolis, USA), thus LFP signals were registered alongside the cortical EEG. Two asterisks (**) next to the number point out the participant who did not have valid cortical EEG data. In this case, only the behavioral data were included for the analysis

ID	Clinical Stimulation Settings
1	*STN left: G+, 5-100%, 130 Hz, 60µs, 3 mA (0-3.2mA); STN right: G+, 7-100%, 130 Hz, 60µs, 3 mA (0-3.2mA)*
3	*STN left: G+, 4-75%, 3-25%, 50µs, 130Hz, 2,9mA; STN right: G+, 5-34%, 6-33%, 7-33%, 50µs, 130Hz, 1,7mA*
5*	*STN left: G+; 2a2b2c(at 0.7mA), 60µs, 125Hz; STN right: G+; 2a2b2c(at 1mA), 60µs, 125Hz;*
6	*STN left: 5-6-7 (100%), 1.7 mA, 60 microsec., 198 Hz; STN right: 5-6-7 (100%), 3.1 mA, 60 microsec., 198 Hz*
7*	*STN left: 2 a b c (at 0.7 mA), 50 microsec., 130 Hz; re: 9 a b c (at 0.7 mA), 50 microsec., 130 Hz*
8*	*STN left: 7- (25%), 6- (75%), 2.7mA, 50us, 130Hz (1-3,2mA); STN right: 5-6-7 (100%), 2.6mA, 50us, 130 Hz (1-3.2mA)*
9*	*STN right: 9 a b c (at 0.6 mA -> 1.8 mA), 50 microsec., 130 Hz; STN left: 2 a b c (at 0.6 mA -> 1.8 mA), 50 microsec., 130 Hz*
10*	*STN left: G+, 2c, (2.3 mA); 7.0 mA, 60 microsec., 180 Hz (6.0-8.1 mA). STN right: G+, 10b (2.2 mA), 11 (0.9 mA); 6.6 mA, 60 microsec., 180 Hz (0.0-8.0 mA)*
11	*STN left: 1a und 2a (1,0mA), 60us, 185Hz; STN right: 9a (0,4mA), 9b (0,1mA), 10a (0,6mA), 10b (0,2mA), 60us, 185 Hz*
12*	*STN left: (G+ 7-100%, 60 microsec. 143 Hz, 1.7 mA). STN right: (G+ 7-100%, 60 microsec. 143 Hz, 1.7 mA). Boundaries: 1.5-2.2*
13**	*STN left: C+, 2bc- (at 1.0mA); 3.1 mA, 60us, 130Hz (0-4.0mA), STN right: C+, 10c- (1.5mA), 4.7mA, 60us, 130 Hz (0-4.7 mA)*
14	*data unavailable*
15	*STN left: G+ 2-,3-4- (ring mode), 130 Hz, 50us, 2.6mA (boundaries 2.2mA-2.7mA); STN right: G+ 5-,6-,7- (ring mode), 130 Hz, 50us, 2.5mA (boundaries 2.2mA-2.7mA)*
16*	*STN left: 2-3-4 (100%), 3.7mA, 60 microsec., 130 Hz; STN right: 5-6-7 (100%), 2.2mA, 30 microsec., 130 Hz*
17*	*STN left: C+, 1(a-c)-; 1.7mA; 60us; 125 Hz; STN right: C+, 10 (a-c)-; 2,1 mA, 60us, 125 Hz*
18	*STN left: G+, 2a- (2.3mA), 2b- (0.9mA), 2c- (0.9mA); 5.0mA, 60us, 130Hz (0-5.5mA); STN right: G+, 10c- (2.4mA); 7.4mA; 60us, 130Hz (0-10mA)*
19	*STN left: G+; 6- (60%), 8- (40%), 2.1 mA, 60us, 130Hz (0-3mA); STN right: G+, 6- (60%), 7- (20%), 8- (20%); 1.5mA; 60us, 130 Hz (0-3mA)*
20	*STN left: G+ 4- (40%), 7- (60%), 1.6mA, 50 us, 130 Hz (0.5-2.5mA); STN right: G+ 1- (40%), 2- (30%), 3- (30%), 2mA, 50us, 130Hz (0.5-2.5mA)*
21	*STN left: 60us, 179Hz, 3mA, 3- 60%, 4- 20%, 6- 15%, 7- 5%, FG: 0-3.5mA; STN right: 60 us, 179 Hz, 3.3 mA, 5- 60%, 7- 20%, 8- 20%, FG: 0-3.5 mA*
22*	*STN left: G+, 5,6,7 at 33%, 60us, 89Hz, 2.8mA; STN right: 5,6,7 at 33%, 60us, 130Hz, 2.7mA*

*23**	*STN left: c+ 2a-/b-/c- at 0.65mA; 1.95mA, 60 us, 130 Hz (1.2-2.2); STN right: c+, 10a-/b-/c- at 0.5mA (100%); 1.55mA, 60us, 130 Hz (0.7-1.8)*
24	*STN left: 2abc(at 0,7mA) 60 microsec., 125Hz, 2,1mA, STN right: 10abc(at 0,6mA) 60 microsec., 125Hz, 1,9mA (-)*
25	*STN left: G+, 5/6/7-, 1mA, 60us, 185Hz (0.5-2.5mA); STN right: G+, 3- (70%), 6- (30%), 4.5mA, 60us, 185 Hz (2-5mA)*
27	*data unavailable*

References included in this section of the Supplementary Material are listed in ***Chapter 4****.*